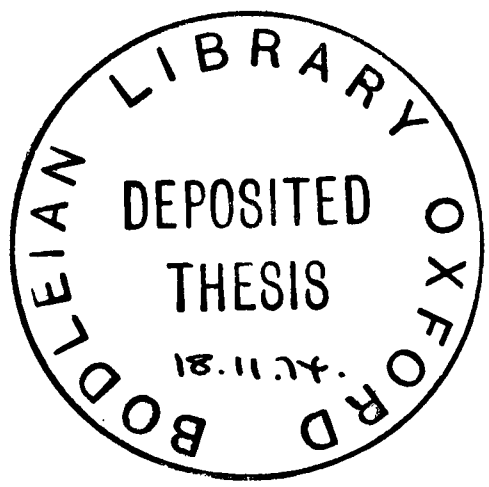
# THE INTERPRETATION OF THE SPECTRA OF DIATOMIC MOLECULES

Abstract of a thesis presented for the degree of D.Phil. in the University of Oxford by

P.R. Scott




Pembroke College,
Oxford.

Michaelmas Term 1974.

Considerable effort has been expended by experimentalists in the last two decades in trying to understand the electronic structure of the simplest transition metal compounds, those containing a metal atom bound to one other atom. Yet in spite of the very detailed information available from the study of the electronic spectra of diatomic molecules, the basic principles of the bonding of these molecules are still largely unknown. This thesis illustrates the important role that molecular orbital calculations can play in helping to elucidate the electronic structure of both the ground and excited states of molecules of chemical, rather than purely physical, interest.

Chapter 1

The theoretical methods to be adopted are outlined. Hartree-Fock theory for closed- and open-shell systems is described, and the errors inherent in the theory are discussed. Several methods of treating the correlation energy problem are outlined, and the computer programmes used in the work are described. A brief survey of the field of diatomic molecules containing one transition metal atom is given, indicating the types of experimental methods that have been used, and the nature of the information which is available.

Chapter 2

Hund's rules for atoms have often been extended in a rather arbitrary way to molecules, without explicit justification, and the validity of this extension is investigated. The model used is an invariant orbital approximation; the limitations of this model are discussed, and it is shown that the model will give the same results as the best possible orbital model. Expressions are derived for the relative energies of the electronic states of linear molecules derived from the same electron configuration. General inequalities relating to coulomb and exchange integrals often permit definite conclusions to be drawn concerning the ordering of the states. The predictions sometimes agree with Hund's rules, sometimes disagree, and also predict the ordering of $\Sigma^+$ and $\Sigma^-$ states, which is not considered by Hund's rules. It is

shown that in cases where sufficient experimental data exist, they are in agreement with the theoretical predictions.

Chapter 3

A theoretical investigation of the excited states of the molecule ScF is described. Single configuration wave functions are calculated for the low-lying and excited states of the molecule; the agreement between the calculated and observed spectroscopic constants for the low-lying states, whose electronic structures are well understood, is very good. It is shown that the lowest $^3\Pi$ state is well described by the electron configuration $4s\sigma 3d\pi$, but that the lowest $^3\Phi$ state corresponds to the configuration $3d\delta 4p\pi$, and not $3d\delta 3d\pi$ as previously thought, and that differences in electron repulsion therefore play an important role in determining the ordering of electronic states in transition metal diatomic molecules. It is further concluded that the observed $^3\Delta$ state corresponds to the configuration $3d\delta 4p\sigma$, and not $3d\delta 3d\sigma$ as previously supposed. These reassignments are shown to resolve a discrepancy which previously existed between the relative energies of the 3d and 4p electrons in ScF and ScO.

Limited configuration interaction studies show that there is no appreciable mixing between the $^3\Phi$ states, but that the excited $^3\Pi$ states are not well described by single configuration wave functions. The difference between the $\Phi$ and $\Pi$ states is explained by the difference in magnitudes of off-diagonal matrix elements representing one- and two-electron excitations. The configuration mixing in the $\Pi$ states allows a rationalisation of the intensity distribution among the $^1\Pi$-$X^1\Sigma^+$ transitions, which is not possible using a single configuration model.

Chapter 4

Ab initio molecular orbital calculations on a number of monohydrides of first row transition metals are described. Although the monohydrides are the simplest transition metal compounds, very little experimental information on them is available, and the calculations attempt to predict and rationalise

the orderings of their ground and low-lying electronic states.

Hartree-Fock calculations are performed on the molecule ScH, and the correlation energies of the low-lying states are estimated semi-empirically from atomic data. Two states are found to be very low-lying, $^1\Sigma^+$ and $^3\Delta$. The suggestion that the transition observed in absorption at 5500 Å is between states of multiplicity greater than three is not supported; it is suggested that this transition could be $^3\Phi$-$^3\Delta$. The splitting of the d orbitals by the hydrogen atom is shown to be $\delta>\pi>\sigma$, with the $\delta$ orbital most stable, although the splitting is rather smaller than in the corresponding fluoride.

Calculations and semi-empirical estimates of correlation energies on TiH suggestthat the low-lying states of the molecule are derived from configurations essentially of the type $4s3d^2$; similar calculations on VH show that in this molecule the low-lying states are derived from configurations which are well described as $4s3d^3$. It is shown that near-degeneracy effects must be taken into account for the $\Sigma^-$ and $\Pi$ states of TiH and VH, and 2×2 configuration interaction calculations are described. It is shown that in each molecule the states may be regarded as the four spatial components of the $^4F$ and $^5F$ states of the ions $Ti^+$ and $V^+$, and the two components of the $^4P$ and $^5P$ states, and that the H atom therefore acts only as a small perturbation on the metal atom. A hole formalism is used to explain why the perturbation in VH has the opposite sign to that in TiH, and it is shown that this perturbation is compatible with the stabilisation of the d orbitals being $\delta>\pi>\sigma$, as in ScH.

A single centre perturbation treatment of the molecule FeH has suggested that the ground state is $^6\Sigma^+$, with the d orbitals stabilised in the order $\delta<\pi<\sigma$. Calculations are described which predict the ground state of FeH to be $^6\Delta$, with the $d\delta$ orbital more stable than $d\pi$ and $d\sigma$. Comparison of other spectroscopic constants calculated by the Hartree-Fock and single-centre techniques show wide discrepancies, and even trends between different states are often not reproduced. It is concluded that the single-centre method is not an appropriate tool for studying transition metal hydrides, as the convergence

characteristics are much slower than had previously been thought.

Calculations on NiH and PdH predict the ground states of these molecules, which have isoelectronic valence shells, to be $^2\Delta$ and $^2\Sigma^+$ respectively, in agreement with experimental results. The bonding in PdH is interpreted as covalent bonding between the $4d\sigma$ and $1s\sigma$ orbitals, giving a $^2\Sigma^+$ ground state with two near-degenerate excited states, $^2\Delta$ and $^2\Pi$. In NiH it is shown that the greater stability of the 4s orbital relative to the 3d stabilises the anti-bonding combination of the $3d\sigma$ and $1s\sigma$ orbitals, and the $^2\Sigma^+$ state lies above the $^2\Delta$ and $^2\Pi$ states. It is further shown that the difference in energies between the $^2\Delta$ and $^2\Pi$ states is 5000 $cm^{-1}$, larger than has previously been supposed, and it is shown that two hypotheses explaining why the $d\pi$ orbital is more stable than the $d\delta$ do not account for a splitting of this magnitude. The splitting is explained by the difference in repulsion energies between a $d\delta$ and $d\sigma$ electron, and a $d\pi$ and $d\sigma$ electron. A population analysis shows that this effect is sufficiently large to explain the calculated splitting, and that it is the same factor, the greater stability of the s orbital relative to the d, which causes the change in ground state and the increase in $^2\Pi$-$^2\Delta$ splitting from PdH to NiH.

# THE INTERPRETATION OF THE SPECTRA OF DIATOMIC MOLECULES

by

P.R. Scott

A thesis submitted for the degree of

Doctor of Philosophy

in the

University of Oxford

Pembroke College,
Oxford.

Michaelmas Term 1974.

ACKNOWLEDGEMENTS

I should like to express my thanks to my supervisors, Dr. W.G. Richards and Dr. R.F. Barrow for their encouragement and advice throughout the work.

I am grateful to Dr. G. Verhaegen for his assistance with the work on correlation energy and for the use of computing time, and to the NATO Science Committee for funding a visit to the Free University of Brussels.

Professors R.N. Zare and J.P. Colpa kindly communicated their work before publication, and their discussions have provided a valuable stimulus to the work in this thesis.

Lastly I am grateful to all my colleagues who were always prepared to give of their time and effort, especially Dr. J. Raftery, who collaborated on the work on Chapter 2, and Les Farnell.

## UNITS AND NOTATION

The atomic system of units is used in this thesis, in which Planck's constant has the value $2\pi$, and the electron has unit mass and charge. The unit of energy is then twice the (non-relativistic) binding energy of the hydrogen atom.

Approximate values of the atomic units are given below.

| | | |
|---|---|---|
| Energy | 1 a.u. | $= 4.3577 \times 10^{-18}$ J. |
| | | $= 219474.6\ \text{cm}^{-1}$. |
| | | $= 27.21$ e.V. |
| Distance | 1 a.u. | $= 52.9167$ pm. |
| | | $= 0.529167$ Å. |
| Mass | 1 a.u. | $= 1.6604 \times 10^{-27}$ Kg. |

Many-particle wave functions are represented by capital Greek letters $\Psi$, $\Phi$, $\Theta$, and one-particle wave functions by small Greek letters $\psi$, $\phi$, $\chi$. Dirac bra-ket notation is used for wave functions.

CONTENTS


| | | Page No. |
|---|---|---|
| Chapter 1. | Introduction | 1 |
| Chapter 2. | Energy Levels in Linear Molecules | 26 |
| Chapter 3. | A Reassignment of the Molecular Orbital Configurations of the Excited States of ScF | 58 |
| Chapter 4. | The Electronic Structure of the Transition Metal Hydrides | 94 |
| References | | 153 |
| Appendix A. | The Roothaan Double Hamiltonian Method | 158 |
| Appendix B. | Atomic Correlation Energies | 162 |

# Chapter 1

## INTRODUCTION


| | | Page No. |
|---|---|---|
| 1.1 | Theoretical Methods | 2 |
| | 1.1.1 The Schrödinger Equation | 2 |
| | 1.1.2 Symmetry Operators | 2 |
| | 1.1.3 Approximate Methods | 3 |
| | 1.1.4 Orbitals | 4 |
| | 1.1.5 Slater Determinants | 5 |
| | 1.1.6 Single Configuration Wave Functions | 6 |
| | 1.1.7 Open Shell Configurations | 9 |
| | 1.1.8 Relativistic Effects | 12 |
| | 1.1.9 Choice of Basis Set | 13 |
| | 1.1.10 Correlation Energy | 15 |
| | 1.1.11 Computer Programmes | 17 |
| 1.2 | Transition Metal Diatomic Molecules | 20 |
| | 1.2.1 Introduction | 20 |
| | 1.2.2 Experimental Methods | 20 |
| | 1.2.3 *Ab Initio* Calculations | 24 |
| | 1.2.4 Summary | 24 |


### Table


Table 1.1 Spectroscopic Constants from Potential Curves 19

## 1.1 Theoretical Methods

### 1.1.1 The Schrödinger equation

The calculations described in this thesis have as their starting-point the Schrödinger equation, which is the equation of non-relativistic quantum mechanics. In quantum mechanics it is postulated that the state of a system may be completely described by a function $\Psi$, which is called the wave function. The wave function is a solution of the Schrödinger equation; in this thesis only stationary states are considered, and for these states the equation takes the form

$$\hat{H}\Psi = E\Psi \qquad (1)$$

where $\hat{H}$ is the hamiltonian operator, which is constructed according to the postulates of quantum mechanics, and E is the energy of the system. If equation (1) is multiplied by $\Psi^*$ and integrated over all space, then

$$\langle \Psi | H | \Psi \rangle = E \langle \Psi | \Psi \rangle \ .$$

The wave function is usually normalised, i.e. $\langle \Psi | \Psi \rangle = 1$, and therefore

$$E = \langle \Psi | H | \Psi \rangle \ .$$

The energy is said to be the expectation value of the hamiltonian, and in general the value of any observable property of the system is equal to the expectation value of some operator.

### 1.1.2 Symmetry Operators

If any operator commutes with the hamiltonian, then the observable corresponding to that operator may be determined simultaneously with the energy, and the wave functions of the system will be eigenfunctions of that operator. This provides a useful tool in classifying molecular wave functions; the most common operators in this context are the angular momentum and symmetry operators of the system. For atomic systems, if a non-relativistic hamiltonian operator is used, then the wave functions are eigenfunctions of the operators

$\hat{L}^2$ and $\hat{L}_z$, the total orbital angular momentum operator and its component along an axis, and $\hat{S}^2$ and $\hat{S}_z$, the corresponding spin operators. The atomic eigenfunctions may be labelled with quantum numbers defining the eigenvalues of these operators, $|L, M_L, S, M_s\rangle$. For linear molecules the operator $\hat{L}^2$ no longer commutes with the hamiltonian. However, if we consider only a non-relativistic electronic hamiltonian, then it still commutes with the operators $\hat{L}_z$, $\hat{S}^2$ and $\hat{S}_z$, where z is the molecular axis.

1.1.3 Approximate Methods

The wave function is a function of the coordinates of all the particles in the system, and for a system of many particles the Schrödinger equation is a partial differential equation in many dimensions. It is not generally possible to obtain analytic solutions of the equation, and it is necessary to resort to approximate methods. The eigenfunctions of the Schrödinger equation form an orthogonal set, and the variation principle therefore applies to approximate solutions. If $\Phi$ is a trial wave function, then the expectation value $\langle\Phi|\hat{H}|\Phi\rangle$ is necessarily greater than or equal to the lowest eigenvalue of $\hat{H}$. An approximate eigenfunction depending on various parameters may therefore be optimised by minimising this expectation value. The calculated value of $\langle\Phi|\hat{H}|\Phi\rangle$ puts an upper bound on the exact eigenvalue.

Perturbation theory may also be used to solve the Schrödinger equation; here the hamiltonian is split into two parts, an unperturbed part whose eigenfunctions and values are known, and a small perturbation. The energy is then approximated as a sum involving diagonal and off-diagonal matrix elements of the perturbation operator over the known eigenfunctions.

The commonest and most important approximation in the solution of the Schrödinger equation for molecular systems is the Born-Oppenheimer approximation, where the wave function is separated into two factors

$$\Psi = \Psi_{\text{electronic}} \cdot \Psi_{\text{nuclear}} .$$

In atomic units the hamiltonian for a molecule is:

$$\hat{H} = -\tfrac{1}{2}\sum_{k=1}^{N} \nabla_k^2/M_k - \tfrac{1}{2}\sum_{i=1}^{M} \nabla_i^2 - \sum_{ik} Z_k/r_{ik} + \sum_{ij} {}^{1}/r_{ij} + \sum_{kl} Z_k Z_l/r_{kl} \ ,$$

where i,j refer to electrons, and k,l to nuclei. The Schrödinger equation may therefore be represented

$$[-\tfrac{1}{2}\sum_{k} \nabla_k^2/M_k - \tfrac{1}{2}\sum_{i} \nabla_i^2 - V_{en}(R,r) + V_{ee}(r) + V_{nn}(R)]\ \Psi = E\Psi$$

where R refers to nuclear coordinates, and r to electronic coordinates. In the Born-Oppenheimer approximation, the electronic wave function is a solution of the clamped-nucleus equation

$$\{-\tfrac{1}{2}\sum_{i} \nabla_i^2 + V_{ee}(r) - E_{en}(R,r)\}\ \Psi_{el} = U_{el}(R)\ \Psi_{el} \qquad (2)$$

If the nuclear repulsion $V_{nn}(R)$ is added to $U_{el}(R)$, then the potential energy surface U(R) is obtained. This may be used as the potential in the nuclear Schrödinger equation, whose eigenfunction is $\Psi_{nuc}$ .

$$\{-\tfrac{1}{2}\sum_{k} \nabla_k^2/M_k + U(R)\}\ \Psi_{nuc} = E\Psi_{nuc} \ .$$

It may be shown that the Born-Oppenheimer approximation is equivalent to neglecting the terms

$$\Psi_{nuc} \sum \nabla_k^2/M_k\ \Psi_{el} + 2\sum_{k}\sum_{\alpha_k} \frac{\partial\Psi_{nuc}}{\partial\alpha_k}\frac{\partial\Psi_{el}}{\partial\alpha_k}\ \frac{1}{M_k}$$

These terms have been shown by Born and Oppenheimer (1926) to be very small compared with the terms that are retained provided that $M_k >> 1$. Even for the lightest nuclei $M_k > 10^3$, and so the approximation is generally valid.

### 1.1.4 Orbitals

The electronic Schrödinger equation may be written

$$\{-T_e - V_{en} + V_{ee}\}\Psi = E\Psi.$$

But for the term $V_{ee}$ this equation would be separable into N one-particle equations:

$$\{-\tfrac{1}{2}\nabla_i^2 - \sum_k {}^{Z_k}/_{r_{ik}}\}\,\phi(r_i) = \varepsilon\phi(r_i).$$

These one-electron wave functions $\phi$ form the basis of many of the approximate methods of solution of the Schrödinger equation, and they are called orbitals. The total electronic wave function $\Psi$ would then be an orbital product

$$\Psi_{el} = \prod_i \phi_i(r_i).$$

If electron spin is included, then the wave function becomes the product of spin-orbitals, each of which may be factorised

$$\psi(r_i,s_i) = \phi(r_i)\,\eta(s_i)$$

The function $\eta$ may have two forms, depending on the value of the $M_s$ quantum number; these are $\alpha(M_s=\frac{1}{2})$ and $\beta(M_s=-\frac{1}{2})$. It is common to represent spin-orbitals as follows:

$$\phi_i(r_i)\,\alpha(s_i) = \phi_i$$

$$\phi_i(r_i)\,\beta(s_i) = \overline{\phi}_i$$

1.1.5 Slater Determinants

A simple spin-orbital product is not a satisfactory wave function as it is not an eigenfunction of the operator $\hat{P}_{ij}$ which permutes electrons i and j. This operator clearly commutes with the hamiltonian, as electrons are indistinguishable. The antisymmetry principle states that for electrons the eigenvalue of $\hat{P}_{ij}$ must be -1. A form of wave function which satisfies this criterion is the Slater determinant

$$\Psi = {}^{1}/_{\sqrt{N!}} \begin{vmatrix} \psi_1(1) & \cdots & \psi_1(N) \\ \psi_2(1) & & \\ \vdots & & \\ \psi_N(1) & \cdots & \psi_N(N) \end{vmatrix}$$

which is commonly written $\Psi = |\psi_1(1) \ldots \psi_N(N)|$. The determinant is antisymmetric to electron permutation as a determinant changes sign when rows or columns are interchanged. It also ensures that no spin-orbital may be doubly occupied, as the determinant vanishes when two rows or columns are identical. As the spin part may only have one of two values, no space orbital may be more than doubly occupied, and the wave function therefore satisfies the Pauli principle.

It may be shown (McWeeny and Sutcliffe 1969 and op. cit.) that if a complete set of $\phi_i$ are taken and combined with spin functions to give a complete set of spin-orbitals $\phi_i$, then the set of functions $\theta_m$ formed by taking all possible subsets of N spin-orbitals from that set, and forming the antisymmetrical product from each subset, is a complete set of functions in the N-electron configuration space. The exact electronic wave function may therefore be expanded as

$$\Psi = \sum_m a_m \theta_m \qquad (2)$$

The expression for the energy is

$$E = \sum_{mn} a_n^* a_n \langle m|H|n \rangle$$

if the orbitals $\phi_i$ are orthogonal, in which case the $\theta_m$ are necessarily orthonormal. These matrix elements may be reduced to matrix elements of one- and two-electron operators by Slater's rules (Slater 1929, 1931) for matrix elements between Slater determinants. Unfortunately as this set of $\theta$ is also infinite, it does not provide a tractable method of solving the wave equation, and in practice some truncation of the infinite series is necessary.

### 1.1.6 Single Configuration Wave Functions

The most commonly employed truncation of the expansion in equation (2) is the single term, and the wave function takes the form

$$\Psi = A \prod_i \psi_i$$

where A is the antisymmetrising operator. To be a suitable wave function for the system, this must be an eigenfunction of $\hat{S}_z$ and $\hat{S}^2$. This is generally true only if the spin orbitals occur in pairs, each with the same space part; these functions have zero eigenvalues of both $\hat{S}_z$ and $\hat{S}^2$ and are called closed-shell functions. The expectation value of the Hamiltonian is given by Slater's first rule:

$$\hat{H} = \sum_i \varepsilon_i^N + \sum_{ij} J_{ij} - \sum_{ij}' K_{ij}$$

where $\varepsilon_i^N = \langle i|\hat{h}|j\rangle$, $J_{ij} = \langle ij|\hat{g}|ij\rangle$ and $K_{ij} = \langle ij|\hat{g}|ji\rangle$. The summations are over spin-orbitals, and the primed summation is over spin-orbitals with the same spin part. It is convenient to define operators $\hat{J}_i$ and $\hat{K}_i$ such that:

$$\hat{J}_i|j(\mu)\rangle = \langle i(\nu)|g_{\mu\nu}|i(\nu)\rangle\,|j(\mu)\rangle$$

$$\hat{K}_i|j(\mu)\rangle = \langle i(\nu)|g_{\mu\nu}|j(\nu)\rangle\,|i(\mu)\rangle$$

Then $J_{ij} = \langle i|\hat{J}_j|i\rangle$ and $K_{ij} = \langle i|\hat{K}_j|i\rangle$.

Closed-shell wave functions may be optimised using the variation principle; the method was first derived by Fock (1930), following the work of Hartree (1928). The best set of orbitals for a given functional form gives a value of the expectation value of the hamiltonian which is a minimum, and therefore invariant to infinitesimal changes in the orbitals.

$$\delta E = 2\sum_i \delta\varepsilon_i^N + \sum_{ij}(2\delta J_{ij} - \delta K_{ij})$$

where the summation is now over orbitals.

$$\delta E = 2\sum_i \langle \delta\phi_i|\hat{h} + \sum_i (2\hat{J}_j - \hat{K}_j)|\phi_i\rangle$$

$$+2\sum_i \langle \phi_i|\hat{h} + \sum_j (2\hat{J}_j - \hat{K}_j)|\delta\phi_i\rangle$$

The orbitals must remain orthogonal during the infinitesimal variation, therefore

$$\langle \phi_i|\delta\phi_j\rangle + \langle \delta\phi_i|\phi_j\rangle = 0.$$

This problem is treated by the method of Lagrangian multipliers, giving the equations:

$$\{\hat{h} + \sum_i (2\hat{J}_j - \hat{K}_j)\}\ \phi_i = \sum_j \varepsilon_{ij}\ \phi_j$$

$$\{h^* + \sum_j (2\hat{J}_j^* - \hat{K}_j^*)\}\ \phi_i^* = \sum_j \varepsilon_{ji}\ \phi_j^*$$

$$\text{or} \quad \hat{F}\ \phi_i = \sum_j \varepsilon_{ij}\ \phi_j . \qquad (3)$$

For a closed shell system, the wave function and energy are invariant to any unitary transformation of the orbitals; this is a consequence of the determinantal form of $\Psi$; the determinant of a matrix is invariant to a unitary transformation. Thus if U is the unitary transformation which diagonalises the matrix $\varepsilon_{ij}$, then the wave function may be constructed from a new set of orbitals $\{\phi'\}$ such that

$$\phi'_j = \sum_j U_{ij}\ \phi_j \ . \qquad (4)$$

The transformation U does not affect $\hat{F}$, so, dropping the primes, the equation becomes

$$\hat{F}\ \phi_i = \varepsilon_i \phi_i \qquad (5)$$

These equations, the Hartree-Fock equations, are pseudo-eigenvalue equations. They are not true eigenvalue equations, as the operator F depends on the orbitals, and they must accordingly be solved iteratively. Methods of this type are called self-consistent field methods, as the iteration is continued until the Fock operator $\hat{F}$ from a set of orbitals has these orbitals as its eigenfunctions.

Direct numerical solution of the Hartree-Fock equations is very difficult, and is only practicable for atomic systems where the spherical symmetry simplifies the mathematics. The most common procedure is to obtain approximate solutions by expanding the orbitals as a linear combination of a set of basis functions $\{\chi\}$. Then

$$\phi_i = \sum_p c_{pi}\ \chi_p . \qquad (6)$$

The problem is conveniently expressed in matrix notation, the functions $\{\phi\}$ and $\{\chi\}$ being expressed as vectors, and the coefficients as a matrix $\underline{C}$. Then equation (6) becomes $\vec{\phi} = \underline{C}\vec{\chi}$. Defining the matrix $\underline{h}$ such that $h_{pq} = \langle p|\hat{h}|q \rangle$, and a density matrix $\underline{R}$ such that $\underline{R} = \underline{C}\underline{C}^{+}$, then the energy expression becomes:

$$E = 2\underline{R}:\underline{h} + \underline{R}:G:\underline{R} \ ,$$

where $\underline{A}:\underline{B} = \text{tr } \underline{A}\underline{B}$, and $G_{pqrs} = 2\langle pr|\hat{g}|qs\rangle - \langle ps|\hat{g}|rq\rangle$. If $\underline{G}=G:\underline{R}$, then

then $$E = 2\underline{R}:\underline{h} + \underline{R}:\underline{G} = \underline{R}:(2\underline{h}+\underline{G}).$$

If the matrix R is subject to an infinitesimal variation $\underline{\delta R}$, then the resulting change in energy $\delta E$ is given by

$$\delta E = 2\underline{\delta R}:\underline{h} + \underline{\delta R}:\underline{G} + \underline{R}:\underline{\delta G}$$

$$= 2\underline{\delta R}:\underline{h} + \underline{\delta R}:G:\underline{R} + \underline{R}:G:\underline{\delta R}$$

$$= 2\underline{\delta R}:(\underline{h}+\underline{G}) = 2\underline{\delta R}:\underline{F} \ . \qquad (7)$$

$\underline{F}$, the Fock matrix, is the matrix representative of the operator $\hat{F}$. Roothaan (1951) has shown that the condition for $\delta E$ to be zero, subject to the orbitals remaining orthogonal, is

$$\underline{F}\ \underline{C} = \vec{\epsilon}\ \underline{S}\ \underline{C}, \qquad (8)$$

where $\underline{S}$ is the overlap matrix, $\langle p|q\rangle = S_{pq}$.

1.1.7 Open Shell Configurations

Many molecular ground states are well represented by closed shell electron configurations; however, to represent electronically excited states, and also the spectroscopically important ground states of radicals and triplets, it is necessary to use open-shell wave functions. For wave functions with non-zero eigenvalues of $\hat{S}^2$, a single determinant may not be a suitable eigenfunction. In these cases, and in other cases where a closed shell description is not appropriate, it is necessary to project from a single $\theta$ a linear combination of determinants which is an eigenfunction with the required eigenvalue. For example the determinant $|\phi_a\overline{\phi}_b|$ is not an eigen-

function of $\hat{S}^2$. However the linear combinations $2^{-\frac{1}{2}}\{|\phi_a\bar{\phi}_b|+|\bar{\phi}_a\phi_b|\}$ and $2^{-\frac{1}{2}}\{|\phi_a\bar{\phi}_b|-|\bar{\phi}_a\phi_b|\}$ have eigenvalues 2 and 0 respectively. These projected functions have been called 'configuration state functions' (Bagus et al. 1971) or 'configurations' (Das 1973), although the latter term is commonly used to mean the set of space orbitals from which the determinants are constructed.

The equations of Fock (5) and Roothaan (6) are applicable only to closed shell wave functions. For a configuration $\phi_a^2\phi_b^2 \ldots \phi_u\phi_v$, where the orbitals $\phi_a,\phi_b$ are doubly occupied, and $\phi_u,\phi_v$ are singly occupied, then the wave function with the maximum eigenvalues of $\hat{S}^2$ and $\hat{S}_z$ may be written as a single determinant:

$$\Psi = \hat{A}|\phi_a\bar{\phi}_a\phi_b\bar{\phi}_b \ldots \phi_u\phi_v|$$

The energy for this function may be written in terms of two $\underline{R}$ matrices, one for the spin-orbitals of each spin, and the derivation of the Roothaan equations above followed. Two eigenvalue equations are then obtained, (McWeeny and Sutcliffe, 1969):

$$\underline{F}_\alpha\underline{C}_\alpha = \vec{\varepsilon}_\alpha\underline{S}\underline{C}_\alpha$$

$$\underline{F}_\beta\underline{C}_\beta = \vec{\varepsilon}_\beta\underline{S}\underline{C}_\beta$$

where

$$\underline{F}_\alpha = \underline{h} + \underline{J}(\underline{R}_\alpha) - \underline{K}(\underline{R}_\alpha) + \underline{J}(\underline{R}_\beta)$$

$$\underline{F}_\beta = \underline{h} + \underline{J}(\underline{R}_\beta) - \underline{K}(\underline{R}_\beta) + \underline{J}(\underline{R}_\alpha)$$

As the number of α and β spin-orbitals is different, $\underline{R}_\alpha \neq \underline{R}_\beta$ and $\underline{F}_\alpha \neq \underline{F}_\beta$, and so different solutions are obtained for the space parts of $\phi_a$ and $\bar{\phi}_a$. The resulting wave function no longer consists of doubly-occupied orbitals with a common space part, and consequently is no longer an eigenfunction of $\hat{S}^2$. This method is the Unrestricted Hartree-Fock method (Pople and Nesbet 1954, Berthier 1954); as the resulting wave functions are not eigenfunctions of $\hat{S}^2$, nor are suitable wave functions readily obtained from them, this method is not considered further.

It is usual to constrain the wave function such that the closed shell spin orbitals fall into pairs with the same space part. This is the Restricted Hartree-Fock method, and the wave function naturally splits into open- and closed-shell parts. The difficulty in performing open-shell calculations lies in the transformation whereby equation (3) becomes equation (4), casting the problem into pseudo-eigenvalue form. For a closed-shell wave function, all the orbitals are doubly occupied, and a unitary transformation among the orbitals leaves the wave function invariant. However in an open-shell wave function there are doubly and singly occupied orbitals, and although the wave function is invariant to unitary transformations within these blocks, it is not invariant to transformations which mix singly and doubly occupied orbitals.

The energy of an open shell wave function, where i and j are orbitals in shells I and J is:

$$E = 2 \sum_{i,I} f_I \, \epsilon_i^N + \sum_{I,J} \sum_{i,j} f_I f_J \, (2a_{IJ} J_{ij} - b_{IJ} K_{ij}) \qquad (9)$$

Here $f_I$ is the fractional occupation of shell I, and $a_{IJ}$ and $b_{IJ}$ are characteristic of the interaction between shells I and J. For a closed shell c, $f_c=1$, $a_{cc}=b_{cc}=a_{Ic}=b_{Ic}=1$. If the orbitals are again expanded in the basis $\{\chi\}$, then a density matrix $\underline{R}_I$ may be defined for each shell:

$$(R_I)_{pq} = \sum_i C^*_{pi} \, C^*_{qi}$$

The energy expression is now:

$$E = 2 \sum_I f_I \, \underline{R}_I : \underline{h} + \sum_{IJ} f_I f_J \underline{R}_I : (2a_{IJ} J - b_{IJ} K) : \underline{R}_J$$

where $J_{pqrs} = \langle pr|\hat{g}|qs \rangle$ and $K_{pqrs} = \langle ps|\hat{g}|rq \rangle$. Defining:

$$\underline{G}_I = \sum_J f_J (2a_{IJ} J - b_{IJ} K) : R_J \quad ,$$

small variations in the $\underline{R}$ matrices give:

$$\delta E = 2 \sum_I f_I \underline{\delta R}_I : (h+G_I) = 2 \sum_I f_I \underline{\delta R}_I : \underline{F}_I$$

This expression is very similar to equation (7), there now being one Fock matrix per shell. However the minimisation procedures may not be carried out independently, as this does not ensure orthogonality between the orbitals of different shells. It is not therefore clear that the condition for a stationary energy may be expressed as a set of eigenvalue equations. Various solutions to the open-shell problem have been proposed, and the more widely-used techniques have been reviewed by Todd (1972), who discussed the applicability and convergence characteristics of the methods.

In Roothaan's method the open-shell problem is obviated by the use of coupling operators $\hat{L}_o$ and $\hat{L}_c$ such that the problem reduces to two eigenvalue equations

$$\hat{F}_c \phi_i = \varepsilon_i \phi_i$$

$$\hat{F}_o \phi_u = \varepsilon_u \phi_u$$

where $\hat{F}_c$ and $\hat{F}_o$ are the usual Fock operators modified by the coupling operators. The method was originally formulated by Roothaan (1960), and later extended by Roothaan and Bagus (1963) and by Bagus (unpublished), to include all possible open-shell wave functions with energy expressions of the form given in equation (9). A derivation of the method is given in both operator and matrix form in Appendix A. It is the method used in the computer programme ALCHEMY.

1.1.8 Relativistic Effects

There are several defects in the analytical self-consistent field theory described above, and these are now discussed in turn. In the Schrödinger equation as defined in equation (2) relativistic terms are omitted, and only electrostatic terms are considered. This error has been treated by Fröman (1958), Hartmann and Clementi (1964) and Walker (1971) by perturbation theory, and is found to be large in absolute terms. Thus in Ar the relativistic energy is approximately -1.8 a.u., which is about 0.3% of the total energy.

This energy is an order of magnitude higher than a typical electronic excitation energy. However in most calculations it is the energy differences with rearrangement of valence electrons that is studied, and as by far the largest part of the relativistic energy is associated with the core electrons, it is generally assumed that relativistic effects have negligible chemical significance (Schwenzer et al. 1973). However relativistic effects are much more important in investigations of inner-shell ionisations.

1.1.9 Choice of Basis Set

In the calculation of molecular wave functions it is usual to expand the molecular orbitals in a finite basis set. This is not true for the calculation of atomic wave functions, where the simplification of spherical symmetry renders the direct numerical solution of the Hartree-Fock equations a practical alternative. Such numerical calculations are described in Chapter 4. To represent molecular orbitals well, it is necessary to choose the basis functions carefully. Clearly the larger the number of basis functions used, the more closely the orbitals will approach the optimum for the type of wave function under consideration. However, the time required to perform a calculation also depends critically on the size of the basis set. For a basis set of m functions, there are $N_1 = \frac{1}{2}m(m+1)$ one-electron integrals, and $N_2 = \frac{1}{2}N_1(N_1+1)$ two-electron integrals to be calculated. This number may in practice be reduced by symmetry or other considerations, but nevertheless it increases very rapidly with m. For a calculation on ScF using 40 basis functions, 156,896 two-electron integrals were evaluated. It is clearly not possible to use an arbitrarily large basis set.

Basis sets must be chosen on two criteria. They must be able to represent well the form of the orbitals, and also lead to integrals which can be readily evaluated. It is therefore usual to choose functions which resemble the exact solutions for the hydrogen atom; they are centred on the nuclei, and are separable into an angular part which is a spherical harmonic, and a radial part which tends to zero as $r \to \infty$. A functional form which has been found to

be particularly suitable for atomic wave functions is the Slater-type orbital (Slater 1930):

$$\chi_{nlm}(r,\theta,\phi) = Y_{lm}(\theta,\phi)\,\frac{(2\zeta)^{n+\frac{1}{2}}}{\sqrt{(2n)!}}\,r^{n-1}\,e^{-\zeta r} \qquad (10)$$

where $Y_{lm}$ represents a spherical harmonic. For L=n-1, this function is the hydrogen-like function with $\zeta$=Z/n, and for lower l values it is the eigenfunction of the effective radial potential

$$V(r) = -\frac{\zeta n}{r} + \frac{n(n-1) - l(l+1)}{2r^2}$$

Hartree-Fock atomic orbitals are often well represented by a linear combination of two to four Slater functions. Atomic orbitals could provide a suitable basis set for the calculation of wave functions, but when the atomic orbitals are expanded as Slater-type functions, it is usual to employ the basis functions which are suitable for representing the atomic orbitals, and to retain them independently. In this way variations in the electron distribution between atoms and molecules, and between the different molecular states, are better allowed for. This differs from the common practice of using 'contracted Gaussians', in which the basis functions are fixed linear combinations of Gaussian-type orbitals. In calculations using Slater-type functions, the time required for SCF iterations is not generally rate-determining and it is possible to retain the basis functions independently.

There are two approaches to the selection of a basis set for a molecular calculation. Either the exponents ($\zeta$ in equation (10)) may be carefully optimised by the variational principle, and wave functions of comparable quality obtained from relatively small basis sets (see e.g. Cade and Huo 1967), or alternatively a larger basis set may be employed, but without any exponent optimisation (see e.g. Clementi 1967). For the calculation of individual energies, the former method is undoubtedly preferable. However, in the work presented in this thesis, calculations are performed for given

molecules at various internuclear distances and for various electronic states. If the technique of using a small, highly optimised set were adopted, then the optimisation would have to be carried out for each distance and state. The procedure used in the calculations in this thesis is that recommended by Clementi (1967). A set of functions centred on each atom is chosen which represents well the atomic wave function. This may be one of the sets given by Clementi (1967), or by Bagus (1972, unpublished). Functions of higher n or l quantum number are then added to allow for the polarisation caused by molecule formation; thus 2p functions are added on hydrogen, and 4p and 4f functions on transition metals. Where these polarisation functions make a large contribution to the wave function, their exponents may be optimised. Current procedures for exponent optimisation are rather inefficient, trial and error being the most common technique in published sets. More sophisticated techniques are not generally available, and in the present work, where only one or two exponents are optimised, trial and error has been used.

One added advantage in the use of the same basis set for all the calculations on a given molecule is that the calculation of perturbation matrix elements between states is virtually impossible if the wave functions are constructed in different bases. Although no such matrix elements are not computed in this work, it is hoped that it may be possible to evaluate these elements in the future.

1.1.10 Correlation Energy

A further error in the analytical Hartree-Fock method arises from the truncation of the expansion of the wave function in spin eigenfunctions after the first term. The method does describe interelectronic repulsion, since the Fock operator for one electron contains a term due to the averaged effect of all other electrons. However this does not reflect the instantaneous correlation of the electronic positions. For a Hartree-Fock wave function, the probability of finding two infinitesimal volume elements occupied by two

electrons of opposite spin is simply the product of each element being occupied independently. This is a defect in the method, since the electrons repel each other, and the probability of finding two in the same volume element simultaneously would be expected to be reduced below that for independent particles. Some correlation is introduced for electrons of the same spin, due to the antisymmetry of the wave function, which prevents two electrons of the same spin simultaneously occupying the same volume element.

The difference between the Hartree-Fock energy and the energy expectation value of the exact solution of the non-relativistic Schrödinger equation is called the correlation energy, and is not accounted for by any wave function which consists of a single spin eigenfunction. The simplest approach to the correlation energy problem is to choose a wave function which explicitly includes the interelectronic separation. This technique has been used very successfully for two electron atoms (Hylleraas 1929, Pekeris 1959), but has proved extremely difficult to extend to systems more complicated than the $H_2$ molecule.

A great proportion of the attempts to compute wave functions which include electron correlation have been based on the expansion in equation (5) where the wave function is a linear combination of Slater determinants. The wave function may be written as a sum of spin eigenfunctions, all having the same eigenvalues of all the operators commuting with the hamiltonian, as the matrix element of the hamiltonian between two functions having different eigenvalues of an operator which commutes with the hamiltonian is zero.

$$\Psi = \sum_m a_m \Phi_m$$

Each $\Phi$ is a linear combination of Slater determinants from the same configuration, with varying spin parts. The configurations are constructed from a set of space orbitals $\{\phi\}$ (which must contain more orbitals than are required for the total number of electrons). Full optimisation of this wave function requires simultaneous optimisation of the coefficients $a_m$ and the orbitals $\{\phi\}$.

The orbitals $\{\phi\}$ are generally expanded in a basis set $\{\chi\}$, and the condition for stationary energy leads to matrix equations which are not easy to solve. Methods for performing such calculations have been described (e.g. Das and Wahl 1972), and have obtained good results, but there can be severe problems in getting the method to converge. This method is generally referred to as multi-configuration SCF.

A more common procedure is to choose a fixed set of orbitals $\{\phi\}$, and then optimise only the coefficients $a_m$. This is the method of configuration interaction, and the set $\{\phi\}$ is often chosen to be the set of solutions of the Hartree-Fock equations, including the virtual orbitals. If this full set is used, and all the possible $\Phi_m$ are constructed, then the best possible energy for the basis set is obtained (the 'basis set limit'). However, this is a very lengthy process; for five electrons and ten basis functions, the number of linearly independent terms with $S=M_S=\frac{1}{2}$ is 3300. Truncation of the expansion is clearly necessary, though unfortunately the convergence of the process appears to be very slow, and there is no guarantee that the 'lowest' virtual orbitals provide the most rapidly convergent expansion.

Perturbation theory indicates that the most likely contributors to the wave function are those configurations which correspond to double replacements of the SCF spin-orbitals. Brillouin (1933) showed that configurations differing from a closed-shell SCF determinant by a single spin-orbital have no first-order contribution to the wave function. Furthermore, the electron density, and hence all one-electron properties, are unaffected to first order by the inclusion of double replacements, being altered only by single replacements. Thus one-electron properties for closed-shell molecules are correct to first order.

### 1.1.11 Computer Programmes

Three computer programmes have been used in the work described in this thesis. Molecular electronic wave functions have been calculated using the ALCHEMY programme (Bagus 1971), which calculates analytical Hartree-Fock wave

functions for linear molecules using Roothaan's open-shell method. It employs a basis set of Slater type orbitals, and requires trial eigenvectors as input data. The output consists of the energy, virial coefficient, eigenvectors, Mulliken population analysis, and one-electron expectation values. It also performs configuration interaction calculations, using virtual orbitals to construct excited states.

Spectroscopic constants have been obtained from the calculated potential energy curves using the programme MCFIT, written by Todd (1967). This programme employs a method of fitting points to a Morse function; this method has the merit of being relatively insensitive to the choice of points, provided that they do not lie too far up the left arm of the curve, where the Morse function is known to be inadequate. The programme requires between five and ten points as input data. Use of the MCFIT programme on data from the literature shows that the results obtained by the method are always essentially identical to those obtained by a Dunham analysis or by fitting to a polynomial. Table 1.1 shows the results of analyses of the potential curves of O'Hare and Wahl for NaO, $Li_2^+$ and SeF by MCFIT and by Dunham analysis (O'Hare and Wahl 1972, Henderson et al. 1973, O'Hare 1974). The differences between the methods are not significant in the work described below.

The third programme employed performs numerical calculations on atoms; in principle it can obtain multiconfiguration wave functions, but in this thesis it has been used to calculate the energies of Hartree-Fock wave functions only. Atomic correlation energies are then obtained by comparison of experimental data and calculated energies.

Table 1.1

Spectroscopic Constants from Potential Curves

1) NaO $^2\Sigma^+$ State

| R(a.u.) | E(a.u.) | | Dunham | MCFIT |
|---|---|---|---|---|
| 3.20 | -236.674287 | $r_e$(Å) | 1.95 | 1.95 |
| 3.45 | .689283 | | | |
| 3.70 | .692860 | $\omega_e$($cm^{-1}$) | 519 | 519 |
| 3.87 | .691554 | | | |
| 3.95 | .690266 | $\omega_e x_e$($cm^{-1}$) | 4 | - |

2) NaO $^2\Pi$ State

| R(a.u.) | E(a.u.) | | Dunham | MCFIT[a] | MCFIT[b] |
|---|---|---|---|---|---|
| 2.90 | -236.596262 | $r_e$(Å) | 2.05 | 2.05 | 2.04 |
| 3.20 | .664208 | | | | |
| 3.45 | .689607 | $\omega_e$($cm^{-1}$) | 504 | 502 | 534 |
| 3.70 | .699526 | | | | |
| 3.87 | .700994 | $\omega_e x_e$($cm^{-1}$) | 3 | - | - |
| 3.95 | .700693 | | | | |
| 4.20 | .696987 | | | | |
| 4.45 | .690654 | | | | |
| 4.80 | .679743 | | | | |
| 5.50 | .656693 | | | | |

(a) Omitting points 2.90 and 3.20 a.u.

(b) Including all points.

3) $Li_2^+$ $^2\Sigma_g^+$ State

| R(a.u.) | E(a.u.) | | Dunham | MCFIT |
|---|---|---|---|---|
| 4.75 | -14.70552 | | | |
| 5.05 | .71019 | $r_e$(Å) | 3.14 | 3.14 |
| 5.25 | .71226 | | | |
| 5.75 | .71470 | $\omega_e$($cm^{-1}$) | 254.7 | 254.7 |
| 6.00 | .71485 | | | |
| 6.25 | .71449 | $\omega_e x_e$($cm^{-1}$) | 1.5 | - |

4) SeF $^2\Pi$ State

| R(a.u.) | E(a.u.) | | Dunham | MCFIT |
|---|---|---|---|---|
| 2.90 | -2499.29411 | | | |
| 3.10 | .31725 | $r_e$(Å) | 1.715 | 1.715 |
| 3.24 | .32095 | | | |
| 3.29 | .32053 | $\omega_e$($cm^{-1}$) | 757 | 752 |
| 3.50 | .31217 | | | |
| 3.70 | .29774 | $\omega_e x_e$($cm^{-1}$) | 5 | - |

## 1.2 Transition Metal Diatomic Molecules

### 1.2.1 Introduction

The last two decades have seen a rapid increase of interest in the spectroscopy and electronic structure of diatomic molecules which contain one transition metal atom. There are several reasons why these molecules are important; many of them are of astrophysical interest, and feature strongly in the spectra of cool stars (with temperatures up to 3000$^{o}$K), in particularly stars of types M and S. Because the group also contains some of the most stable diatomic molecules known, they play an important role in high temperature equilibria, and are of great importance in the rocket and space industries. From a theoretical point of view, they represent the simplest systems in which to study the effects of d electrons on bonding. Contributions of d electrons to chemical bonds have been studied mostly in those systems where their overlap with ligand orbitals is either zero or small, as in crystal and ligand field theories. One of the main advantages in studying diatomic molecules to obtain information on d-orbital contributions is the high quality and accuracy of the data obtained from the many line band spectra of the gas phase diatomic molecules in contrast to that obtained from the largely featureless band spectra of polyatomic molecules generally in condensed phases.

### 1.2.2 Experimental Methods

The high lattice energies of the transition metals (M) and their simple salts demand high temperature sources for the observation of the diatomic molecules MH, MX and MO, generally using temperatures of the order of 2000$^{o}$K.

Gas phase electronic spectroscopy has been the most widely used technique in the study of transition metal diatomic molecules. Arcs have been used to obtain emission spectra of hydrides, oxides and halides; hydrides and oxides are obtained in atmospheres of hydrogen and oxygen or air, and halides obtained when one of the electrodes contains solid halide. However, the

method is not without problems; atomic spectra are often excited simultaneously with high intensity, background continua may lead to rather poor contrast, and the rotational temperature may be very high, with the result that rotational structure is developed to very high J values, and there is overlapping of adjacent bands. A further problem is that the Doppler width is proportional to the square root of the temperature, and at very high temperatures the resolution may be limited by the Doppler effect. Flames do not suffer from many of the disadvantages of arcs, though they operate at rather lower temperatures, and give less intensity. They may also consume large amounts of material.

High temperature furnaces have proved a most useful and versatile source of spectra; the King furnace, in which a hollow carbon tube containing the sample is heated in vacuo by passing an electric current through it, is the most common. Only very involatile or reactive species may not be obtained. King furnaces may be used to photograph molecules in emission or absorption, and indeed it is often convenient to obtain both emission and absorption spectra on the same photographic plate. Heating oxides and sulphides produces the corresponding monoxides and monosulphides; monofluorides may be obtained by heating the metal with $AlF_3$, and monohydrides by heating the metal in an atmosphere of hydrogen.

Electrodeless discharges excited by radio-frequency oscillators can give relatively clean spectra; microwave discharges are particularly attractive as they require very small amounts of material. Submilligram quantities may be used, which makes the use of artificially enriched isotopes a possibility (Rao et al. 1962a-c). Hollow cathode discharges have also been used, particularly for exciting the spectra of fluorides (Hayes and Nevin 1955); hollow cathodes have often been used to excite the spectra of ionised molecules, although no transition metal molecule ions have been reported yet.

Techniques in which involatile molecules are studied by producing an environment in which their equilibrium concentration is relatively high are

unable to obtain those molecules at low rotational temperatures. Methods of producing transient high temperatures may be capable of obtaining lower rotational temperatures; flash photolysis, exploding wires and shock heating have been used to excite molecules (Callear and Norrish 1960, Bass et al. 1964).

Optical spectra in principle give information on the symmetries of states, internuclear distances, vibrational frequencies, and term values. Emission spectra may give information about a large number of states, both low-lying and excited, but are often hard to analyse, especially if there is extensive overlapping between different systems. Absorption spectra, which show bands based on only a few very low-lying electronic states, are often more suitable for a preliminary investigation.

In the last decade matrix isolation spectroscopy has proved to be of great value in the study of transition metal diatomic molecules. The molecules are trapped in a matrix of an inert gas at $4^{o}K$, and absorption spectra then give information on the positions of 0-0 transitions, and upper-state vibration frequencies. Ground state vibration frequencies may be observed in the infra-red, or by fluorescence studies, which may also provide information on manifolds of a different multiplicity from the ground state. Electron spin resonance studies of matrix isolated molecules have given important information on the characters of the ground states of odd-electron molecules. Matrix spectra therefore greatly assist in the interpretation of gas phase spectra, which may be too complex to analyse. However, perturbations due to the matrix, which are poorly understood, may reverse the ordering of two low-lying states, and so the ground state in the matrix is not necessarily the gas-phase ground state.

It is not possible to determine the dissociation energies of transition metal diatomic molecules from purely spectroscopic considerations. This is partly because the change in internuclear distance on excitation is generally so small that all the intensity is concentrated in a few bands; long

vibrational progressions are virtually unknown, and as many of the molecules are quite ionic, there is no reason to suppose that long Birge-Sponer extrapolations will be valid. Also the relatively large number of low-lying atomic states means that even when reliable dissociation limits are obtained, the correlation of atomic and molecular states is still uncertain. Dissociation energies have been measured mostly by mass spectrometric studies of high temperature equilibria. However the third-law treatment of such equilibria requires a knowledge of the partition function, and hence the identities and term valences of low-lying electronic states; the uncertainties in these in many cases are quite large.

Small perturbations in gas phase spectra have been used to obtain information on the nature of the electron distribution in transition metal diatomic molecules. Hyperfine structure effects which are large enough to be observed in optical spectra at commonly employed resolutions have been observed in ScO, LaO, VO, NbO and $NbO^+$, and hyperfine effects have also been observed in matrix spectra. The dominant effect seems to be a magnetic one, and large effects occur in molecular ground states where there is an unpaired $\sigma$ electron for which the contact term depending on $\Psi^2(0)$ can be large, i.e. s orbitals and in heavy atoms $p_{\frac{1}{2}}$ orbitals. $\Lambda$-doubling and spin-splitting constants have also been used to interpret the electronic structure of excited states in transition metal diatomic molecules; in ScO the excited $^2\Pi_{\frac{1}{2}}$ and $^2\Sigma^+$ states mutually perturb each other, and the equality of the $\Lambda$-doubling and spin-splitting constants in the two states have been interpreted as evidence that both states have an unpaired $4p$ electron in pure precession. It has not however proved possible to fix the relative positions of different spin manifolds by observation of perturbations between states of different multiplicity; this is probably due to the small differences in B values for the different states in transition metal molecules. As a result of this there is almost no information on the relative energies of states of different multiplicities; temperature coefficients of intensities have been used by

Phillips (1952) on TiO, but the method is not very accurate, and has been little used.

1.2.3 Ab Initio Calculations

Matrix Hartree-Fock calculations on transition metal diatomic molecules were first performed ten years ago. In a series of papers Carlson and co-workers performed small basis set calculations on ScO, ScF, TiO, TiN, VO and $Mn_2$, and these proved to be a reliable source of information on the nature of the ground states of these molecules (Carlson et al. 1965, Carlson and Nesbet 1964, Carlson and Moser 1967, Carlson et al. 1967, Carlson and Moser 1966, Nesbet 1964). They did not seriously consider the nature of any of the excited states. In spite of the success of these calculations, very little work appeared after these early papers. Walker et al. (1972) published a calculation on FeH using a single-centre method, and Bagus and Schaefer (1973) performed a matrix Hartree-Fock calculation on MnH which was much closer to the Hartree-Fock limit. Bagus and Preston (1973) published a configuration interaction calculation on FeO, but was unable to identify the ground state. The calculations presented in this thesis extend the range of calculations on transition metal diatomic molecules, and shed further light on their electronic structure, and the validity of the models used to describe them.

1.2.4 Summary

This section has very briefly introduced the field of transition metal diatomic molecules; it gives an indication of the type of techniques which have been used in the field, and the type of information which may be obtained. It is not appropriate here to discuss any of these techniques in detail, nor to survey the experimental data and discuss electronic structure. This information has been reviewed by several authors. Carlson and Claydon (1967) reviewed theoretical work on many molecules, matrix isolation on molecules of stellar interest was discussed by Weltner (1967), transition metal monosulphides have been discussed by Barrow and Cousins (1971), nuclear hyperfine effects were reviewed by Barrow (1971) in an article on transition metal

monoxides, and a general survey, including a comprehensive compilation of data, was given by Cheetham and Barrow (1967). More recent compilations of experimental data have been given by Rosen (1970) and Barrow (1973), and bibliographies of calculations by Richards et al. (1971, 1974).

## Chapter 2

## ENERGY LEVELS IN LINEAR MOLECULES


| | Page No. |
|---|---|
| 2.1 Introduction | 28 |
| 2.2 The Model | 29 |
| 2.3 Notation | 33 |
| 2.4 Configurations with 2 Open-Shell Electrons | 36 |
| 2.4.1 The Configuration $\sigma_1\sigma_2$ | 36 |
| 2.4.2 The Configuration $\pi^2$ | 36 |
| 2.4.3 The Configuration $\pi_1\pi_2$ | 37 |
| 2.4.4 The Configuration $\pi\delta$ | 38 |
| 2.5 Configurations with 3 Open-Shell Electrons | 41 |
| 2.5.1 The Configuration $\sigma_1\sigma_2\pi$ | 41 |
| 2.5.2 The Configuration $\pi^2\sigma$ | 41 |
| 2.5.3 The Configuration $\pi_1\pi_2\sigma$ | 43 |
| 2.5.4 The Configuration $\pi_1^2\pi_2$ | 45 |
| 2.5.5 The Configuration $\pi^2\delta$ | 45 |
| 2.5.6 The Configuration $\delta^2\pi$ | 47 |
| 2.5.7 The Configuration $\sigma\pi\delta$ | 47 |
| 2.6 Configurations with more than 3 Open-Shell Electrons | 51 |
| 2.6.1 Configurations with more than half-filled shells | 51 |
| 2.6.2 The Configuration $\pi_1^3\pi_2$ | 52 |
| 2.6.3 The Configuration $\pi^3\delta$ | 54 |
| 2.6.4 The Configuration $\sigma\pi^3\delta$ | 54 |
| 2.6.5 The Configuration $\sigma\pi_1^3\pi_2$ | 56 |
| 2.7 Conclusions | 57 |

## Figures


Page No.

Figure 2.1 Energy Differences in the Invariant Orbital Approximation 31

Figure 2.2 The Configuration $\pi_1\pi_2$ 39

Figure 2.3 The Configuration $\pi\delta$ 40

Figure 2.4 The Configuration $\sigma_1\sigma_2\pi$ 42

Figure 2.5 The Configuration $\pi^2\sigma$ 44

Figure 2.6 The Configuration $\pi_1\pi_2\sigma$ 46

Figure 2.7 The Configuration $\pi^2\delta$ 48

Figure 2.8 The Configuration $\sigma\pi\delta$ 50

Figure 2.9 The Configuration $\pi_1^3\pi_2$ 53

Figure 2.10 The Configuration $\pi^3\delta$ 55

## 2.1 Introduction

When a spectroscopist attempts to assign observed molecular band systems to states from an open-shell configuration, there are tables which show which states may arise from that configuration (see e.g. Herzberg 1950). However, these tables give no indication of the relative energies of the states, and it is common practice to use an extended form of Hund's rules. The practice has no theoretical justification, and can often lead to erroneous interpretations, even for the lowest state.

In their original form, Hund's rules were empirical observations, and stated that for atomic configurations of equivalent electrons, the state of lowest energy is that with the highest spin multiplicity, and that if there are several such states, then the lowest state is that with the highest value of the L quantum number (Hund, 1925). These rules have often been extended, without explicit justification, to linear molecules; the second rule is modified to predict that for a given multiplicity, the state with the higher value of the quantum number $\Lambda$ is that with lowest energy. It is also commonly assumed that the rules apply to configurations of non-equivalent electrons, and to states of less than maximum multiplicity. In this work (Raftery *et al.* 1972, Scott *et al*. 1973a, 1973b) the generality of these extensions is investigated, and more rigorous criteria for the labelling of observed states are deduced.

## 2.2 The model

The model employed in these calculations is essentially an invariant orbital approximation. The wave functions of the states considered are assumed to be anti-symmetrized products, that is Slater determinants, of spin-orbitals, chosen to be eigenfunctions of $\hat{S}^2$, the total spin angular momentum operator, and of $\hat{L}_z$, the component of the orbital angular momentum along the molecular axis. For $\Sigma$ states, the wave functions are also eigenfunctions of the reflection operator. Methods for obtaining suitable wave functions are given by Richards and Horsley (1971). When these orbitals are chosen to minimize the expectation value of the energy, according to the variation principle, then this becomes the Hartree-Fock approximation. However, no particular form is assumed for the orbitals, and the results are valid for all sets of orbitals, including the Hartree-Fock orbitals. It is further assumed that for a given configuration, the orbitals remain unchanged from one state to another. The energies of the states are then deduced, by Slater's rules, using the non-relativistic electronic hamiltonian, and appear as functions of one-electron core integrals, and two-electron coulomb and exchange integrals. Slater's rules for evaluating matrix elements $\langle \psi_a | H | \psi_b \rangle$ between Slater determinants are given below, in section 2.3. The differences in energies between the states are then obtained in terms of coulomb and exchange integrals; using relationships between the magnitudes of these integrals, it is often possible to deduce the ordering of the states.

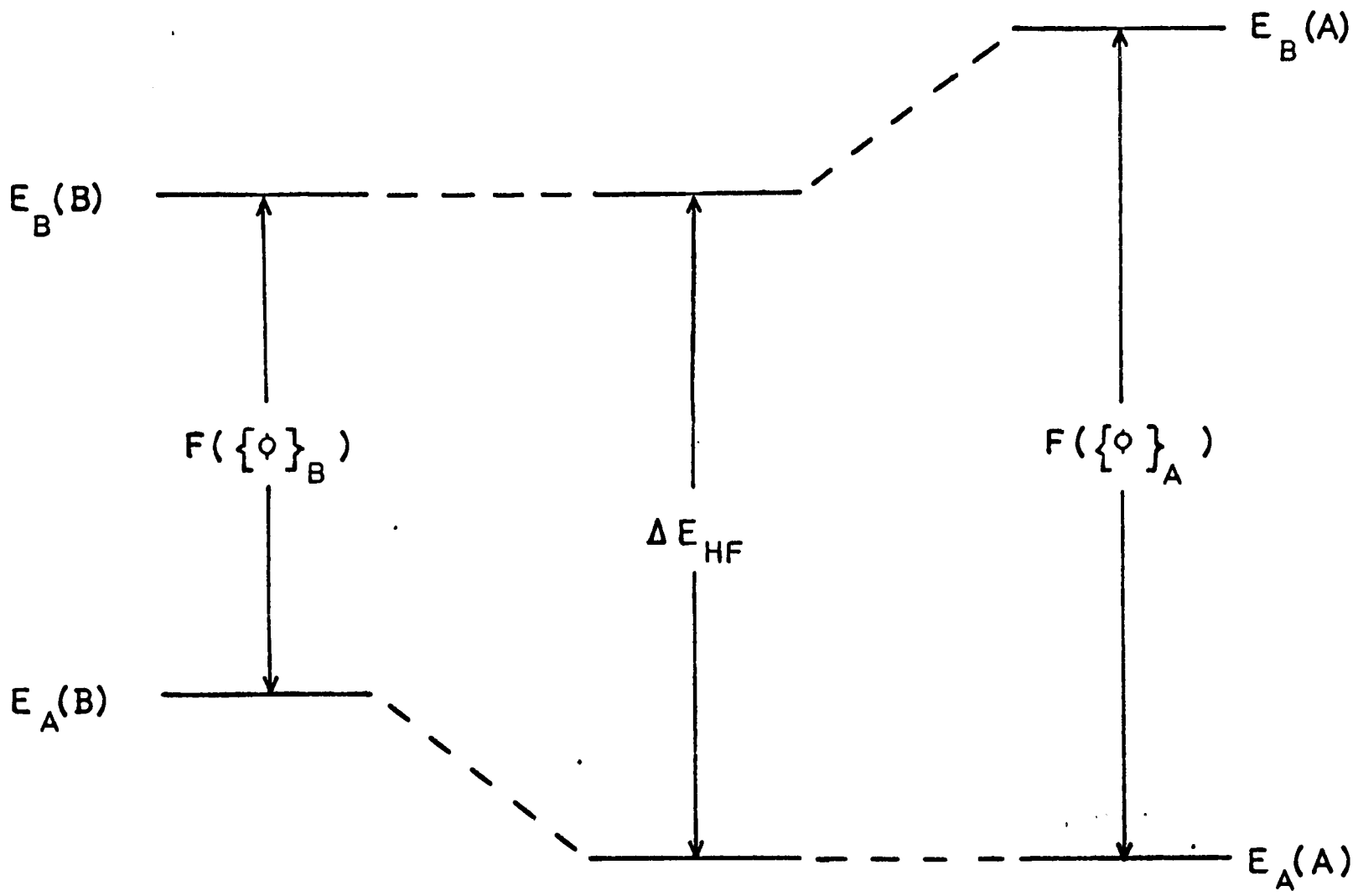
Before the results of the calculations are presented it is appropriate to discuss the limitations of the model. Firstly, the model neglects the effects of electron correlation, as indeed must any model in which meaning is attached to the term 'electron configuration'. The effects of electron correlation are generally small for low-lying states, except in cases where near-degeneracy may be important. In such cases, two different configurations give rise to states of the same symmetry at similar energies, and then

deviations from the simple rules presented below may well be observed. The best known example of the importance of near-degeneracy effects is in the breaking of Hund's first rule in the Mg atom. The configuration [Ne]3s3d gives rise to two states, $^3D$ and $^1D$, and the singlet is found to lie lower than the triplet. This has been attributed to the near-degeneracy of the configuration [Ne]3s3d with the configuration [Ne]$3p^2$, which gives rise to the states $^3P$, $^1D$ and $^1S$. The $^1D$ states interact, giving a $^1D$ state whose wave function is a linear combination [Ne]3s3d and Ne[$3p^2$], and which has a correspondingly lower energy.

A second limitation is the invariance of the orbitals between different states of the same configuration. In this model the differences in energies between the states arise from changes in the electron repulsion terms; the electron-nuclear attraction and kinetic energy terms are the same for all the states. Recent studies by Colpa and Islip (1973) and Colbourn (1973) on several atomic and molecular systems have shown that in many cases the largest contribution to the energy differences is from the electron-nuclear attraction, and that the change in electron-electron repulsion is of the opposite sign to that predicted by the invariant orbital model. It has been suggested (Colpa and Islip 1973) that this could cast doubts on calculations of the type presented below, but fortunately this is not the case.

Suppose that a given configuration may give rise to two electronic states of different symmetries A and B, and that the invariant orbital model predicts that the energies of these states should differ by an amount $F(\{\phi\})$, where F is a function of the set of orbitals $\{\phi\}$ used to construct the wave function. In many cases given below it is possible to show that F is necessarily positive, whatever $\{\phi\}$ is used; in this case B would be predicted to lie above A. Now if we take $\{\phi\}$ to be the set of Hartree-Fock orbitals for B, $\{\phi_B\}$, then the energy difference between the states will be $F(\{\phi_B\})$. If we now substitute the Hartree-Fock orbitals for A, $\{\phi_A\}$, into the wave function for A, then this will lower the energy of A, as the Hartree-Fock orbitals by definition give

Figure 2·1·




Energy Differences in the Invariant Orbital Approximation.

a lower energy than any other set. The energy difference between A and B is now the Hartree-Fock energy difference, as both states are described by their respective Hartree-Fock orbitals. Now if the energy of B is calculated using $\{\phi_A\}$, it must similarly be greater than that calculated using $\{\phi_B\}$, and the difference between it and the energy of A is $F(\{\phi_A\})$. This is shown in Figure 2.1. Thus:

$$F(\{\phi_B\}) \leqslant \Delta E_{HF} \leqslant F(\{\phi_A\}) \qquad (1)$$

and any conclusion about the magnitude of F which is true for all $\{\phi\}$ must also be true for $\Delta E_{HF}$.

The explanation of the results of Colpa and Colbourn is as follows. On changing from one state to another, the orbitals undergo a slight change in size; this produces a very small change in the total energy, but produces rather larger changes in the separate components of the energy, the electron repulsion, electron-nuclear attraction and kinetic energy terms. These changes are typically of comparable magnitude to the change in electron repulsion due to the change in electron coupling, and of course the changes in electron repulsion due to change in size and change of coupling have opposite signs. It therefore may happen that the change in electron repulsion is very small, and not necessarily of the expected sign. However, this does not mean that the invariant orbital model does not give a good representation of the states; the inequalities in (1) still hold, and typically the quantities involved in that inequality are very similar. In a calculation on the singlet and triplet $\Delta$ states in CuF, the singlet-triplet splitting was calculated to be 0.0106 a.u. using the singlet orbitals, and 0.0127 a.u. using the triplet orbitals. The Hartree-Fock splitting was 0.0116 a.u.

## 2.3 Notation

The wave functions are represented as Slater determinants of orbital products; a bar over an orbital signifies β spin. Only the open-shell spin-orbitals are explicitly shown, and degenerate orbitals are shown in their complex form (e.g. $\pi^{+},\delta^{2-}$).

The energies are expressed in terms of coulomb and exchange integrals, which are defined as follows:

$$J_{ij} = \langle \phi_i(1)\phi_j(2)|\frac{1}{r_{12}}|\phi_i(1)\phi_j(2)\rangle = \iint \phi_i^*(1)\phi_i(1)\phi_j^*(2)\phi_j(2)\,\frac{1}{r_{12}}\,d\tau_1 d\tau_2$$

$$K_{ij} = \langle \phi_i(1)\phi_j(2)|\frac{1}{r_{12}}|\phi_j(1)\phi_i(2)\rangle = \iint \phi_i^*(1)\phi_j(1)\phi_i(2)\phi_j^*(2)\,\frac{1}{r_{12}}\,d\tau_1 d\tau_2$$

For degenerate orbitals, different types of integral may be distinguished, depending on the relative phases of the orbitals. If a complex orbital is written as $\pi_i\, e^{i\phi}$, where $\pi_i$ is real, then:

$$J^0_{\pi_i\pi_j} = \iint \pi_i(1)e^{-i\phi_1}\pi_i(1)e^{i\phi_1}\pi_j(2)e^{-i\phi_2}\pi_j(2)e^{i\phi_2}\,\frac{1}{r_{12}}\,d\tau_1 d\tau_2$$

$$= \iint \pi_i(1)\pi_i(1)\pi_j(2)\pi_j(2)\,\frac{1}{r_{12}}\,d\tau_1 d\tau_2 = J_{\pi_i^+\pi_j^+} = J_{\pi_i^+\pi_j^-} = J_{\pi_i^-\pi_j^+} = J_{\pi_i^-\pi_j^-}$$

$$J^2_{\pi_i\pi_j} = \iint \pi_i(1)e^{i\phi_1}\pi_i(1)e^{i\phi_1}\pi_j(2)e^{-i\phi_2}\pi_j(2)e^{-i\phi_2}\,\frac{1}{r_{12}}\,d\tau_1 d\tau_2$$

$$= \iint \pi_i(1)\pi_i(1)\pi_j(2)\pi_j(2)\,e^{2i(\phi_1-\phi_2)}\,\frac{1}{r_{12}}\,d\tau_1 d\tau_2$$

$$K^0_{\pi_i\pi_j} = \iint \pi_i(1)e^{-i\phi_1}\pi_j(1)e^{i\phi_1}\pi_i(2)e^{i\phi_2}\pi_j(2)e^{-i\phi_2}\,\frac{1}{r_{12}}\,d\tau_1 d\tau_2$$

$$= \iint \pi_i(1)\pi_j(1)\pi_i(2)\pi_j(2)\,\frac{1}{r_{12}}\,d\tau_1 d\tau_2 = K_{\pi_i^+\pi_j^+} = K_{\pi_i^-\pi_j^-}$$

$$K^2_{\pi_i\pi_j} = \iint \pi_i(1)e^{i\phi_1}\pi_j(1)e^{i\phi_1}\pi_i(2)e^{-i\phi_2}\pi_j(2)e^{-i\phi_2}\frac{1}{r_{12}}d\tau_1 d\tau_2$$

$$= \iint \pi_i(1)\pi_j(1)\pi_i(2)\pi_j(2)e^{2i(\phi_1-\phi_2)}\frac{1}{r_{12}}d\tau_1 d\tau_2 = K^{+-}_{\pi_i\pi_j} = K^{-+}_{\pi_i\pi_j} .$$

For $\delta\delta$ integrals, $J^0$, $J^4$, $K^0$ and $K^4$ may similarly be defined, and for $\pi\delta$ integrals, $J^0$, $K^1$ and $K^3$.

Slater's rules for obtaining matrix elements $\langle\psi_A|H|\psi_B\rangle$ between determinants are given below. Four separate cases are considered. If $\psi_A = \psi_B$, then if $\psi_A = |\phi_1^2\phi_2^2 \ldots \phi_n|$,

$$\langle\psi_A|H|\psi_B\rangle = \sum_{k=1} \varepsilon_k^N + \sum_{kl} J_{kl} - \sum_{kl}' K_{kl}$$

where the summation is over electrons and electron pairs, and the primed summation indicates summation only over electron pairs of the same spin.

If $\psi_A$ and $\psi_B$ differ by one spin-orbital, such that $\psi_A = |\phi_1^2\phi_2^2 \ldots \phi_k|$ and $\psi_B = |\phi_1^2\phi_2^2 \ldots \phi_l|$, then

$$\langle\psi_A|H|\psi_B\rangle = \varepsilon^N_{kl} + \sum_m \zeta^{kl}_{mm} - \sum_m' \zeta^{km}_{lm}$$

where the primed sum indicates summation only over pairs of electrons of the same spin, and $\varepsilon^N_{kl} = \int \phi_k H^N \phi_l \, dv$.

If $\psi_A$ and $\psi_B$ differ by two spin-orbitals, such that $\psi_A = |\phi_1^2\phi_2^2 \ldots \phi_k\phi_p|$ and $\psi_B = |\phi_1^2\phi_2^2 \ldots \phi_l\phi_q|$, then

$$\langle\psi_A|H|\psi_B\rangle = \zeta^{kl}_{pq} - \zeta^{kq}_{pl}$$

These terms will only both be non-zero if all four spin-orbitals have the same spin.

If $\psi_A$ and $\psi_B$ differ by more than two spin-orbitals, then the matrix element between them will be zero.

Given Slater's rules it is possible to evaluate energy expressions for the states considered below from their wave functions. One problem which remains is that certain configurations give rise to two or more states of

the same symmetry. In these cases it is necessary to construct appropriate combinations of determinants for which the energy is minimised. The energies are found by taking appropriate simple basis determinants which are eigenfunctions of $\hat{S}^2$; particularly simple examples are given by Richards and Horsley (1971). The energy is then minimised with respect to variation in the coefficients of the determinants by diagonalising the matrix of the hamiltonian. In such cases the wave function has a rather complex form, and is not given below.

Several inequalities are useful in comparing the energy expressions for different states; proofs of some of these inequalities have appeared in a paper by Power and Pitzer (1974). For any i, j,

$$J^n_{ij} > K^n_{ij}$$

unless i=j, when $J^n_{ii} = K^n_{ii}$

Furthermore $J^0_{ij} > J^n_{ij}$

where n=2 for $\pi$ orbitals and 4 for $\delta$ orbitals. A similar relationship exists for K integrals, $K^n_{ij} > K^{n+m}_{ij}$

where m is positive. It may also be shown that all J and K integrals are necessarily greater than zero. One inequality which is also useful in comparing energy expressions is:

$$K^0_{ij} > J^2_{ij}$$

This inequality may not be proved analytically, but a large number of ab initio molecular orbital calculations have shown that it is almost always obeyed. One calculation has been published where the inequality did not hold, on some excited repulsive states of AlF (So and Richards 1974). Here the open-shell orbitals were almost entirely localised on different nuclei, and the integrals were so small that all the states were virtually degenerate.

## 2.4 Configurations with Two Open-Shell Electrons

The possible types of configuration with two open-shell electrons, if we consider only $\sigma$, $\pi$ and $\delta$ orbitals, are as follows; $\sigma\sigma'$, $\sigma\pi$, $\sigma\delta$, $\pi\pi'$, $\pi\delta$, $\delta\delta'$, $\pi^2$ and $\delta^2$. Of these, $\pi\pi'$ and $\delta\delta'$, and $\pi^2$ and $\delta^2$, are formally analogous, giving similar energy expressions for corresponding states.

### 2.4.1 The Configuration $\sigma_1\sigma_2$

The configurations $\sigma_1\sigma_2$, $\sigma\pi$ and $\sigma\delta$ each give two states, a singlet and triplet with the same value of $\Lambda$. In each case the triplet is the lower state. The wave functions and energy expressions are given below; only the two-electron terms appear, as the one-electron terms are invariant for a given configuration.

| | | | |
|---|---|---|---|
| $\sigma_1\sigma_2$ | $^3\Sigma^+$ | $\Psi = \lvert\sigma_1\sigma_2\rvert$ | $E = J_{\sigma_1\sigma_2} - K_{\sigma_1\sigma_2}$ |
| | $^1\Sigma^+$ | $\Psi = 1/\sqrt{2}\{\lvert\sigma_1\bar{\sigma}_2\rvert - \lvert\bar{\sigma}_1\sigma_2\rvert\}$ | $E = J_{\sigma_1\sigma_2} + K_{\sigma_1\sigma_2}$ |
| $\sigma\pi$ | $^3\Pi$ | $\Psi = \lvert\sigma\pi^+\rvert$ | $E = J_{\sigma\pi} - K_{\sigma\pi}$ |
| | $^1\Pi$ | $\Psi = 1/\sqrt{2}\{\lvert\sigma\bar{\pi}^+\rvert - \lvert\bar{\sigma}\pi^+\rvert\}$ | $E = J_{\sigma\pi} + K_{\sigma\pi}$ |
| $\sigma\delta$ | $^3\Delta$ | $\Psi = \lvert\sigma\delta^{2+}\rvert$ | $E = J_{\sigma\delta} - K_{\sigma\delta}$ |
| | $^1\Delta$ | $\Psi = 1/\sqrt{2}\{\lvert\sigma\bar{\delta}^{2+}\rvert - \lvert\bar{\sigma}\delta^{2+}\rvert\}$ | $E = J_{\sigma\delta} + K_{\sigma\delta}$ |

These all obey Hund's first rule, with the triplet lying below the singlet by 2K. An example of this ordering is the $\sigma\delta$ configuration in TiO, where the $^3\Delta$ state is estimated to be 600 $cm^{-1}$ below the $^1\Delta$ state (Phillips 1950).

### 2.4.2 The Configuration $\pi^2$

This configuration gives rise to the states $^3\Sigma^-$, $^1\Delta$ and $^1\Sigma^+$. The wave functions and energy expressions are:

$^3\Sigma^-$ $\quad \Psi = |\pi^+\pi^-| \quad E = (J^0 - K^2)_{\pi\pi}$

$^1\Delta$ $\quad \Psi = |\pi^+\bar{\pi}^+| \quad E = J^0_{\pi\pi}$

$^1\Sigma^+$ $\quad \Psi = 1/\sqrt{2}\{|\pi^+\bar{\pi}^-| - |\bar{\pi}^+\pi^-|\} \quad E = (J^0 + K^2)_{\pi\pi}$

The ordering of the states is thus $^3\Sigma^- < {}^1\Delta < {}^1\Sigma^+$, in agreement with the extended forms of Hund's first and second rules. The $\delta^2$ configuration, giving the states $^3\Sigma^-$, $^1\Gamma$ and $^1\Sigma^+$, gives analogous results.

2.4.3 The Configuration $\pi_1\pi_2$

This gives rise to the states $^3\Delta$, $^1\Delta$, $^3\Sigma^+$, $^1\Sigma^+$, $^3\Sigma^-$, and $^1\Sigma^-$. The wave functions and energy expressions are:

$^3\Delta$ $\quad \Psi = |\pi^+_1\pi^+_2| \quad E = (J^0 - K^0)_{\pi_1\pi_2}$

$^1\Delta$ $\quad \Psi = 1/\sqrt{2}\{|\pi^+_1\bar{\pi}^+_2| - |\bar{\pi}^+_1\pi^+_2|\} \quad E = (J^0 + K^0)_{\pi_1\pi_2}$

$^3\Sigma^+$ $\quad \Psi = 1/\sqrt{2}\{|\pi^+_1\pi^-_2| + |\pi^-_1\pi^+_2|\} \quad E = (J^0 + J^2 - K^0 - K^2)_{\pi_1\pi_2}$

$^3\Sigma^-$ $\quad \Psi = 1/\sqrt{2}\{|\pi^+_1\pi^-_2| - |\pi^-_1\pi^+_2|\} \quad E = (J^0 - J^2 + K^0 - K^2)_{\pi_1\pi_2}$

$^1\Sigma^+$ $\quad \Psi = \tfrac{1}{2}\{|\pi^-_1\bar{\pi}^+_2| - |\bar{\pi}^-_1\pi^+_2| + |\pi^+_1\bar{\pi}^-_2| - |\bar{\pi}^+_1\pi^-_2|\}$

$\quad E = (J^0 + J^2 + K^0 + K^2)_{\pi_1\pi_2}$

$^1\Sigma^-$ $\quad \Psi = \tfrac{1}{2}\{|\pi^-_1\bar{\pi}^+_2| - |\bar{\pi}^-_1\pi^+_2| - |\pi^+_1\bar{\pi}^-_2| + |\bar{\pi}^+_1\pi^-_2|\}$

$\quad E = (J^0 - J^2 - K^0 + K^2)_{\pi_1\pi_2}$

Using the relationships between the integrals $J^0 > J^2$, $K^0 > K^2$, $J^2 > K^2$ and $J^0 > K^0$,

and assuming that $K^0$ is appreciably larger than $J^2$, the following general conclusions may be made.

The ordering of the states is not that which would be expected from Hund's rules; the $^1\Sigma^-$ state is that of lowest energy, contrary to the rules of maximum multiplicity and maximum $\Lambda$. However the positions of the other singlet and triplet pairs, and of the $\Sigma^+$ and $\Delta$ states, do conform to these rules. The ordering is shown in Figure 2.2. This ordering is, as far as is known, that of the experimentally observed states of the $\pi_u^3\pi_g^3$ configuration of $O_2$ (Rosen 1970). The $\delta_1\delta_2$ configuration, giving $^3\Gamma$, $^1\Gamma$, $^3\Sigma^\pm$ and $^1\Sigma^\pm$ states, gives analogous results.

2.4.4 The Configuration $\pi\delta$

This configuration gives rise to four states, $^3\Phi$, $^3\Pi$, $^1\Phi$ and $^1\Pi$. The wave functions and energy expressions are:

$$^3\Phi \qquad \Psi = |\pi^+\delta^{2+}| \qquad E = (J^0-K^1)_{\pi\delta}$$

$$^1\Phi \qquad \Psi = 1/\sqrt{2}\{|\pi^+\bar{\delta}^{2+}|-|\bar{\pi}^+\delta^{2+}|\} \qquad E = (J^0+K^1)_{\pi\delta}$$

$$^3\Pi \qquad \Psi = |\pi^-\delta^{2+}| \qquad E = (J^0-K^3)_{\pi\delta}$$

$$^1\Pi \qquad \Psi = 1/\sqrt{2}\{|\pi^-\bar{\delta}^{2+}|-|\bar{\pi}^-\delta^{2+}|\} \qquad E = (J^0+K^3)_{\pi\delta}$$

As $K^1>K^3>0$, the ordering of the states is $^3\Phi<^3\Pi<^1\Pi<^1\Phi$, as shown in Figure 2.3. The triplets therefore follow the second rule, although the singlets do not; the first rule is obeyed by both the $\Phi$ and $\Pi$ states. It is interesting to note that the ordering of these states is incorrectly predicted by Brewer and Green (1969) in the molecule ScF, where the unobserved $^1\Phi$ state is said to lie below the observed $^1\Pi$ state.

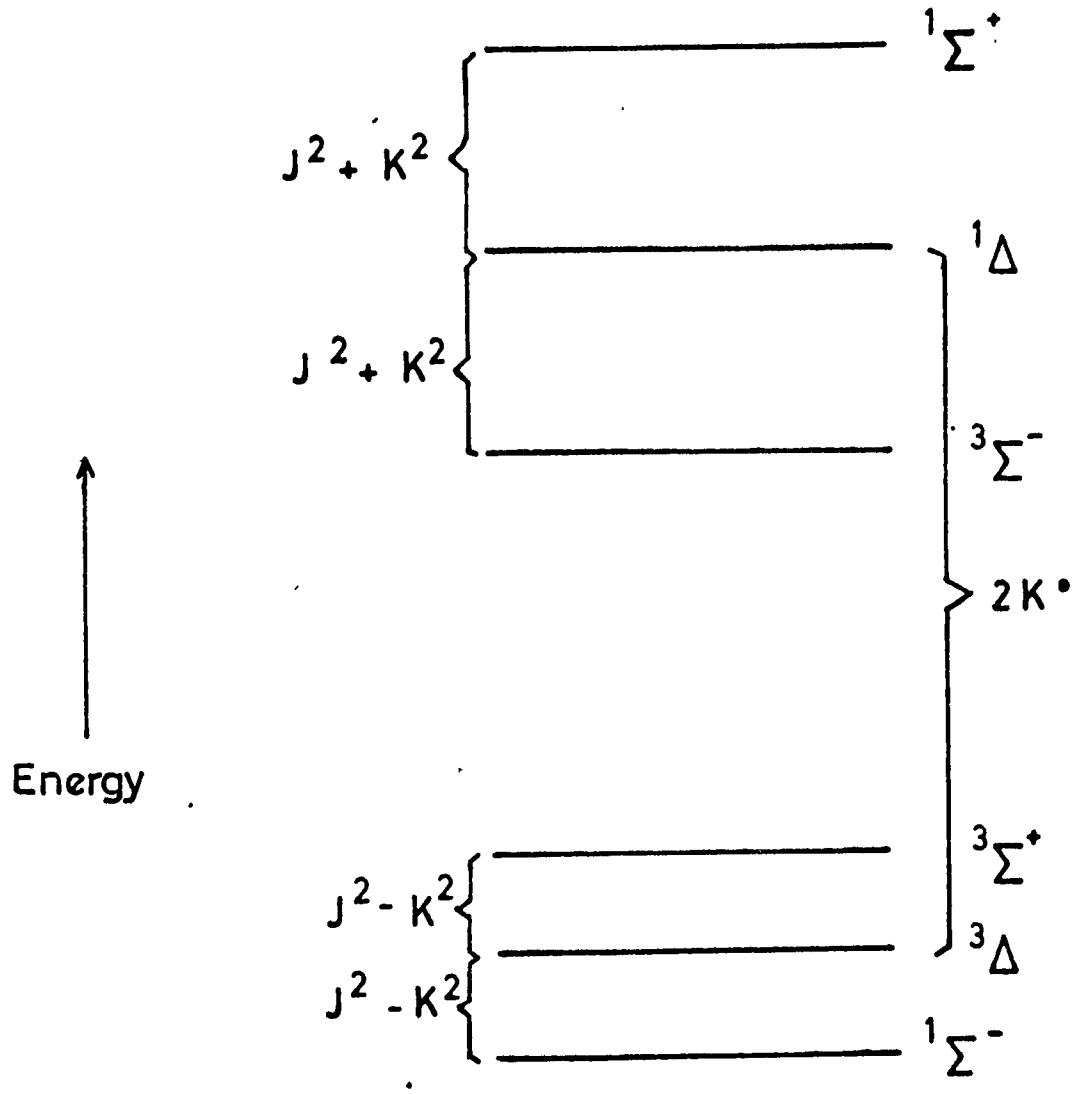



Figure 2.2.

The Configuration $\pi_1 \pi_2$

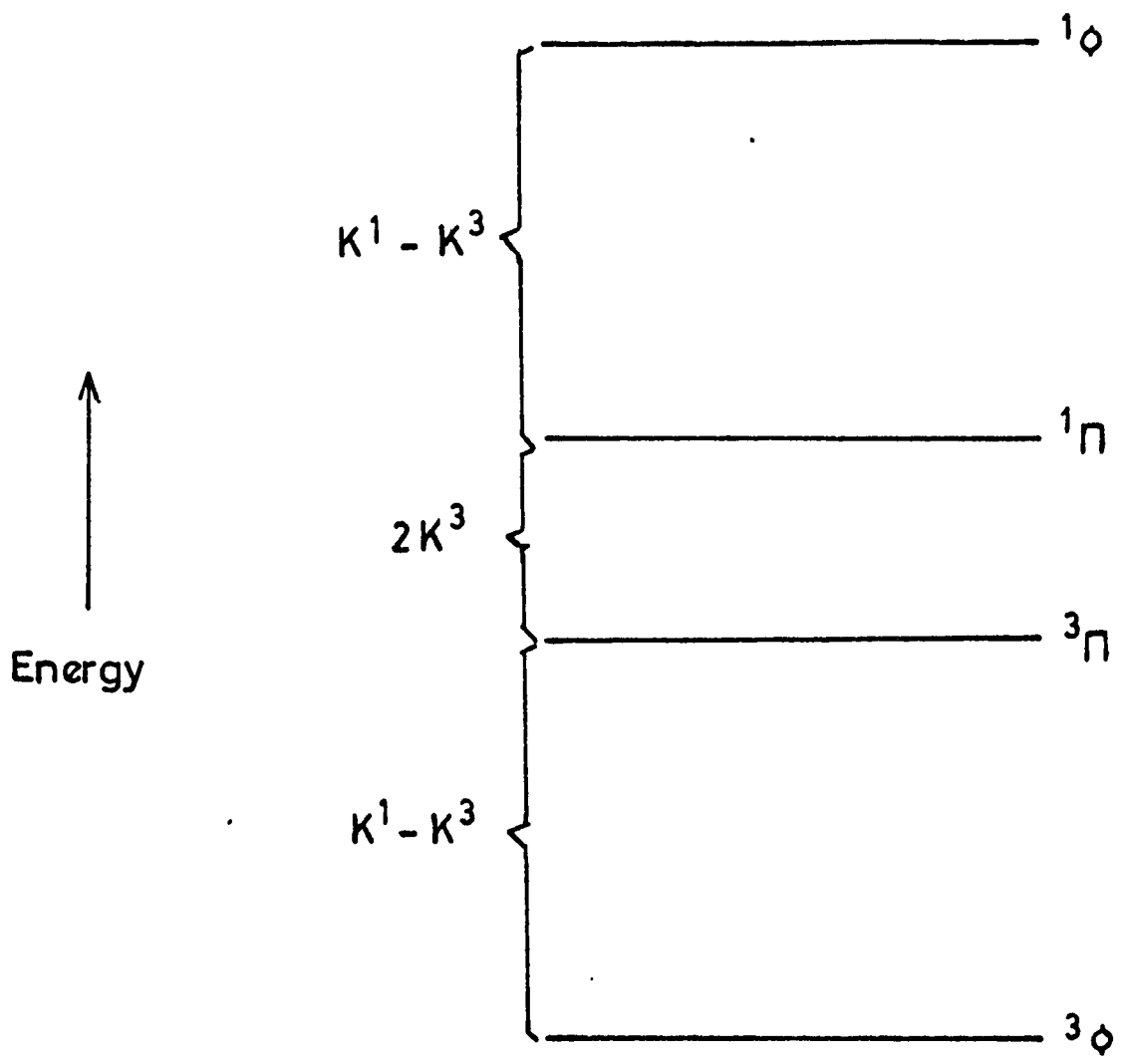



Figure 2.3.

The Configuration $\pi\delta$

## 2.5 Configurations with 3 Open-Shell Electrons

In the cases of configurations with three open-shell electrons, the energy expressions may depend on three or four independent quantities, and it is not always possible to make as many general conclusions about the ordering of the states as for configurations with two open-shell electrons.

### 2.5.1 The Configuration $\sigma_1\sigma_2\pi$

This configuration gives rise to three states, one $^4\Pi$ and two $^2\Pi$ states. The method for obtaining the energies of the $^2\Pi$ states has been described before; the wave functions are not given below.

$$^4\Pi \qquad \Psi = |\sigma_1\sigma_2\pi^+| \qquad E = (J-K)_{\sigma_1\sigma_2} + (J-K)_{\sigma_1\pi} + (J-K)_{\sigma_2\pi}$$

$$^2\Pi \qquad E = J_{\sigma_1\sigma_2} + J_{\sigma_1\pi} + J_{\sigma_2\pi} \pm \{(K_{\sigma_1\sigma_2})^2 + (K_{\sigma_1\pi})^2 + (K_{\sigma_2\pi})^2 - K_{\sigma_1\pi}K_{\sigma_2\pi} - K_{\sigma_1\pi}K_{\sigma_1\sigma_2} - K_{\sigma_2\pi}K_{\sigma_1\sigma_2}\}^{\frac{1}{2}}$$

As $(K_{\sigma_1\sigma_2} + K_{\sigma_1\pi} + K_{\sigma_2\pi})$ is necessarily greater than the square root of the quantity in brackets, the quartet state lies below both $^2\Pi$ states; this is shown in Figure 2.4.

The $^4\Delta$ and two $^2\Delta$ states from the configuration $\sigma_1\sigma_2\delta$, and the $^4\Sigma^+$ and and two $^2\Sigma^+$ states from the configuration $\sigma_1\sigma_2\sigma_3$, are analogously ordered.

### 2.5.2 The Configuration $\pi^2\sigma$

This configuration gives rise to the states $^4\Sigma^-$, $^2\Delta$, $^2\Sigma^-$ and $^2\Sigma^+$. The wave functions and energy expressions are:

$$^4\Sigma^- \qquad \Psi = |\pi^+\pi^-\sigma| \qquad E = (J^0-K^2)_{\pi\pi} + (2J-2K)_{\pi\sigma}$$

$$^2\Delta \qquad \Psi = |\pi^+\bar{\pi}^+\sigma| \qquad E = J^0_{\pi\pi} + (2J-K)_{\pi\sigma}$$

$$^2\Sigma^+ \qquad \Psi = 1/\sqrt{2}\{|\bar{\pi}^+\pi^-\sigma| - |\pi^+\bar{\pi}^-\sigma|\} \qquad E = (J^0+K^2)_{\pi\pi} + (2J-K)_{\pi\sigma}$$

$$^2\Sigma^- \qquad \Psi = 1/\sqrt{6}\{2|\pi^+\pi^-\bar{\sigma}| - |\bar{\pi}^+\pi^-\sigma| - |\pi^+\bar{\pi}^-\sigma|\} \qquad E = (J^0-K^2)_{\pi\pi} + (2J-K)_{\pi\sigma}$$

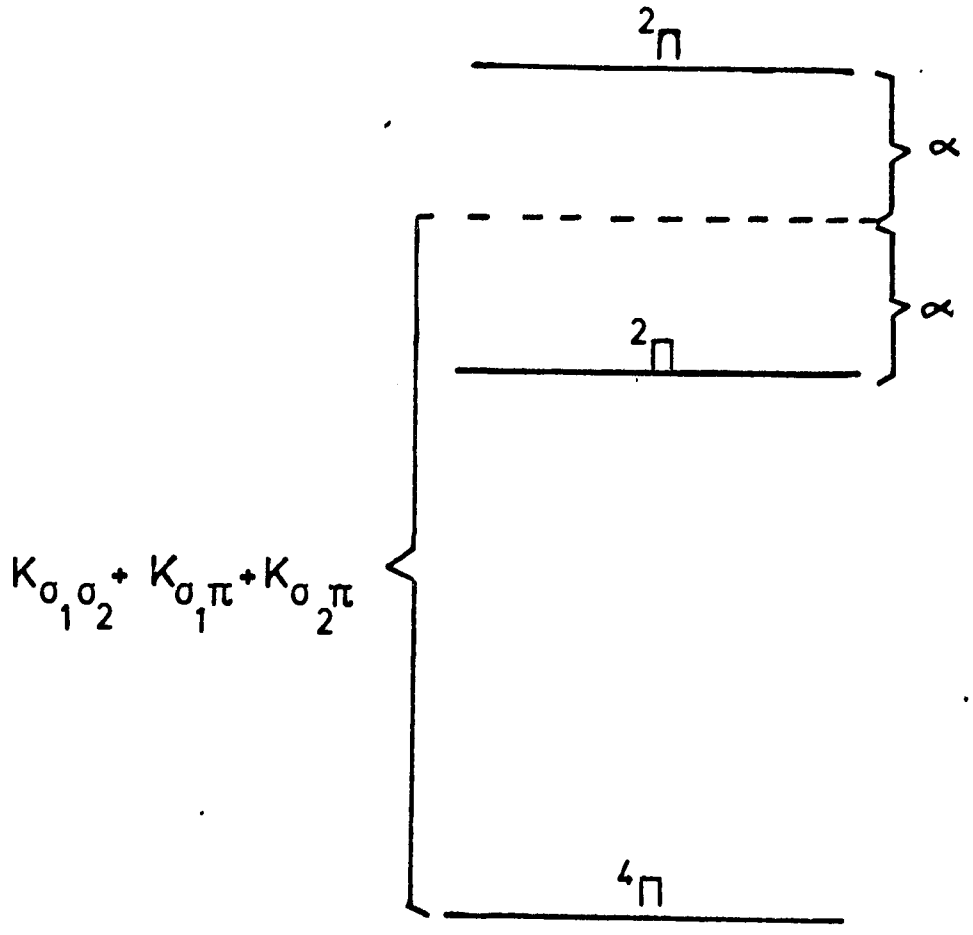



Figure 2.4.

The Configuration $\sigma_1 \sigma_2 \pi$

$$\alpha = \left\{ (K_{\sigma_1\sigma_2})^2 + (K_{\sigma_1\pi})^2 + (K_{\sigma_2\pi})^2 - K_{\sigma_1\pi}K_{\sigma_2\pi} - K_{\sigma_1\pi}K_{\sigma_1\sigma_2} - K_{\sigma_2\pi}K_{\sigma_1\sigma_2} \right\}^{1/2}.$$

From these expressions it may be deduced that the $^4\Sigma^-$ state is the lowest in energy. Little may be said about the ordering of the doublet states without some knowledge of the relative magnitudes of $K^2_{\pi\pi}$ and $K_{\pi\sigma}$. If $K_{\pi\sigma}<\frac{1}{2}K^2_{\pi\pi}$, then the ordering of the states is $^2\Sigma^-<^2\Delta<^2\Sigma^+$. If $\frac{1}{2}K^2_{\pi\pi}<K^2_{\pi\sigma}<K^2_{\pi\pi}$, then the ordering is $^2\Delta<^2\Sigma^-<^2\Sigma^+$. If $K_{\pi\sigma}>K^2_{\pi\pi}$, the ordering is $^2\Delta<^2\Sigma^+<^2\Sigma^-$. This is shown schematically in Figure 2.5. An example of this configuration is $0^+_2$, where the order of the states is $^4\Sigma^-_g<^2\Delta_g<^2\Sigma^-_g$; the $^2\Sigma^+_g$ state has not been observed (Edqvist et al. 1970, Jonathan et al. 1971). The $\delta^2\sigma$ configuration, giving $^4\Sigma^-$, $^2\Gamma$, $^2\Sigma^+$ and $^2\Sigma^-$ states, gives analogous results.

2.5.3 The Configuration $\pi_1\pi_2\sigma$

This configuration gives rise to nine states, $^4\Delta$, $^4\Sigma^+$, $^4\Sigma^-$, two $^2\Delta$, two $^2\Sigma^+$ and two $^2\Sigma^-$ states. As previously the wave functions are not given for the doublet states.

$^4\Delta$ $\quad \Psi = |\pi^+_1\pi^+_2\sigma|$ $\quad E = (J^0-K^0)_{\pi_1\pi_2}+(J-K)_{\pi_1\sigma}+(J-K)_{\pi_2\sigma}$

$^4\Sigma^+$ $\quad \Psi = 1/\sqrt{2}\{|\pi^+_1\pi^-_2\sigma|-|\pi^-_1\pi^+_2\sigma|\}$ $\quad E = (J^0-J^2+K^0-K^2)_{\pi_1\pi_2}+(J-K)_{\pi_1\sigma}+(J-K)_{\pi_2\sigma}$

$^4\Sigma^-$ $\quad \Psi = 1/\sqrt{2}\{|\pi^+_1\pi^-_2\sigma|+|\pi^-_1\pi^+_2\sigma|\}$ $\quad E = (J^0+J^2-K^0-K^2)_{\pi_1\pi_2}+(J-K)_{\pi_1\sigma}+(J-K)_{\pi_2\sigma}$

$^2\Delta$ $\quad E = J^0_{\pi_1\pi_2}+J_{\pi_1\sigma}+J_{\pi_2\sigma}\pm\{(K_{\pi_1\sigma})^2+(K_{\pi_2\sigma})^2+(K^0_{\pi_1\pi_2})^2-K_{\pi_1\sigma}K^0_{\pi_2\sigma}-K_{\pi_1\sigma}K^0_{\pi_1\pi_2}$

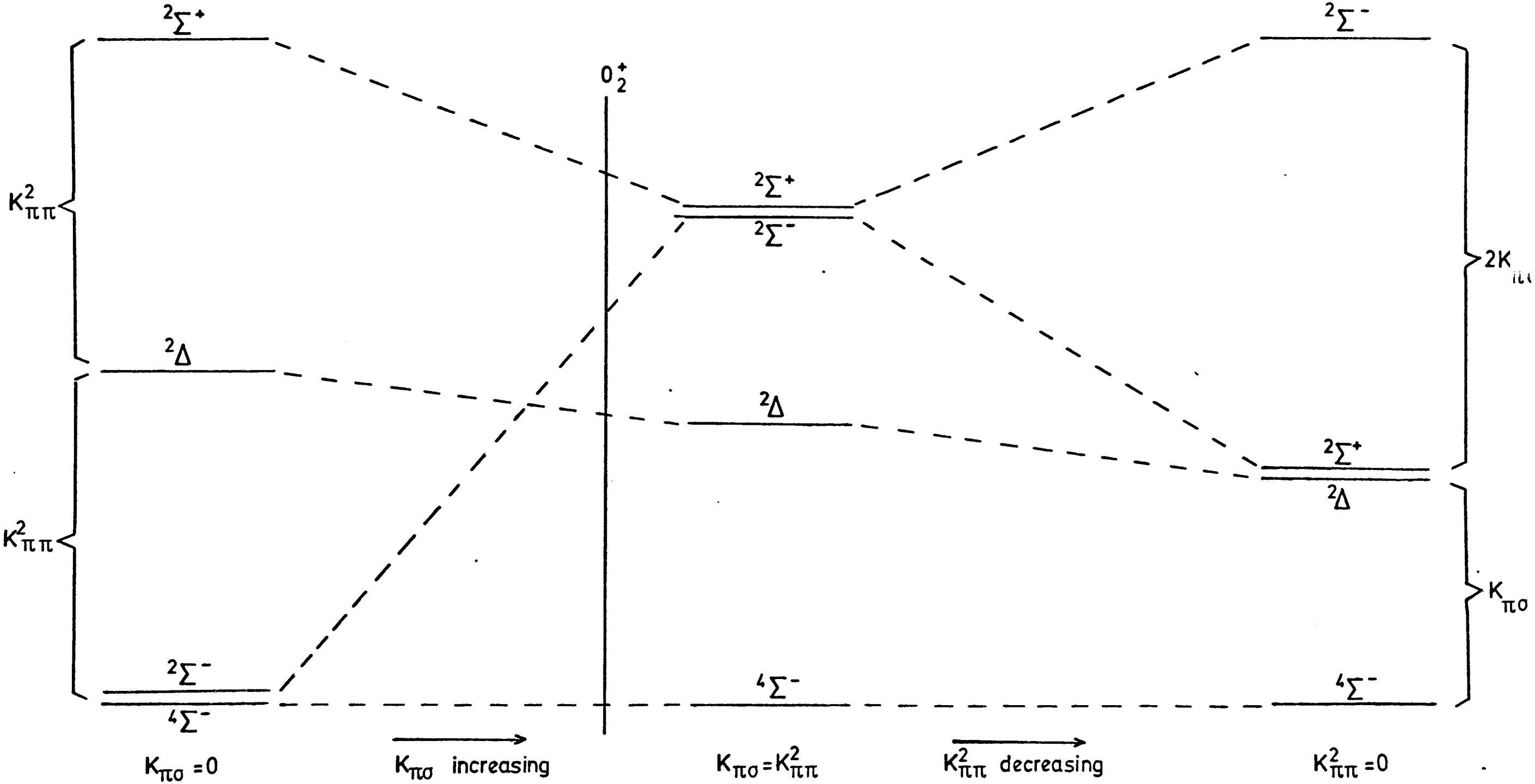
$$-K_{\pi_2\sigma}K_{\pi_1\pi_2}\}^{\frac{1}{2}}$$

$^2\Sigma^+$ $\quad E = (J^0+J^2)_{\pi_1\pi_2}+J_{\pi_1\sigma}+J_{\pi_2\sigma}\pm\{(K^0+K^2)^2_{\pi_1\pi_2}+(K_{\pi_1\sigma})^2+(K_{\pi_2\sigma})^2$

$$-(K^0+K^2)_{\pi_1\pi_2}K_{\pi_1\sigma}-(K^0+K^2)_{\pi_1\pi_2}K_{\pi_2\sigma}-K_{\pi_1\sigma}K_{\pi_2\sigma}\}^{\frac{1}{2}}$$

$^2\Sigma^-$ $\quad E = (J^0-J^2)_{\pi_1\pi_2}+J_{\pi_1\sigma}+J_{\pi_2\sigma}\pm\{(K^0-K^2)^2_{\pi_1\pi_2}+(K_{\pi_2\sigma})^2+(K_{\pi_2\sigma})^2$

$$-(K^0-K^2)_{\pi_1\pi_2}K_{\pi_1\sigma}-(K^0-K^2)_{\pi_1\pi_2}K_{\pi_2\sigma}-K_{\pi_1\sigma}K_{\pi_2\sigma}\}^{\frac{1}{2}}.$$




The Configuration $\pi^2\sigma$
Figure 2.5.

From these expressions it may be deduced that the $^4\Delta$ state lies below the $^2\Delta$ states, and the $^4\Sigma^+$ below the $^2\Sigma^+$ states. These states therefore follow the rule of maximum multiplicity. Furthermore, the $^4\Sigma^+$ state lies above the $^4\Delta$, and on the reasonable assumption that $K^0>J^2$, the $^4\Sigma^-$ state lies above the $^4\Sigma^+$. Nothing may be deduced about the positions of the $^2\Sigma^-$ states, which may lie anywhere. The quartet states are shown in Figure 2.6.

2.5.4 The Configuration $\pi^2\pi$

This configuration gives rise to five states, $^4\Pi$, $^2\Phi$ and three $^2\Pi$ states. As there are three $^2\Pi$ states, analytical solution of the problem requires the diagonalization of a three by three matrix; this makes general results hard to obtain, and too complex to allow interpretation. Specific examples of the numerical treatment of the analogous $\pi_u^3\pi_g^2$ configuration in $O_2^+$ may be found in Dixon and Hull (1969) and Raftery and Richards (1971). The energy expressions and wave functions for the $^4\Pi$ and $^2\Phi$ states are:

$^4\Pi$ $\quad \Psi = |\pi_1^+\pi_1^-\pi_2^+| \quad E = (J^0-K^2)_{\pi_1\pi_1} + (2J^0-K^0-K^2)_{\pi_1\pi_2}$

$^2\Phi$ $\quad \Psi = |\pi_1^+\bar{\pi}_1^+\pi_2^+| \quad E = J^0_{\pi_1\pi_1} + (2J^0-K^2)_{\pi_1\pi_2}$

The $^4\Pi$ state therefore lies below the $^2\Phi$; experimental evidence for $O_2^+$ (Jonathan et al. 1971) indicates that for this example that the lowest $^2\Pi$ state lies between the $^4\Pi$ and $^2\Phi$ states, with the $^4\Pi$ lying lowest.

2.5.5 The Configuration $\pi^2\delta$

This configuration gives rise to the states $^4\Delta$, $^2\Gamma$, $^2\Sigma^+$, $^2\Sigma^-$ and two $^2\Delta$ states. The wave functions and energy expressions are:

$^4\Delta$ $\quad \Psi = |\pi^+\pi^-\delta^{2+}| \quad E = (J^0-K^2)_{\pi\pi} + (2J^0-K^1-K^3)_{\pi\delta}$

$^2\Gamma$ $\quad \Psi = |\pi^+\bar{\pi}^+\delta^{2+}| \quad E = J^0_{\pi\pi} + (2J^0-K^1)_{\pi\delta}$

$^2\Sigma^+$ $\quad \Psi = 1/\sqrt{2}\{|\pi^+\bar{\pi}^+\delta^{2-}| + |\pi^-\bar{\pi}^-\delta^{2+}|\} \quad E = J^0_{\pi\pi} + (2J^0-K^3)_{\pi\delta}$

$^2\Sigma^-$ $\quad \Psi = 1/\sqrt{2}\{|\pi^+\bar{\pi}^+\delta^{2-}| - |\pi^-\bar{\pi}^-\delta^{2+}|\} \quad E = J^0_{\pi\pi} + (2J^0-K^3)_{\pi\delta}$

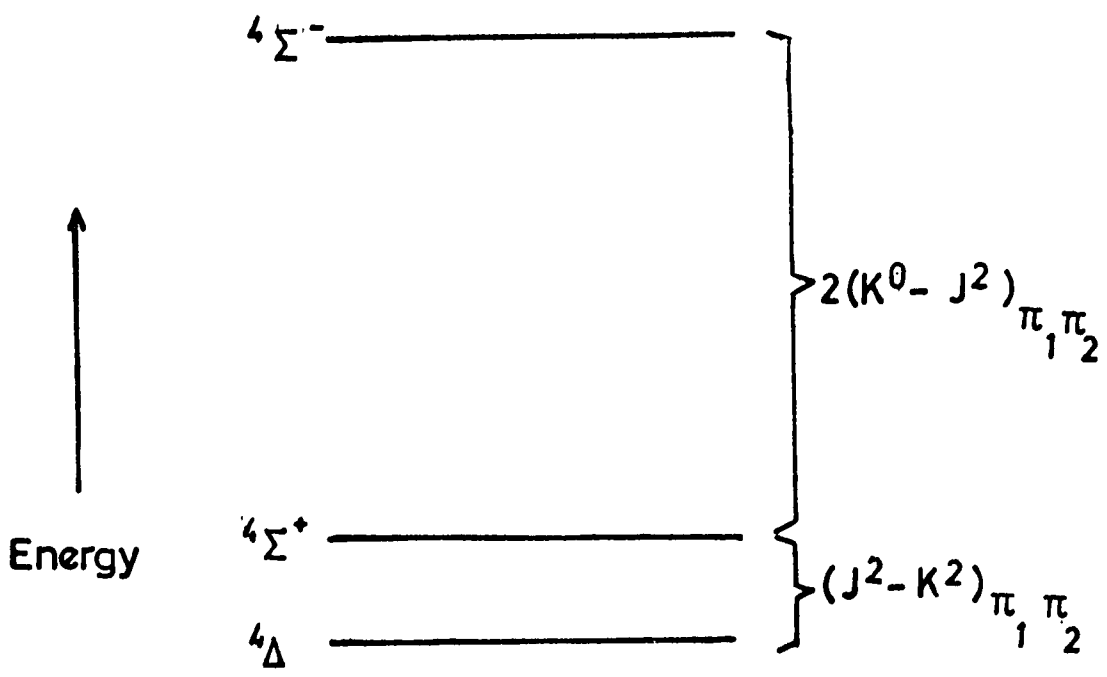



Figure 2.6.

The Configuration $\pi_1 \pi_2 \sigma$

$$^2\Delta \qquad E = J^0_{\pi\pi}+2J^0_{\pi\delta}\pm\{(K^1_{\pi\delta})^2+(K^2_{\pi\pi})^2+(K^3_{\pi\delta})^2-K^1_{\pi\delta}K^3_{\pi\delta}-K^2_{\pi\pi}K^1_{\pi\delta}-K^2_{\pi\pi}K^3_{\pi\delta}\}^{\frac{1}{2}}$$

The $^4\Delta$ state therefore lies lowest in energy. The $^2\Sigma^+$ and $^2\Sigma^-$ states in this approximation are degenerate, and they lie above the $^2\Gamma$ state. The position of the lower $^2\Delta$ state may not be predicted, except that it always lies above the $^4\Delta$ state. The higher $^2\Delta$ state is always the highest state. This is shown in Figure 2.7. Thus the rule of maximum multiplicity is always obeyed, though in the doublets the rule of maximum $\Lambda$ is not necessarily obeyed.

2.5.6 The Configuration $\delta^2\pi$

This configuration gives rise to the states $^2\Pi$, $^2H$, $^2\Phi$, and $^2\Pi$ twice. The wave functions and energy expressions are:

$$^4\Pi \qquad \Psi = |\delta^{2+}\delta^{2-}\pi^+| \qquad E = (J^0-K^4)_{\delta\delta}+(2J^0-K^1-K^3)_{\pi\delta}$$

$$^2H \qquad \Psi = |\delta^{2+}\bar{\delta}^{2+}\pi^+| \qquad E = J^0_{\delta\delta}+(2J^0-K^1)_{\pi\delta}$$

$$^2\Phi \qquad \Psi = |\delta^{2+}\delta^{2+}\pi^-| \qquad E = J^0_{\delta\delta}+(2J^0-K^3)_{\pi\delta}$$

$$^2\Pi \qquad E = J^0_{\delta\delta}+2J^0_{\delta\pi}\pm\{(K^1_{\pi\delta})^2+(K^3_{\pi\delta})^2+(K^4_{\delta\delta})^2-K^1_{\pi\delta}K^3_{\pi\delta}-K^1_{\pi\delta}K^4_{\delta\delta}-K^3_{\pi\delta}K^4_{\delta\delta}\}^{\frac{1}{2}}$$

The $^4\Pi$ state is therefore the lowest state, and the $^2\Phi$ state lies higher than the $^2H$ state. The lower $^2\Pi$ state may be anywhere higher than the $^4\Pi$ state, and the higher $^2\Pi$ state is the highest state. The ordering is thus similar, though not identical, to that found for the $\pi^2\delta$ configuration.

2.5.7 The Configuration $\sigma\pi\delta$

The states derived from the configuration $\sigma\pi\delta$ are $^4\Phi$, $^4\Pi$, $^2\Phi$(twice) and $^2\Pi$ (twice). The wave functions and energy expressions are:

$$^4\Phi \qquad \Psi = |\sigma\pi^+\delta^{2+}| \qquad E = (J-K)_{\sigma\pi}+(J-K)_{\sigma\delta}+(J^0-K^1)_{\pi\delta}$$

$$^4\Pi \qquad \Psi = |\sigma\pi^-\delta^{2+}| \qquad E = (J-K)_{\sigma\pi}+(J-K)_{\sigma\delta}+(J^0-K^3)_{\pi\delta}$$

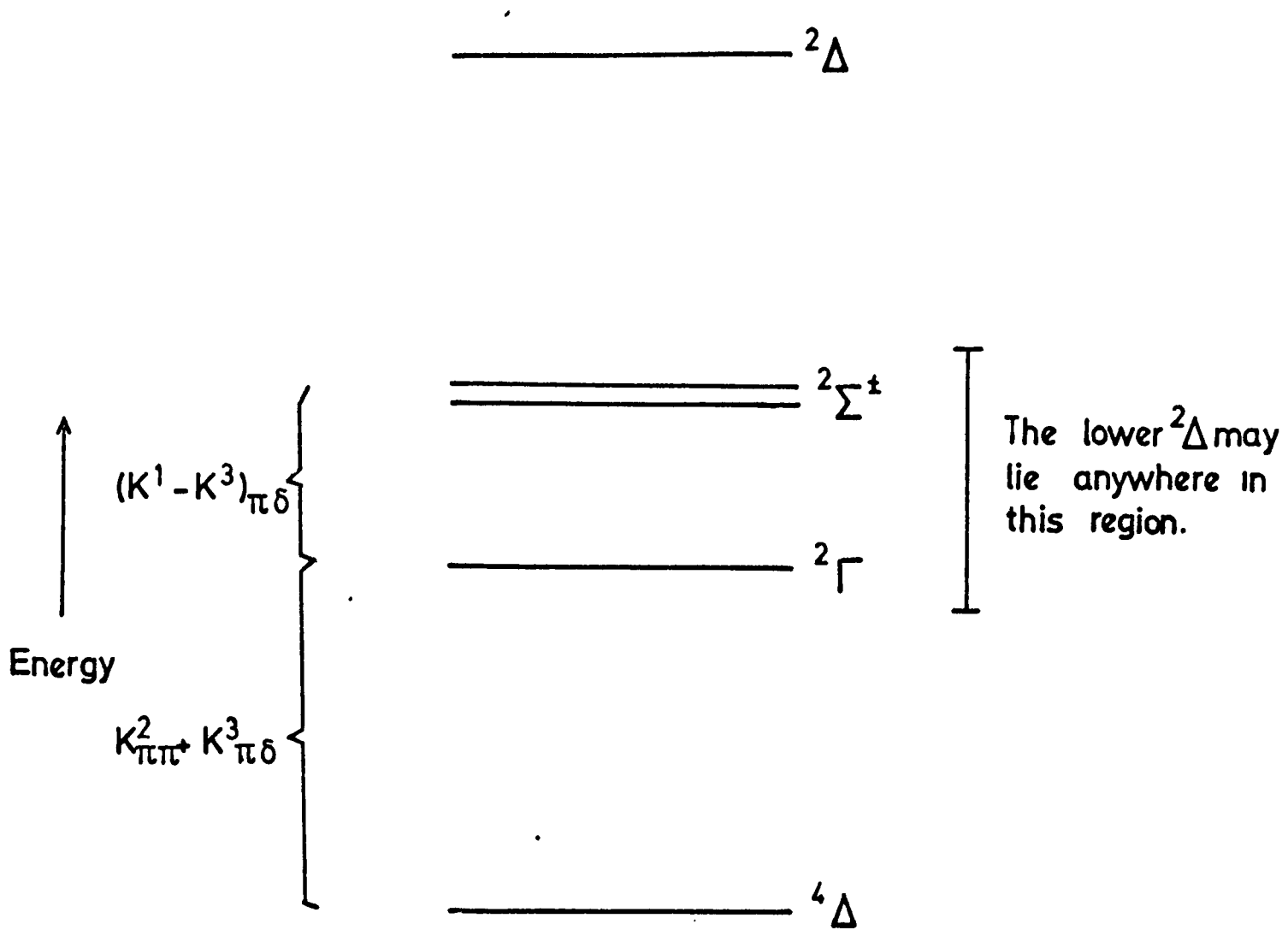



Figure 2.7.

The Configuration $\pi^2\delta$

$$^2\Phi \qquad E = J_{\sigma\pi}+J_{\sigma\delta}+J^0_{\pi\delta}\pm\{(K_{\sigma\pi})^2+(K_{\sigma\delta})^2+(K^1_{\pi\delta})^2-K^1_{\pi\delta}K_{\sigma\pi}-K^1_{\pi\delta}K_{\sigma\delta}-K_{\sigma\pi}K_{\sigma\delta}\}^{\frac{1}{2}}$$

$$^2\Pi \qquad E = J_{\sigma\pi}+J_{\sigma\delta}+J^0_{\pi\delta}\pm\{(K_{\sigma\pi})^2+(K_{\sigma\delta})^2+(K^3_{\pi\delta})^2-K^3_{\pi\delta}K_{\sigma\pi}-K^3_{\pi\delta}K_{\sigma\delta}-K_{\sigma\pi}K_{\sigma\delta}\}^{\frac{1}{2}}$$

From these expressions it may be deduced that the $^4\Phi$ state lies below the $^4\Pi$, and that each quartet lies below the corresponding pair of doublets. In addition, for the lower $^2\Phi$ state to lie below the lower $^2\Pi$ state, the condition is $K^1_{\pi\delta}+K^3_{\pi\delta}>K_{\sigma\pi}+K_{\sigma\delta}$. The ordering of the upper doublets is the opposite of the lower doublets. In cases where the lower $^2\Phi$ lies below the lower $^2\Pi$, it is also possible that it lies below the $^4\Pi$ state. This is shown schematically in Figure 2.8.

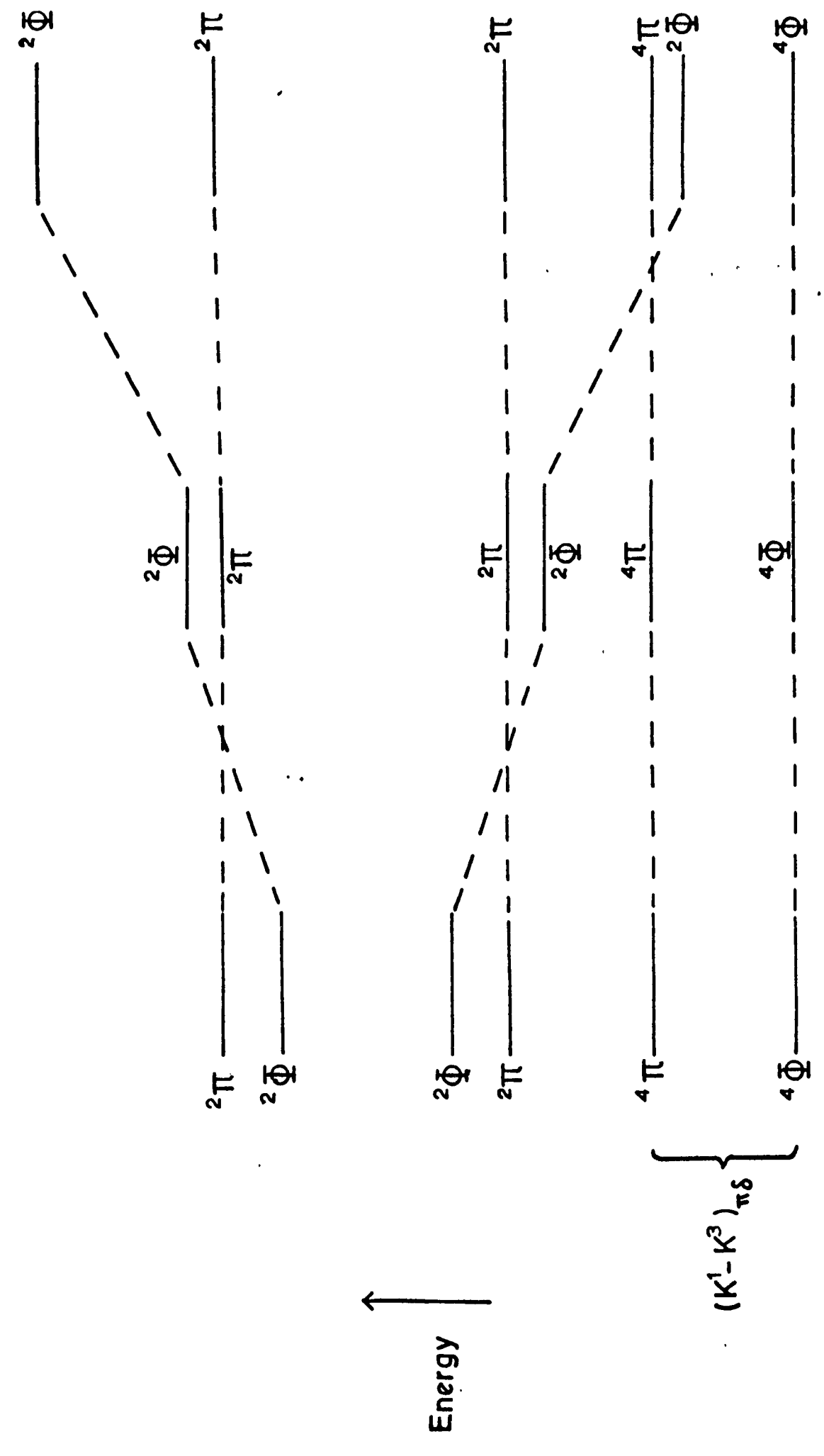



Figure 2·8

The Configuration $\sigma\pi\delta$.

## 2.6 Configurations with more than Three Open-Shell Electrons

As the number of open-shell electrons increases, it becomes more difficult to generalise about the ordering of states in the above manner for two reasons. Firstly, the number of independent quantities involved in the energy expressions increases, greatly reducing the number of predictions which may be made. Secondly, with an increasing number of open-shell electrons, the number of derived states increases rapidly, and configuration interaction becomes an important factor in determining the ordering of the states.

### 2.6.1 Configurations with more than half-filled shells

The complications associated with a large number of open-shell electrons do not apply if the configurations contains shells which are more than half-filled, e.g. $\delta^3$. In these cases, fewer independent interactions need to be considered, and the number of states is the same as for the analogous configuration containing a shell which is less than half-filled, i.e. $\sigma\delta^3$ is analogous to $\sigma\delta$.

In general, configurations in which all the open shells of degenerate orbitals are at least half-filled (i.e. $\lambda^2$ or $\lambda^3$, where $\lambda$ is $\pi$, $\delta$, etc.) will have analogous ordering to the corresponding states from the configurations in which the shells are at most half-filled. Thus the $\pi_1^3\pi_2^3$ configuration has the same ordering as $\pi_1\pi_2$; an example of this configuration is the $O_2$ molecule (Rosen 1970). Similarly, configurations such as $\pi_1^3\pi_2^2$ and $\sigma\delta^3$ behave similarly to $\pi_1\pi_2^2$ and $\sigma\delta$. However, if a configuration contains one shell which is more than half-filled, and another which is less than half-filled, then the ordering of the states will follow a different pattern from that in which all the shells are no more than half-filled, even though the same states are obtained from that configuration. Thus positive holes interact with positive holes in a similar way to negative electrons with negative electrons; but the interaction of positive holes with negative electrons is not analogous to that of electrons with electrons.

For cases where the configuration contains both less than half-filled shells and more than half-filled shells, some predictions of the ordering of states are given below.

2.6.2 The $\pi^3\pi$ Configuration

This configuration gives rise to six states, $^3\Delta$, $^1\Delta$, $^3\Sigma^-$, $^3\Sigma^+$, $^1\Sigma^+$ and $^1\Sigma^-$. The wave functions and energy expressions are:

$$^3\Delta \quad \Psi = |\pi_1^+\bar{\pi}_1^+\pi_1^-\pi_2^+| \qquad E = (3J^0-K^2)_{\pi_1\pi_1}+(3J^0-K^0-K^2)_{\pi_1\pi_2}$$

$$^1\Delta \quad \Psi = 1/\sqrt{2}\{|\pi_1^+\bar{\pi}_1^+\pi_1^-\bar{\pi}_2^+|-|\pi_1^+\bar{\pi}_1^+\pi_1^-\bar{\pi}_2^+|\} \quad E = (3J^0-K^2)_{\pi_1\pi_1}+(3J^0-K^0+K^2)_{\pi_1\pi_2}$$

$$^3\Sigma^+ \quad \Psi = 1/\sqrt{2}\{|\pi_1^+\bar{\pi}_1^+\pi_1^-\pi_2^-|+|\pi_1^-\bar{\pi}_1^-\pi_1^+\pi_2^+|\} \quad E = (3J^0-K^2)_{\pi_1\pi_1}+(3J^0-J^2-K^0-K^2)_{\pi_1\pi_2}$$

$$^3\Sigma^- \quad \Psi = 1/\sqrt{2}\{|\pi_1^+\bar{\pi}_1^+\pi_1^-\pi_2^-|-|\pi_1^-\bar{\pi}_1^-\pi_1^+\pi_2^+|\} \quad E = (3J^0-K^2)_{\pi_1\pi_2}+(3J^0+J^2-K^0-K^2)_{\pi_1\pi_2}$$

$$^1\Sigma^+ \quad \Psi = \tfrac{1}{2}\{|\pi_1^+\bar{\pi}_1^+\pi_1^-\bar{\pi}_2^-|-|\pi_1^+\bar{\pi}_1^+\pi_1^-\bar{\pi}_2^-|-|\pi_1^+\bar{\pi}_1^-\pi_1^-\bar{\pi}_2^+|+|\bar{\pi}_1^+\pi_1^-\bar{\pi}_1^-\pi_2^+|\}$$

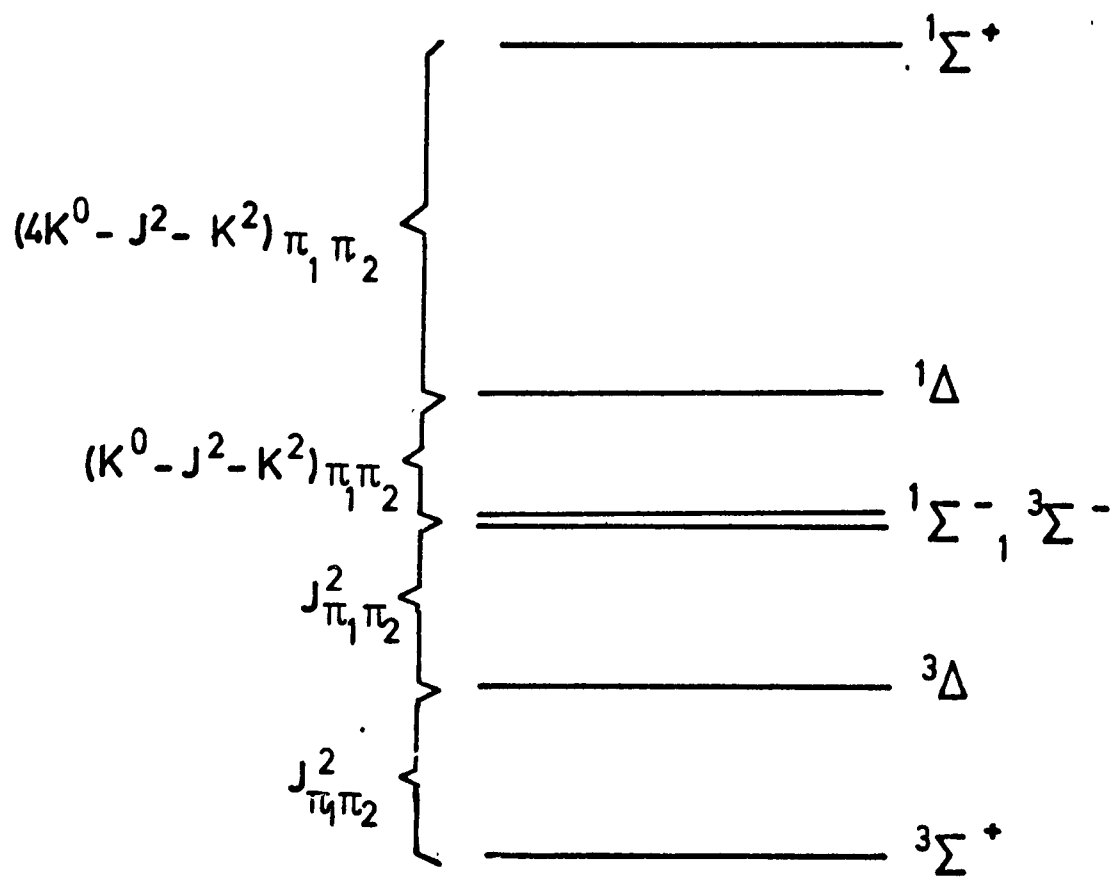
$$E = (3J^0-K^2)_{\pi_1\pi_2}+(3J^0-J^2+3K^0-K^2)_{\pi_1\pi_2}$$

$$^1\Sigma^- \quad \Psi = \tfrac{1}{2}\{|\pi_1^+\bar{\pi}_1^+\pi_1^-\bar{\pi}_2^-|-|\pi_1^+\bar{\pi}_1^+\pi_1^-\bar{\pi}_2^-|+|\pi_1^+\bar{\pi}_1^-\pi_1^-\bar{\pi}_2^+|-|\bar{\pi}_1^+\pi_1^-\bar{\pi}_1^-\pi_2^+|\}$$

$$E = (3J^0-K^2)_{\pi_1\pi_2}+(3J^0+J^2-K^0-K^2)_{\pi_1\pi_2}$$

Making the assumption, based on a large number of ab initio calculations, that $K^0_{12}$ is greater than $(J^2_{12}+K^2_{12})$, the following conclusions may be drawn about the states. The triplets are ordered $^3\Sigma^+ < ^3\Delta < ^3\Sigma^-$, and the singlets $^1\Sigma^- < ^1\Delta < ^1\Sigma^+$; in this approximation the $^1\Sigma^-$ and $^3\Sigma^-$ states are degenerate. This is shown in Figure 2.9. This ordering is experimentally observed in the $\pi_u^3\pi_g$ configuration of $N_2$ and CO (Rosen 1970). The $\delta_1^3\delta_2^2$ configuration is analogously ordered.

Figure 2.9.




The Configuration $\pi_1\,^3\pi_2$

2.6.3 The Configuration $\pi^3\delta$

This gives rise to four states, $^3\Phi$, $^1\Phi$, $^3\Pi$ and $^1\Pi$. The wave functions and energy expressions are:

$$^3\Phi \quad \Psi = |\pi^{+}\bar{\pi}^{+}\pi^{-}\delta^{2+}| \qquad E = (3J^0-K^2)_{\pi\pi}+(3J^0-K^1-K^3)_{\pi\delta}$$

$$^1\Phi \quad \Psi = 1/\sqrt{2}\{|\pi^{+}\bar{\pi}^{+}\pi^{-}\bar{\delta}^{2+}|-|\pi^{+}\bar{\pi}^{+}\pi^{-}\bar{\delta}^{2+}|\} \quad E = (3J^0-K^2)_{\pi\pi}+(3J^0-K^1+K^3)_{\pi\delta}$$

$$^3\Pi \quad \Psi = |\pi^{-}\bar{\pi}^{-}\pi^{+}\delta^{2+}| \qquad E = (3J^0-K^2)_{\pi\pi}+(3J^0-K^1-K^3)_{\pi\delta}$$

$$^1\Pi \quad \Psi = 1/\sqrt{2}\{|\pi^{-}\bar{\pi}^{-}\pi^{+}\delta^{2+}|-|\pi^{-}\bar{\pi}^{-}\pi^{+}\bar{\delta}^{2+}|\} \quad E = (3J^0-K^2)_{\pi\pi}+(3J^0+K^1-K^3)_{\pi\delta}$$

The ordering of the states is therefore $^3\Phi\simeq{}^3\Pi<{}^1\Phi<{}^1\Pi$. This is shown in Figure 2.10. The $\pi\delta^3$ configuration is analogously ordered.

2.6.4 The Configuration $\sigma\pi^3\delta$

The wave functions and energy expressions for the six states from this configuration are:

$$^4\Phi \quad \Psi = |\sigma\pi^{+}\bar{\pi}^{+}\pi^{-}\delta^{2+}| \qquad E = (3J-2K)_{\sigma\pi}+(J-K)_{\sigma\delta}+(3J^0-K^1-K^3)_{\pi\delta}+(3J^0-K^2)_{\pi\pi}$$

$$^4\Pi \quad \Psi = |\sigma\pi^{-}\bar{\pi}^{-}\pi^{+}\delta^{2+}| \qquad E = (3J-2K)_{\sigma\pi}+(J-K)_{\sigma\delta}+(3J^0-K^1-K^3)_{\pi\delta}+(3J^0-K^2)_{\pi\pi}$$

$$^2\Phi \qquad E = (3J-K)_{\sigma\pi}+J_{\sigma\delta}+(3J^0-K^1)_{\pi\delta}+(3J^0-K^2)_{\pi\pi}$$

$$\pm\{(K_{\sigma\pi})^2+(K^3_{\pi\delta})^2+(K_{\sigma\delta})^2-K_{\sigma\pi}K^3_{\pi\delta}-K_{\sigma\pi}K_{\sigma\delta}-K^3_{\pi\delta}K_{\sigma\delta}\}^{\frac{1}{2}}$$

$$^2\Pi \qquad E = (3J-K)_{\sigma\pi}+J_{\sigma\delta}+(3J^0-K^3)_{\pi\delta}+(3J^0-K^2)_{\pi\pi}$$

$$\pm\{(K_{\sigma\pi})^2+(K_{\pi\delta})^2+(K_{\sigma\delta})^2-K_{\sigma\pi}K^1_{\pi\delta}-K_{\sigma\pi}K_{\sigma\delta}-K^1_{\pi\delta}K_{\sigma\delta}\}^{\frac{1}{2}}$$

It may hence be shown that in this approximation, the two quartet states are degenerate, and that both $^2\Phi$ states lie above the quartet states, as do both $^2\Pi$ states. It is not possible to make predictions about the relative orderings of the doublet states. The $\sigma\pi\delta^3$ configuration is analogously ordered.

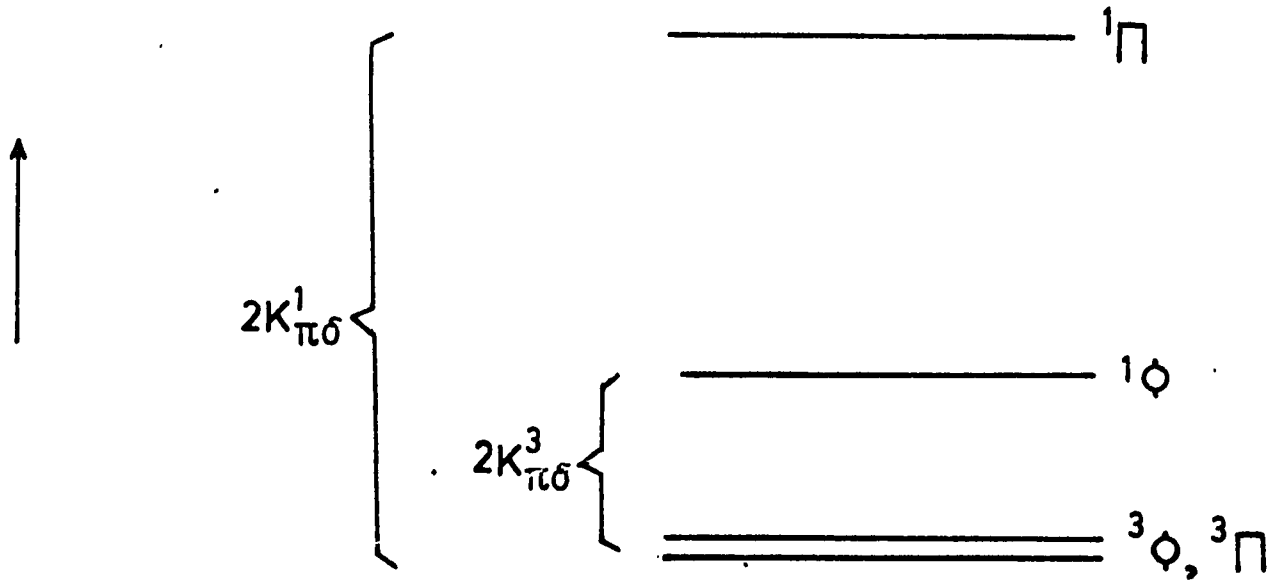



Figure 2.10.

The Configuration $\pi^3\delta$

2.6.5 The Configuration $\sigma\pi_1^3\pi_2$

This configuration gives rise to a $^4\Delta$, a $^4\Sigma^+$, a $^4\Sigma^-$, two $^2\Delta$, two $^2\Sigma^+$ and two $^2\Sigma^-$ states. The energy expressions are:

$$^4\Delta \quad \Psi = |\pi_1^+\bar{\pi}_1^+\pi_1^-\pi_2^+\sigma| \qquad E = (3J^0-K^2)_{\pi_1\pi_1}+(3J^0-K^0-K^2)_{\pi_1\pi_2}+(3J-2K)_{\pi_1\sigma}+(J-K)_{\pi_2\sigma}$$

$$^4\Sigma^+ \quad \Psi = 1/\sqrt{2}\{|\pi_1^+\bar{\pi}_1^+\pi_1^-\pi_2^-\sigma|+|\pi_1^-\bar{\pi}_1^-\pi_1^+\pi_2^+\sigma|\}$$

$$E = (3J^0-K^2)_{\pi_1\pi_1}+(3J^0-J^2-K^0-K^2)_{\pi_1\pi_2}+(3J-2K)_{\pi_1\sigma}+(J-K)_{\pi_2\sigma}$$

$$^4\Sigma^- \quad \Psi = 1/\sqrt{2}\{|\pi_1^+\bar{\pi}_1^+\pi_1^-\pi_2^-\sigma|-|\pi_1^-\bar{\pi}_1^-\pi_1^+\pi_2^+\sigma|\}$$

$$E = (3J^0-K^2)_{\pi_1\pi_1}+(3J^0+J^2-K^0-K^2)+(3J-2K)_{\pi_1\sigma}+(J-K)_{\pi_2\sigma}$$

$$^2\Delta \qquad E = (3J^0-K^2)_{\pi_1\pi_1}+(3J^0-K^0)_{\pi_1\pi_2}+(3J-K)_{\pi_1\sigma}+J_{\pi_2\sigma}$$

$$\pm\{(K^2_{\pi_1\pi_2})^2+(K_{\pi_1\sigma})^2+(K_{\pi_2\sigma})^2-K^2_{\pi_1\pi_2}K_{\pi_1\sigma}-K^2_{\pi_1\pi_2}K_{\pi_2\sigma}-K_{\pi_1\sigma}K_{\pi_2\sigma}\}^{\frac{1}{2}}$$

$$^2\Sigma^+ \qquad E = (3J^0-K^2)_{\pi_1\pi_1}+(3J^0-J^2+K^0-K^2)_{\pi_1\pi_2}+(3J-K)_{\pi_1\sigma}+J_{\pi_2\sigma}$$

$$\pm\{4(K^0_{\pi_1\pi_2})^2+(K_{\pi_1\sigma})^2+(K_{\pi_2\sigma})^2-2K^0_{\pi_1\pi_2}K_{\pi_1\sigma}-2K^0_{\pi_1\pi_2}K_{\pi_2\sigma}-K_{\pi_1\sigma}K_{\pi_2\sigma}\}^{\frac{1}{2}}$$

$$^2\Sigma^- \qquad E = (3J^0-K^2)_{\pi_1\pi_1}+(3J^0+J^2-K^0-K^2)_{\pi_1\pi_2}+(3J-K)_{\pi_1\sigma}+J_{\pi_2\sigma}$$

$$\pm\{(K_{\pi_1\sigma})^2+(K_{\pi_2\sigma})^2-K_{\pi_1\sigma}K_{\pi_2\sigma}\}^{\frac{1}{2}}$$

From these energy expressions it may be deduced that the ordering of the quartet states is $^4\Sigma^+<^4\Delta<^4\Sigma^-$, which is not in agreement with the rule of maximum $\Lambda$. It may also be shown that all the doublet states lie above all the corresponding quartet states.

## 2.7 Conclusions

In the preceding sections expressions have been derived for the electronic energies of states arising from open-shell electron configurations. Using inequalities between coulomb and exchange integrals, it has been possible in many cases to make general predictions of the ordering of the states from a given configuration; these predictions are supported by the available experimental evidence. The predictions show that although extended forms of Hund's rules often used are correct in some simple cases, they are not universally valid; in many cases alternative rules may be proposed, but in a few cases it is shown that it is not possible to formulate any general conclusions. It is also often possible to predict the relative ordering of $\Sigma^+$ and $\Sigma^-$ states, which is not treated by Hund's rules.

The predictions are derived from the assumption that the electronic states are well represented by single configurations, and that the form of the orbitals does not vary significantly from one state to another. The limitations of the latter assumption have been discussed; it has been shown that predictions based on this model invariably give the same ordering as accurate Hartree-Fock calculations. Where deviations from the predicted orderings are observed, then the effects of configuration interaction must be appreciable. It is hoped that these predictions will be of value in the assignment of band spectra to electronic states.

A possible extension of this work is to the states of molecules of non-linear symmetry. Much of the nomenclature described above may be carried over to non-linear symmetry; one problem which remains to be studied is the importance of Jahn-Teller splittings in determining the ordering of states; in linear molecules no Jahn-Teller distortions are possible.

# Chapter 3

## A REASSIGNMENT OF THE MOLECULAR ORBITAL CONFIGURATIONS OF THE EXCITED STATES OF ScF


| | | Page No. |
|---|---|---|
| 3.1 | Introduction | 60 |
| 3.2 | The Electronic Structure of ScF | 61 |
| 3.3 | The Nature of the Problem | 67 |
| 3.4 | Summary of Previous Work on ScF and TiO | 70 |
| 3.5 | Choice of the Basis Set | 72 |
| 3.6 | The Results of Hartree-Fock Calculations | 76 |
| | 3.6.1 Calculations on the Sc and F Atoms | 76 |
| | 3.6.2 Calculations in the Low-lying States of ScF | 76 |
| | 3.6.3 Calculations on the Excited States of ScF | 78 |
| 3.7 | The Results of Configuration Interaction Calculations | 85 |
| 3.8 | Discussion | 90 |
| 3.9 | Conclusions | 92 |

## Tables


| | | Page No. |
|---|---|---|
| Table 3.1 | Observed and Estimated Energy Levels in ScF | 66 |
| Table 3.2 | S.T.O. Basis Functions | 74 |
| Table 3.3 | Energies of the Sc and F Atoms | 76 |
| Table 3.4 | Energies and Spectroscopic Constants of the Low-Lying States of ScF | 77 |
| Table 3.5 | Energies and Spectroscopic Constants of the $\Pi$ States of ScF | 79 |
| Table 3.6 | The $3d\delta 3d\pi$ Configuration of ScF | 84 |
| Table 3.8 | C.I. Calculations on the $^3\Phi$ States of ScF | 87 |
| Table 3.9 | C.I. Calculations on the $^3\Pi$ States of ScF | 89 |


## Figures


| | | |
|---|---|---|
| Figure 3.1 | Known Electronic States of ScF | 62 |
| Figure 3.2 | Known Electronic States of TiO | 64 |
| Figure 3.3 | Known Electronic States of ScO | 68 |
| Figure 3.4 | Proposed Configurations for the Electronic States of ScF | 93 |

## 3.1 Introduction

Scandium monofluoride is a diatomic molecule of wide interest and importance; its valence electronic structure is similar to that of the much studied series $N_2$, CO and AlF, and it acts as a model system for the understanding of binding in transition metal compounds. It has been extensively studied, and twelve electronic states have been identified, seven singlet states and five triplets. Accordingly it has been possible to assign molecular orbital configurations to the states with some confidence, and these assignments have been generally accepted for some years (Cheetham and Barrow 1967, Brewer and Green 1969, Balfour and Tatum 1973). Although more detailed information about the electronic states is available for ScF than for any other transition metal diatomic molecule, there are nevertheless several points at which current understanding of the structure of the molecules is not able to explain experimental observations. In particular, the difference in energy between the 3d and 4p electrons does not seem to be compatible with that found in related molecules, and the intensities of the bands are not correctly predicted by simple molecular orbital considerations. In this chapter it is shown that molecular orbital calculations can play a valuable part in the interpretation of the electronic structure of the transition metal diatomic molecules; reassignments of several states of ScF are proposed, and it is also shown that other states may not be described adequately by a single molecular orbital configuration. These conclusions remove many of the problems in the understanding of the electronic structure of ScF, and may be extended to apply to other molecules with isoelectronic valence shells.

## 3.2 The Electronic Structure of ScF

There are three reasons why scandium monofluoride has become the most comprehensively understood of the transition metal diatomic molecules. The first reason is the large number of electronic transitions which fall in the visible and near ultra-violet regions of the spectrum. The second is the relatively small number of electrons involved in the binding of ScF, which simplifies both the analysis of the spectrum and also the assignment of molecular orbital configurations to observed electronic states. A third factor of great importance is the availability of data on molecules which have isoelectronic valence shells; TiO, which is isoelectronic, provides the most important information, but comparisons with YF, LaF and ZrO have also been helpful. ScF and TiO illustrate well the principles of bonding in the transition metal diatomic molecules, as far as they are understood, and also illustrate the ways in which the interpretation of experimental data is achieved.

ScF was first observed only eleven years ago (Gurvich and Shenyavskaya, 1963) but TiO has been known for many years, having been originally detected in stellar spectra. However its ground state was not correctly identified until as late as 1950 (Phillips, 1950). ScF has been studied in the gas phase in King furnaces both in absorption and thermal emission (Barrow et al. 1967). It shows band systems based on a $^1\Sigma^+$ and a $^3\Delta$ state, which appear with comparable intensities at 2000$^\circ$K. It has also been observed in inert gas matrices (McLeod and Weltner, 1966) where absorption spectra which correspond to singlet-singlet transitions appear. There are six singlet-singlet, and four triplet-triplet transitions known; to date no intercombination singlet-triplet transitions have been reported. The known states of ScF are shown in Figure 3.1. The spectrum of TiO shows many similarities to that of ScF; bands are observed based on three low-lying states, $^1\Delta$, $^1\Sigma^+$ and $^3\Delta$. Five singlet transitions are known, and four triplet transitions (Rosen 1970, Phillips and Davis 1971);

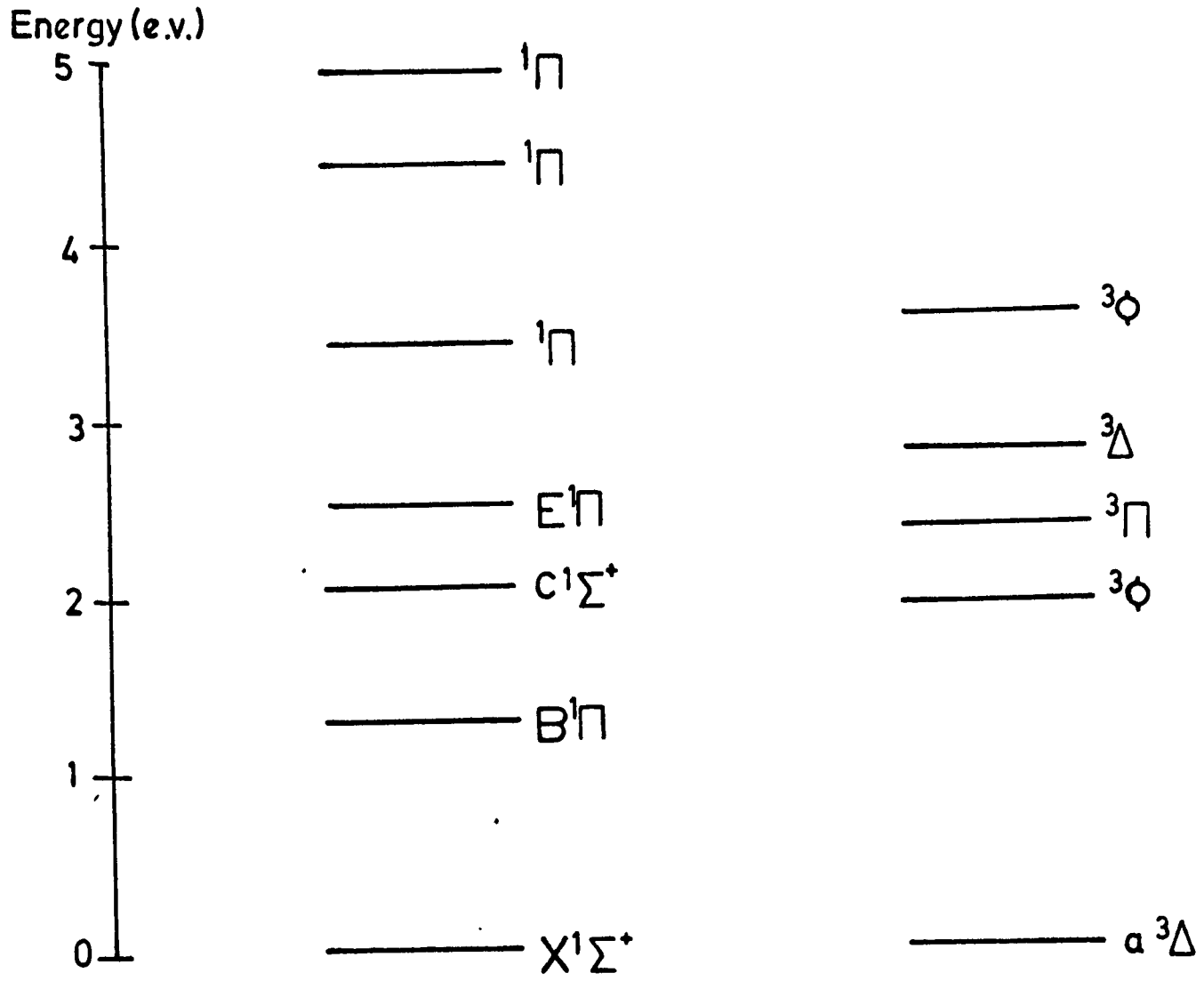



Figure 3.1.

Known Electronic States of ScF.

again no forbidden singlet-triplet transitions are known. These states are shown in Figure 3.2.

The lowest lying triplet states of both ScF and TiO have been identified spectroscopically as $^3\Delta$, and they are certainly derived from the same electron configuration in each molecule. In TiO a low-lying $^1\Delta$ state is known, and this would be expected to be derived from the same configuration as the $^3\Delta$ state. The splitting between these two states is not known accurately as no intercombination bands are known, not have any suitable perturbations been analysed, but it has been estimated as 600 $cm^{-1}$ by Phillips (1952) from the variation of the intensities of the bands with temperature. However the uncertainty in this value may be as high as 100%. In ScF the splitting is perhaps rather larger, as no transitions from the $^1\Delta$ state have been observed. The lowest singlet state in ScF is $^1\Sigma$; in TiO the $^1\Sigma$ state is known to lie 2200 $cm^{-1}$ above the $^1\Delta$, as both states give transitions to the $b^1\Pi$ state. In neither case is a $^3\Sigma$ state observed, and it is therefore expected that the $^1\Sigma$ state corresponds to a closed shell electron configuration. These arguments have been supported by molecular orbital calculations by Carlson and Nesbet (1964) and Carlson and Moser (1967), which show that the low-lying states are derived from the configurations $9\sigma^2$ and $9\sigma 1\delta$, where the $9\sigma$ orbital is mainly 4s (Sc) and the $1\delta$ is 3d (Sc).

Two $^3\Phi$ states are known in ScF, and they play an important role in the assignment of configurations to the excited states. No $^1\Phi$ states are known, as they would only be expected in combination with the $^1\Delta$ state, but one $^1\Phi$ state is known in TiO. The $\Phi$ states arise from configurations of the type $\delta\pi$, and these configurations also give rise to $\Pi$ states; thus the $\Phi$ states may be used as a guide to the assignment of configurations to the $\Pi$ states, provided that there is some knowledge of the relative energies of the $\Phi$ and $\Pi$ states from $\delta\pi$ configurations. This problem has been tackled in Chapter 2. There are four $^1\Pi$ states known in ScF; the lowest state, $B^1\Pi$, is assigned an energy of 10,700 $cm^{-1}$, although this is based on the assumption that the longest

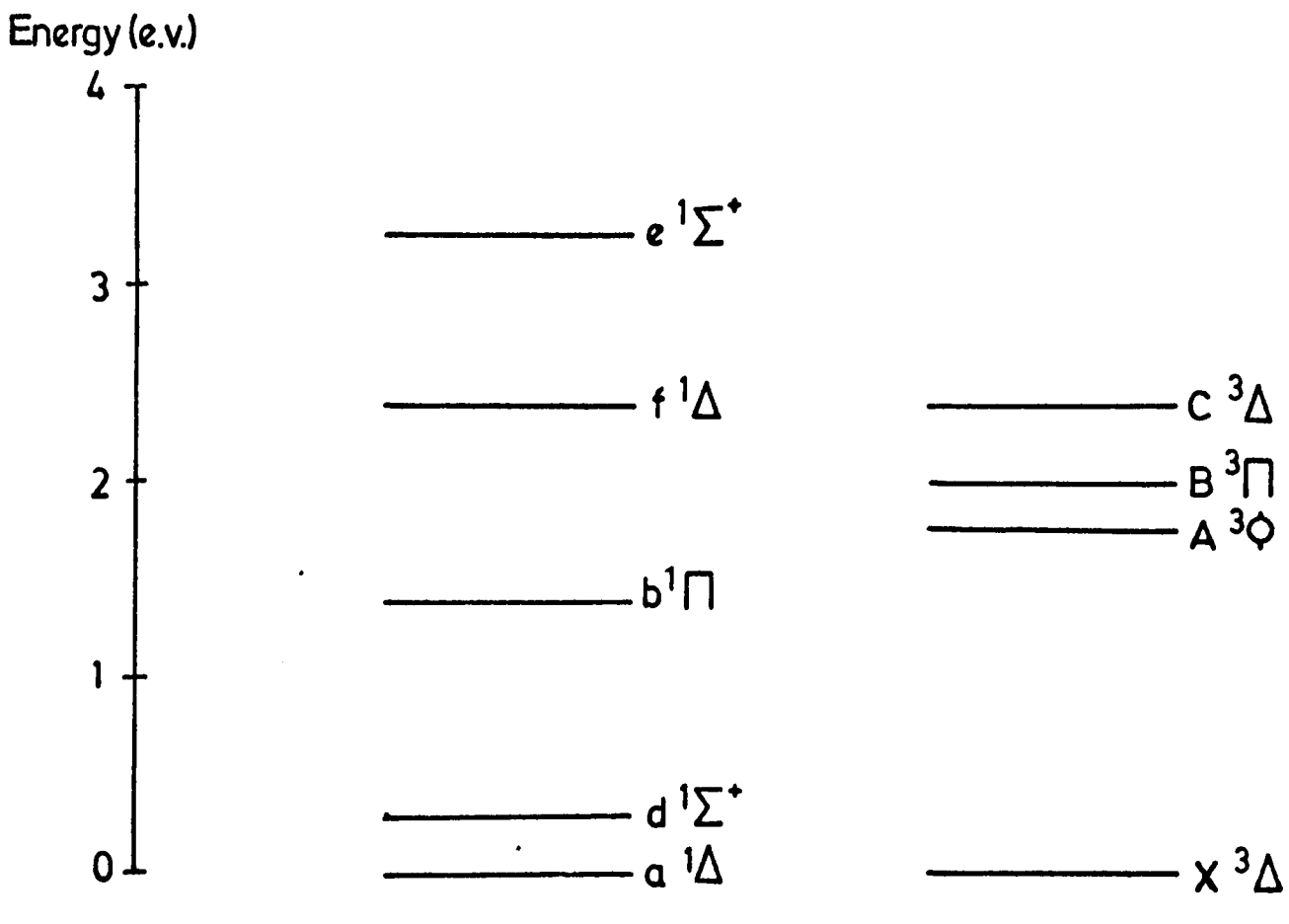



Figure 3.2.

Known Electronic States of TiO.

wavelength band so far observed is the 0-0 band. So far it has proved experimentally difficult to observe bands at longer wavelengths which could confirm this assignment. The $B^1\Pi$ state may be assigned the configuration $9\sigma 4\pi$, where the $4\pi$ orbital is mainly 3d (Sc), and the $E^1\Pi$ state at 20,200 $cm^{-1}$ assigned the $3d\delta\ 3d\pi$ configuration. In this way it is possible to account for all the observed $\Pi$ and $\Phi$ states using the 4s, 4p and 3d scandium orbitals, and to predict approximate positions of undetected states. From these predictions it is possible to suggest reasonable assignments for the remaining $\Delta$ and $\Sigma$ states, and this has been done by Brewer and Green (1969). Table 3.1 shows the configurations of all the states of ScF, along with their observed or estimated energies. An error in their proposed energies of the $^1\Phi$ states in ScF has been corrected (see Chapter 2).

This analysis of the low-lying and excited states of ScF may be carried over to the isoelectronic molecule TiO; however, one problem presents itself. In ZrO, which has an isoelectronic valence shell, many of the states have been assigned to configurations of the type $3\pi^3$...., where the $3\pi$ orbital is mainly non-metal $2p\pi$ (Weltner and McLeod 1965). There is little doubt that such configurations are not important in ScF; Scott (1972) has shown that these configurations do not give rise to bound states, and similar evidence exists in the case of other fluorides (So and Richards 1974), but it is possible that in the oxides they are more important. It has been suggested (Cheetham and Barrow 1967) that in PbO some of the low-lying states may be derived from the configuration $\pi_0^3\sigma^2\pi$. We may therefore conclude that although all the available experimental evidence on TiO may be explained by analogy with ScF, that this is not necessarily the only possible explanation.

Table 3.1

Observed and Estimated Energy Levels in ScF

| Configuration | State | Energy ($cm^{-1} \times 10^3$) |
|---|---|---|
| $s\sigma^2$ | $^1\Sigma^+$ | 0.0 |
| $s\sigma$ $d\delta$ | $^3\Delta$ | 0.0 |
| | $^1\Delta$ | 2 |
| $s\sigma$ $d\pi$ | $^3\Pi$ | 8 |
| | $^1\Pi$ | 10.7 |
| $d\delta$ $d\pi$ | $^3\Phi$ | 15.3 |
| | $^1\Phi$ | 21 |
| | $^3\Pi$ | 18.3 |
| | $^1\Pi$ | 20.3 |
| $s\sigma$ $d\sigma$ | $^3\Sigma^+$ | 14 |
| | $^1\Sigma^+$ | 16.1 |
| $d\delta$ $d\sigma$ | $^3\Delta$ | 21.9 |
| | $^1\Delta$ | 24 |
| $s\sigma$ $p\pi$ | $^3\Pi$ | 24 |
| | $^1\Pi$ | 26.8 |
| $d\delta$ $p\pi$ | $^3\Phi$ | 27.2 |
| | $^1\Phi$ | 36 |
| | $^3\Pi$ | 31 |
| | $^1\Pi$ | 34.9 |

## 3.3 The Nature of the Problem

Two problems remain in the account of the electronic structure of ScF presented above. The first concerns the difference in energies between the 3d and 4p orbitals. The spectrum of scandium monoxide has been extensively studied, and shows that the ground state is $^2\Sigma^+$; e.s.r. work (Weltner et al. 1967) has shown that the unpaired electron has mainly 4s (Sc) character. Two excited states are known, $^2\Pi$ and $^2\Sigma^+$ as shown in Figure 3.3. The equality of the spin-splitting and Λ-doubling constants in these states have been interpreted as evidence that the unpaired electron in both states is essentially a 4p electron in pure precession. The three states in which the 3d orbital is occupied have not been observed in ScO, although a calculation by Green (1971) predicted that the $^2\Delta$ state, which would presumably be the lowest-lying of the 3d states, lies above the observed $^2\Pi$ state. Furthermore, in the molecule LaO, which has an isoelectronic valence shell, two $^2\Pi$ and two excited $^2\Sigma^+$ states are known; here the lower states have been interpreted as arising from the 6p orbital, and the higher states as arising from the 5d orbitals. Inspection of Table 3.1 shows that in ScF the difference in energies of the $^3\Phi$ states, which corresponds to the 3dπ–4pπ energy difference, is 1.5 e.v. Also the difference between the $E^1\Pi$ state ($1\delta 3d\pi$) and the $^1\Pi$ state ($1\delta 4p\pi$) is 1.8 e.v., and that between the $B^1\Pi$ state ($9\sigma 3d\pi$) and the $^1\Pi$ state ($9\sigma 4p\pi$) is 2.0 e.v., in each case with the 3dπ orbital being more stable than the 4pπ. Thus it would seem that in ScO the 3d orbital lies above the 4p orbital, whereas in ScF the reverse is true. Furthermore, the 4s→4p excitation energy is about 2 e.v. in ScO, but about 4 e.v. in ScF. There has been no satisfactory explanation of these discrepancies between the interpretations of the structures of ScF and ScO.

A second problem concerns the intensities of the bands observed in ScF. Four $^1\Pi$–$X^1\Sigma^+$ transitions have been observed in absorption experiments at about 2000°K; they all appear with roughly comparable intensities, and it is not

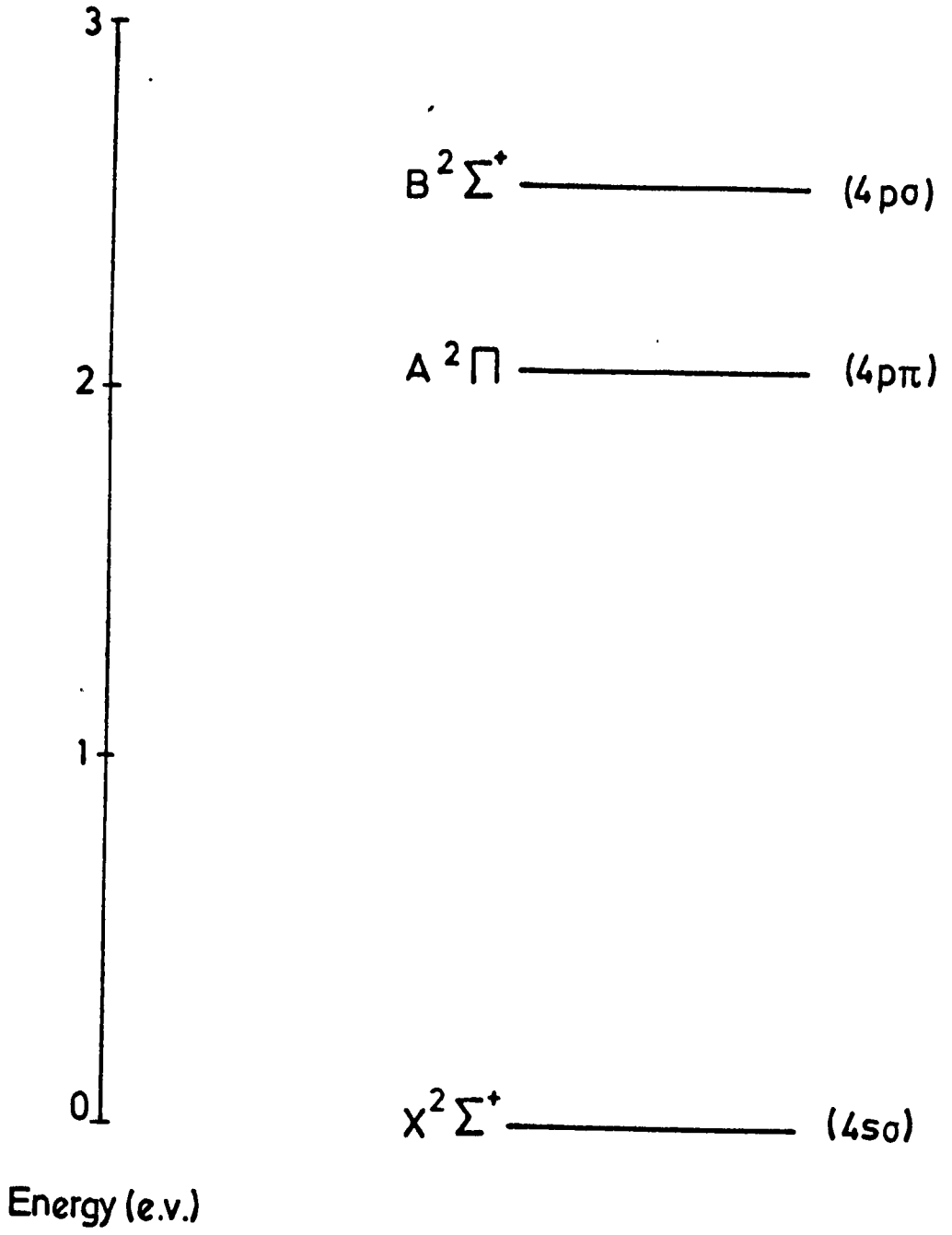



Figure 3.3.

Known Electronic States of ScO.

clear from the spectrum that some transitions are allowed, whereas others are to some extent forbidden. Yet if we assign the configuration $9\sigma^2$ to the $X^1\Sigma^+$ state, then only transitions to the $^1\Pi$ states corresponding to the configurations $9\sigma 4\pi$ and $9\sigma 5\pi$ are allowed. The transitions $9\sigma^2 \rightarrow 1\delta 4\pi$ and $9\sigma^2 \rightarrow 1\delta 5\pi$ are both two-electron jumps, and are formally forbidden.

## 3.4 Summary of Previous Theoretical Work on ScF and TiO

There have been three papers published giving results of ab initio calculations on ScF and the isoelectronic molecule TiO. Carlson and Nesbet (1964) described a calculation on TiO which used a basis set of nineteen Slater-type orbitals. Variational calculations were performed on the $^1\Sigma^+$ and $^3\Delta$ states of the molecule, and excitation energies were obtained for many excited states by the virtual orbital approximation. They showed that the configurations of the low-lying states were $4s^2$ and $4s3d$. The internuclear distances were predicted correct to 10%, but the values of $\omega_e$ were all approximately 1200 $cm^{-1}$, whereas the experimental results are in the range 800-1000 $cm^{-1}$. As is expected from the use of the virtual orbital approximation, the excitation energies were all too large, but also gave some surprising results. The lowest $^1\Pi$ state corresponded to the configuration $1\delta4\pi$, whereas the lowest $^3\Pi$ state was derived from the configuration $9\sigma4\pi$. Configurations involving the excitation of a $3\pi$ electron (mainly $2p\pi$ on oxygen) were predicted to be of comparable energies to configurations such as $1\delta4\pi$.

In 1967, Carlson and Moser published the results of calculations on ScF and TiO using a basis set of twenty four Slater-type orbitals. They calculated the $^1\Sigma^+$ and $^3\Delta$ states variationally, and the $^1\Delta$ state by the use of invariant orbitals. They estimated the defects from the Hartree-Fock limit in the atoms to be 0.642 a.u. for Sc and 0.055 a.u. for F. They concluded that the uncorrelated ground state of ScF is $^3\Delta$, which was predicted to be more stable than the $^1\Sigma^+$ state by 0.0207 a.u., but that empirical estimates of the correlation energy differences would reverse this ordering. The internuclear separations were predicted correct to 3% in ScF, and 6% in TiO. The $\omega_e$ values were inaccurate by 40% in ScF, and again the variation in $\omega_e$ from state to state was not reproduced . In TiO the values of $\omega_e$ were inaccurate by 70%.

In 1972 Scott described calculations on ScF in a much larger basis set of forty two Slater-type orbitals; variational calculations were described for the $^1\Sigma^+$ and $^3\Delta$ states, and also for several configurations in which an electron is excited from the $3\pi$ orbital (mainly $2p\pi$ on F). The spectroscopic constants were found to be in much closer agreement with experiment, and the $^1\Sigma^+ - {}^3\Delta$ splitting was less than half that predicted by Carlson and Moser. States in which an electron was excited from the F atom were shown to be highly excited, and to be repulsive at all distances.

Since 1967 an increase in sophistication in computer programming, speed and capacity has produced the situation where it is now possible to perform calculations on molecules with a relatively large number of electrons such as ScF using a much larger basis set than those of Carlson and co-workers. Wave functions may now be produced which are relatively close to the Hartree-Fock limit, which are not biased in favour of either centre, and which possess sufficient flexibility to represent many states of the molecule satisfactorily; also it is possible to compute wave functions which include a limited amount of configuration interaction. In this work (Scott and Richards, 1974) calculations are performed on the excited states of ScF; the limitations involved in the truncation of the basis set may be estimated by comparing calculations on the low-lying states, whose electronic structures are well-known, with experimental observations. The calculations are then used to suggest reassignments of the configurations of some of the state, and to indicate where single configuration wave functions may be inadequate.

## 3.5 Choice of the Basis Set

Although use of a very large basis set is clearly likely to give wave functions which are very close to the Hartree-Fock limit, as the time involved in integral evaluation increases as the third or fourth power of the size of the basis set, and convergence is harder to obtain the larger the basis set, the availability of computer time limits the size of basis set which may be employed. The starting point for a molecular calculation is usually an atomic basis set, and this is then augmented by other functions. These functions may represent orbitals which are not occupied in the ground state of the atom, or may be orbitals of higher angular momentum to represent polarisation and angular distortion.

There are several sets of functions available for the transition metals, and the one selected in this work is the double zeta set of Clementi et al. (1967). This gives an energy which is quite close to the Hartree-Fock limit, while using a relatively small number of functions. Clementi's double zeta set for the F atom (Clementi 1964) has also been employed as it is important to use basis functions of comparable accuracy for both atoms. Clementi's set for Sc includes no 4p basis functions, and these will be important in work on the excited states of ScF; two 4p functions have been added in each symmetry, one with an exponent taken from the work of Carlson and Moser (1967), and the other with an exponent optimised for the equilibrium internuclear separation of the $X^1\Sigma^+$ state. This is expected to be a satisfactory procedure, as the main difficulty of the basis set is in representing the 4p contributions to the diffuse 9σ orbital; however the effect of varying the 4p exponents on the states in which the 4p orbital is occupied was tested extensively to ensure that the results presented below are not basis set dependent. It was found that although the total energy of the molecule is fairly sensitive to the exact choice of the 4p exponents, the differences in energy between states

is much less sensitive to such variations; the variation in the total energy is due to the part played by the 4p functions in representing the core orbitals of the molecule. Further functions which have been added are 3s and 3d functions on F, following the work of Cade and Huo (1967), and 4f functions to represent angular distortion. The 4f functions make a rather small contributions to the total energy and their exponent has not been optimised. A 3dδ function in fluorine was also added, as it had been suggested that a similar function could be important in ScO (Carlson et al. 1965), but in spite of exponent optimisation the total contribution to the energy was never greater than $3 \times 10^{-5}$ a.u., and so this function was omitted. Details of the full basis set used are given in Table 3.2.

The calculations were performed using the ALCHEMY programme, which has been described above. A typical time for a calculation on ScF using forty two basis functions, with eight iterations, on the 360/195 computer at the Rutherford High Energy Laboratory would be four minutes, of which ninety seconds would be taken in integral evaluation. For a configuration interaction calculation, transformation of the integrals would require a further forty-five seconds; the time required for the other steps is negligible provided that the number of configurations is small.

Table 3.2

STO Basis Functions

| | | | |
|---|---|---|---|
| 1. | 1sσ | Sc | 17.29 |
| 2. | 1sσ | Sc | 22.7566 |
| 3. | 2sσ | Sc | 8.2528 |
| 4. | 2sσ | Sc | 10.8582 |
| 5. | 3sσ | Sc | 3.4054 |
| 6. | 3sσ | Sc | 5.3205 |
| 7. | 4sσ | Sc | 1.9277 |
| 8. | 4sσ | Sc | 1.0507 |
| 9. | 2pσ | Sc | 7.6297 |
| 10. | 2pσ | Sc | 13.4947 |
| 11. | 3pσ | Sc | 4.2055 |
| 12. | 3pσ | Sc | 2.6867 |
| 13. | 4pσ | Sc | 3.5863 |
| 14. | 4pσ | Sc | 1.0837 |
| 15. | 3dσ | Sc | 1.8554 |
| 16. | 3dσ | Sc | 4.5843 |
| 17. | 4fσ | Sc | 2.75 |
| 18. | 1sσ | F | 7.9179 |
| 19. | 1sσ | F | 11.011 |
| 20. | 2sσ | F | 1.9467 |
| 21. | 2sσ | F | 3.076 |
| 22. | 3sσ | F | 9.9254 |
| 23. | 2pσ | F | 1.8454 |
| 24. | 2pσ | F | 4.1710 |

Continued....

Table 3.2 continued

| | | | |
|---|---|---|---|
| 25. | 3dσ | F | 1.8354 |
| 26. | 3dσ | F | 3.368 |
| 27. | 4fσ | F | 2.7001 |
| 28. | 2pπ | Sc | 7.6297 |
| 29. | 2pπ | Sc | 13.4947 |
| 30. | 3pπ | Sc | 4.2055 |
| 31. | 3pπ | Sc | 2.6867 |
| 32. | 4pπ | Sc | 3.5863 |
| 33. | 4pπ | Sc | 1.0837 |
| 34. | 3dπ | Sc | 1.8554 |
| 35. | 3dπ | Sc | 4.5843 |
| 36. | 4fπ | Sc | 2.75 |
| 37. | 2pπ | F | 4.1710 |
| 38. | 2pπ | F | 1.8454 |
| 39. | 3dπ | F | 2.1338 |
| 40. | 4fπ | F | 2.7936 |
| 41. | 3dδ | Sc | 1.8554 |
| 42. | 3dδ | Sc | 4.5843 |

## 3.6 The Results of Hartree-Fock Calculations

### 3.6.1 Calculations on the Sc and F atoms

Initial calculations were performed on the ground states of the Sc and F atoms, which are $^2D$ and $^2P$ respectively. The energies obtained, and the defects from the Hartree-Fock limits are shown in Table 3.3. The values of

Table 3.3

| | Sc | F | |
|---|---|---|---|
| Hartree-Fock limit | -759.73555 | -99.40930 | a.u. |
| This work | -759.72219 | -99.40186 | a.u. |
| Defect | 0.01336 | 0.00744 | a.u. |

the energies of the atoms at the Hartree-Fock limit are taken from Roetti and Clementi (1974).

### 3.6.2 Calculations on the Low-Lying States of ScF

Approximate wave functions for the low-lying $^1\Sigma^+$ and $^3\Delta$ states are already known from the work of Carlson and Moser, and these provide a guide for obtaining trial vectors in the larger basis. The states correspond to the configurations $1\rightarrow 9\sigma^2\ 1\rightarrow 3\pi^4$ and $1\rightarrow 8\sigma^2\ 1\rightarrow 3\pi^4\ 9\sigma 1\delta$ respectively. Calculations were performed for six internuclear separations around the equilibrium value, and the energies obtained are shown in Table 3.4. Spectroscopic constants were obtained by the method of Todd (Richards et al., 1974, Todd 1967), and are given in Table 3.4, along with the experimental values. The agreement between the calculated and observed spectroscopic constants is encouraging. The internuclear distances are accurate to 0.8% and 0.3%, this agreement perhaps being fortuitously good; the vibrational frequencies are too large by 10%, as is expected from the use of single configuration wave functions. However, the differences in frequencies between the two states is satisfactorily reflected in the calculated values. The $^3\Delta$ state is the uncorrelated ground

Table 3.4

Energies and Spectroscopic Constants of the Low-Lying States of ScF

| R (a.u.) | $^1\Sigma^+$ | $^3\Delta$ |
|---|---|---|
| 3.21 | -859.271471 | |
| 3.26 | .273899 | |
| 3.31 | .275252 | |
| 3.36 | .275656 | -859.282248 |
| 3.41 | .275223 | .284041 |
| 3.46 | | .285025 |
| 3.51 | .272245 | .285294 |
| 3.61 | | .284010 |
| 3.66 | | .282602 |

| | $^1\Sigma^+$ | $^3\Delta$ |
|---|---|---|
| $r_e$ (calc.) (Å) | 1.777 | 1.855 |
| $r_e$ (expt.) (Å) | 1.791 | 1.859 |
| $\omega_e$ (calc.) ($cm^{-1}$) | 813 | 708 |
| $\Delta G_{1/2}$ (expt.) ($cm^{-1}$) | 728 | 643 |
| $T_e$ (calc.) ($cm^{-1}$) | 2115 | 0 |

state, but the $^1\Sigma^+$ state lies only 0.3 e.v. higher; correlation effects would be expected to stabilise the $^1\Sigma^+$ state, in which the $9\sigma$ orbital is doubly occupied, relative to the $^3\Delta$ state.

3.6.3 Calculations on the Excited States of ScF

Ideally in order to assign configurations to all the excited $\Pi$ and $\Phi$ states we would wish to perform calculations on the four configurations $9\sigma 3d\pi$, $9\sigma 4p\pi$, $1\delta 3d\pi$ and $1\delta 4p\pi$. Comparison of calculated spectroscopic constants with experimental data should then allow states and configurations to be matched. However the nature of the calculations performed here is variational, and it is therefore in general very difficult to obtain convergence on states which are not the lowest of their symmetry. In this sense the $\Pi$ states from the configurations of the types $\sigma\pi$ and $\delta\pi$ count as being of different symmetries. Thus although we may obtain convergence on two of the $\Pi$ states, it is not possible to obtain variational results for all four configurations. However, those states for which convergence is obtained should be the lowest of their symmetries.

Calculations were performed for the lowest $^3\Pi$ and $^1\Pi$ states, which are derived from the configuration $9\sigma 4\pi$. The energies obtained and the derived spectroscopic constants are given in Table 3.5. Also shown are the population analyses of the valence orbitals, which clearly show that the orbitals are quite well described as $4s\sigma 3d\pi$, which is the conventional assignment of the $B^1\Pi$ state. The agreement between the observed and calculated spectroscopic constants of the $B^1\Pi$ state is quite satisfactory: the calculated $B^1\Pi - X^1\Sigma^+$ excitation energy is too small, as it is expected that correlation effects would stabilise the $^1\Sigma^+$ state relative to the $^1\Pi$. The relative energies of the singlet and triplet manifolds are not known exactly, but the energy difference between the $a^3\Delta$ and $B^1\Pi$ states, which might have rather similar correlation energies, is probably in error by less than 1000 $cm^{-1}$. The $^3\Pi$-$a^3\Delta$ transition is predicted to lie at about 20,000 Å, and this explains why

Table 3.5

Energies and Spectroscopic Constants of the Π States of ScF

| R (a.u.) | $^3\Pi$ | $^1\Pi$ |
|---|---|---|
| 3.41 | -859.260178 | |
| 3.46 | | -859.240890 |
| 3.51 | .262574 | |
| 3.56 | .262800 | .243010 |
| 3.61 | .262468 | .243102 |
| 3.66 | | .242648 |
| 3.71 | .260377 | .241712 |

| | $^3\Pi$ | $^1\Pi$ |
|---|---|---|
| $r_e$ (calc.) (Å) | 1.881 | 1.901 |
| $r_o$ (expt.) (Å) | | $\leq$ 1.923 |
| $\omega_e$ (calc.) ($cm^{-1}$) | 665 | 670 |
| $\Delta G_{\frac{1}{2}}$ (expt.) ($cm^{-1}$) | | $\geq$ 582 |
| $T_e$ (calc.) ($^3\Delta$-$^3\Pi$) | 5002 | |
| ($^1\Sigma^+$-$^1\Pi$) | | 7138 |

Population Analysis ($^1\Pi$ State, R = 3.61 a.u.)

| | 4s(Sc) | 4p(Sc) | 3d(Sc) | 2s(F) | 2p(F) |
|---|---|---|---|---|---|
| 9σ | 0.834 | 0.155 | 0.009 | 0.000 | 0.002 |
| 4π | | 0.007 | 0.977 | | 0.016 |

it has not been observed so far. It would be expected that observation could be experimentally quite difficult.

Calculations were also performed on the lowest $^3\Phi$ state, which is derived from the configuration $1\delta 4\pi$, and also on the $^1\Pi$ state from that configuration. Previous work has shown that configurations such as $3\pi^3 9\sigma^2 1\delta$ are highly excited, and need not be considered (Scott 1972). The energies obtained and the derived spectroscopic constants are given in Table 3.6, with the population analysis of the $^3\Phi$ state at the calculated equilibrium internuclear distance. The most important and striking result is that the $4\pi$ orbital is now almost entirely 4p(Sc), and not 3d(Sc) as previously suggested. This applies to both the $^3\Phi$ and $^1\Pi$ states, and shows that the nature of the $4\pi$ orbital depends on the occupancy of the other orbitals. When the $9\sigma$ orbital (mainly 4s(Sc)) is occupied, the $4\pi$ orbital has mainly 3d(Sc) character, whereas when the $1\delta$ orbital (3d(Sc) character) is occupied, the $4\pi$ orbital becomes mainly 4p(Sc).

The agreement between the calculated and observed spectroscopic constants for the $^3\Phi$ and $^1\Pi$ states is now rather poorer than has been found for the lower-lying states of ScF. The calculated $^3\Phi - a^3\Delta$ excitation energy is in error by about 1 e.v., the vibration frequency is rather too high, and the calculated internuclear separation is not as close to experiment as in other states, although the difference is still not unreasonable for a Hartree-Fock calculation. There are three possible causes of these discrepancies, and these will be discussed in turn.

Firstly it is possible that the observed states may not be described well by a single configuration wave function. This possibility is discussed in section 3.7 when configuration interaction calculations are carried out on the excited $\Pi$ and $\Phi$ states.

A second possibility is that the basis set is able to represent the 3d and 4s orbitals rather better than the 4p orbital, and that for this reason the states involving the 4p orbital appear to be too highly excited. This possibility was excluded by extensive variation of the 4p basis functions;

Table 3.6

The $^3\Phi$ and $^1\Pi$ States of ScF

| R (a.u.) | $^3\Phi$ | $^1\Pi$ |
|---|---|---|
| 3.41 | -859.179290 | -859.151413 |
| 3.51 | .179811 | .156715 |
| 3.61 | .177977 | .160650 |
| 3.71 | .174348 | .162773 |
| 3.81 | .169377 | .162530 |

| | $^3\Phi$ | $^1\Pi$ |
|---|---|---|
| $r_e$ (calc.) (Å) | 1.841 | 1.835 |
| $r_o$ (expt.) (Å) | 1.896 | |
| $\omega_e$ (calc.) ($cm^{-1}$) | 708 | 714 |
| $\Delta G_{\frac{1}{2}}$ (expt.) ($cm^{-1}$) | 564 | |
| $T_e$ (calc.) ($^3\Delta$-$^3\Phi$) | 23125 | |
| ($^1\Sigma^+$-$^1\Pi$) | | 24727 |

Population Analysis

| | 4p(Sc) | 3d(Sc) | 2p(F) |
|---|---|---|---|
| 1δ | - | 1.00 | - |
| 4π | 0.87 | 0.12 | 0.00 |

it was found that no matter what exponents of the 4p functions are used, the $^3\Phi$-$a^3\Delta$ excitation energy remains sensibly unchanged. This is direct evidence that our basis set is sufficiently flexible to represent all the states of the molecules adequately, as is expected from a basis set of double zeta quality.

The third possibility is that the state on which we have obtained convergence is not in fact the lowest state of its symmetry, and that the calculation has become 'trapped' in an excited state. The true lowest $^3\Phi$ state could still correspond to the configuration $3d\delta 3d\pi$, which would explain the relatively poor agreement between the observed and calculated spectroscopic constants. There are several reasons for believing that this is not the case. Firstly, considerable effort has been expended attempting to obtain convergence on the $3d\delta 3d\pi$ state by use of various trial vectors, and by varying the convergence conditions of the calculation. All these have failed to produce the required state. Secondly, we may obtain some evidence on the energy of the $3d\delta 3d\pi$ state from the position of the $^3\Sigma^-$ state from the configuration $3d\delta^2$; a calculation has been performed on this state, which is of interest as it is predicted to be the ground state by crystal field theory (Berg and Sinanoglu, 1960). This state is calculated to lie 1.8 e.v. higher than the $^3\Phi$ state; furthermore, the $3d\pi$ orbital is known to be less stable than the $3d\delta$ orbital by 0.6 e.v. from the calculations on the $^3\Delta$ and $^3\Pi$ states described above. It is possible that the repulsion between two electrons in a $3d\delta$ orbital is greater than that between one electron in a $3d\delta$ orbital and one in a $3d\pi$ orbital, but it seems unlikely that this effect could be larger than the 2.4 e.v. which would be necessary to depress the $3d\delta 3d\pi$ state below the $3d\delta 4p\pi$. Thirdly, further evidence on the position of the $3d\delta 3d\pi$ state may be obtained from performing calculations omitting the more diffuse $4p\pi$ function. It is then easy to obtain convergence on the required state. Now the contribution of the omitted $4p\pi$ function to the $3d\pi$ orbital is expected to be very small,

and may be neglected, but the contribution to the $1\pi$, $2\pi$, and $3\pi$ orbitals may not be so small. This defect may be roughly estimated by performing calculations on the $9\sigma 3d\pi$ state with and without the $4p\pi$ function. The results of these calculations are summarised in Table 3.7. In all cases the calculations are performed at the internuclear distance R=3.61 a.u. Although they may only be regarded as rough calculations, they do provide further evidence that the configuration $3d\delta 3d\pi$ lies appreciably higher than the $3d\delta 4p\pi$, and that the assignment of the configurations $3d\delta 4p\pi$ to the $^3\Phi$ state at 15,000 $cm^{-1}$ is correct.

Table 3.7

The 3dδ3dπ Configuration of ScF

| | | | |
|---|---|---|---|
| $^3\Phi$ | (3dδ4pπ) | 42 basis functions | E = -859.177977 |
| $^3\Phi$ | (3dδ3dπ) | 41 basis functions | E = -859.120716 |
| $^3\Pi$ | (4sσ3dπ) | 42 basis functions | E = -859.262468 |
| $^3\Pi$ | (4sσ3dπ) | 41 basis functions | E = -859.247760 |
| | | | .014708 |
| Estimated $^3\Phi$ | (3dδ3dπ) | 42 basis functions | E = -859.135424 |

## 3.7 The Results of Configuration Interaction Calculations

One important aspect of the structure of the transition metal diatomic molecules which has not so far been studied by any workers is the extent to which it is possible to represent observed electronic states by single configuration wave functions. This is due to the computational difficulties in performing a configuration interaction calculation for a molecule as large as ScF. It is still not computationally feasible to perform the very extensive configuration interaction which would be necessary, for example, to identify unambiguously the correlated ground state of the molecule, or to predict accurately vibration frequencies. This might require of the order of hundreds of thousands of configurations. However, it is possible to obtain some insight into the electronic structure of the electronic states of ScF using only a very limited configuration interaction, with just a few excited configuration state functions.

In the ALCHEMY programme the excited configurations are obtained from the variationally computed wave function by replacing occupied orbitals by virtual orbitals. The virtual orbitals are orthogonal to the occupied orbitals, which simplifies the calculation, but in general the virtual orbitals provide a rather poor description of the excited orbitals; thus excitation energies calculated in a virtual orbital approximation are usually appreciably too large. If many thousands of configurations are to be employed this is not a great disadvantage, as the virtual orbitals act simply as a convenient basis set for the configuration interaction expansion. But if we wish to consider only the interaction of two or three states with each other, in order to gain some chemical insight, then it is important to remember that in general the non-variational states will be rather poorly represented and that the results obtained will not be quantitatively reliable.

One possible limitation to the reassignment of the configurations of the $^3\Phi$ states suggested in section 6 is that, as there are known to be

two $^3\Phi$ states separated by only 1.5 e.v., there may be appreciable mixing between the configurations $3d\delta 3d\pi$ and $3d\delta 4p\pi$, and that it may not be possible to describe either state adequately by a single configuration. A 2 x 2 configuration interaction calculation was therefore performed to obtain the off-diagonal matrix element between these two configurations. The calculation was performed at the internuclear separation R = 3.61 a.u., and the off-diagonal matrix element was found to be less than $4 \times 10^{-6}$ a.u. This is negligibly small in comparison to the energy difference between the two configurations, and even though this value may be slightly too small, owing to the use of the virtual orbital to represent the $3d\pi$ orbital, it may be concluded that there is no first order mixing between the $3d\delta 4p\pi$ and $3d\delta 3d\pi$ configurations.

A second possibility which has been considered is that there could be significant mixing between the $1\delta 4\pi$ configuration and the configuration $3\pi^3 9\sigma^2 1\delta$, in which an electron is excited from the fluorine 2p orbital Although this state is rather more highly excited than the $1\delta 5\pi$ configuration, it is an attractive suggestion for several reasons. The state represents a two-electron excitation from the $1\delta 4\pi$ configuration, and might therefore be expected to give rise to a rather larger off-diagonal matrix element than the $1\delta 5\pi$ configuration. As this is a repulsive state, any configuration mixing would be expected to increase with increasing internuclear separation, and this would have the result of decreasing the vibration frequency of the lower state. Furthermore, as the configuration $3\pi^3 9\sigma^2 1\delta$ would be expected to be the lowest-lying of the 'charge transfer' configurations, it provides a ready mechanism for lowering the calculated $^3\Phi - a^3\Delta$ excitation energy. A 3 x 3 configuration interaction calculation was performed, and the results are shown in Table 3.8. There are several conclusions to be drawn from these results. The second-order mixing between the $3d\delta 4p\pi$ and $3d\delta 3d\pi$ configurations, that is the mixing via the third configuration, is very small, and need not be considered in a discussion of the electronic structure of the

Table 3.8

C.I. Calculations on the $^3\Phi$ States of ScF

| | |
|---|---|
| Configuration I | $3\pi^4\ 1\delta 4\pi$ |
| Configuration II | $3\pi^4\ 1\delta 5\pi$ |
| Configuration III | $3\pi^3\ 9\sigma^2 1\delta$ |

Energy Matrix

| | I | II | III |
|---|---|---|---|
| I | -911.52283 | -0.000004 | -0.003091 |
| II | | -911.44547 | 0.001522 |
| III | | | -911.24809 |

$\Phi_1 = 0.999937\ \Psi_1 \quad -0.000176\ \Psi_2 \quad +0.011250\ \Psi_3$

$\Phi_2 = 0.000262\ \Psi_1 \quad +0.999970\ \Psi_2 \quad -0.007688\ \Psi_3$

$\Phi_3 = -0.011248\ \Psi_1 \quad +0.007690\ \Psi_2 \quad +0.999907\ \Psi_3$

Stabilisation of lowest state = 0.000035 a.u.

of the $^3\Phi$ states. The off-diagonal matrix element for the two-electron excitations is as expected much larger than that for the one-electron excitation, but the coefficient of the excited configuration in the final wave function is still only 0.011. The total change in the energy is only about $10^{-3}$ e.v., which is too small to have any marked effect on any of the calculated spectroscopic constants.

A further problem which must be considered is configuration mixing within the $\Pi$ states. There are two reasons for believing that mixing may be more important in the $\Pi$ states than in the $\Phi$ states. Firstly, there are four low-lying $\Pi$ states, from the configurations $9\sigma 4\pi$, $9\sigma 5\pi$, $1\delta 4\pi$ and $1\delta 5\pi$, and thus many of the off-diagonal matrix elements will correspond to two-electron excitations. Secondly, appreciable configuration mixing would provide a simple mechanism for obtaining comparable intensity in all four $^1\Pi - X^1\Sigma^+$ transitions. Variational calculations were performed on the $^3\Pi$ state from the configuration $9\sigma 4\pi$ at R=3.61 a.u., and the interaction with three excited states was computed. The results are summarised in Table 3.9. The difference between these results and those for the $\Pi$ states is most marked. Although it is unreasonable to attach too great a quantitative significance to these mixing coefficients, it is quite clear that although the lowest $^3\Pi$ state is quite well described by a single configuration wave function, there is very considerable mixing between the remaining three configurations. The $1\delta 4\pi$ configuration has a coefficient of only 0.038 in the lowest state, and the other two excited configurations make an even smaller contribution. However, the remaining three states can clearly not be adequately described by a single configuration. As is expected, the excitation energies of the upper states are too large; nevertheless the calculations do show that if we had been able to use a reasonable representation for the excited states as well as for the lowest state, that the off-diagonal matrix elements would be sufficiently large to produce very extensive configuration mixing.

Table 3.9

C.I. Calculations on the $^3\Pi$ States of ScF

| | |
|---|---|
| Configuration I | $9\sigma\ 3d\pi$ |
| Configuration II | $9\sigma\ 4p\pi$ |
| Configuration III | $1\delta\ 3d\pi$ |
| Configuration IV | $1\delta\ 4p\pi$ |

$$\Phi_1 = 0.999263\ \Psi_1 + 0.001937\ \Psi_2 + 0.006331\ \Psi_3 + 0.037823\ \Psi_4$$

$$E = -859.262651$$

$$\Phi_2 = -0.029188\ \Psi_1 + 0.583728\ \Psi_2 + 0.467911\ \Psi_3 + 0.662925\ \Psi_4$$

$$E = -859.157333$$

$$\Phi_3 = 0.018734\ \Psi_1 + 0.811920\ \Psi_2 - 0.329774\ \Psi_3 - 0.481336\ \Psi_4$$

$$E = -859.142477$$

$$\Phi_4 = -0.016476\ \Psi_1 + 0.006580\ \Psi_2 - 0.819920\ \Psi_3 + 0.572203\ \Psi_4$$

$$E = -859.071843$$

## 3.8 Discussion

The results of the calculations described in sections 3.6 and 3.7 show that the molecular orbital configurations of the Φ states in ScF must be reassigned. The reassignments now prevent generalisations such as 'the 3d orbital lies below the 4p orbital' from having any meaning, as the energies of the orbitals clearly depend on the occupancy of the other orbitals. The calculated ordering of the states would suggest that repulsion between the 4s and 4p electrons is relatively high, allowing the 4s3d states to lie lower than the 4s4p; the alternative suggestion that it is the 3d-3d repulsion which is relatively high is less likely, as in ScO the 4p orbital lies below the 3d, and in TiF the ground state is $^4\Sigma^-$, from the configuration $4s3d^2$ (Diebner and Kay, 1969). It seems likely that this type of consideration will be important in determining the ordering of states in other transition metal diatomic molecules, although so far there are insufficient data to identify other cases. The reassignments of the Φ states also suggest a reassignment of the $^3\Delta$ state at 21,000 $cm^{-1}$, and a confirmation of assignment of the $^1\Sigma^+$ state at 16,000 $cm^{-1}$. The lowest lying $^3\Delta$ state now becomes the $3d\delta\ 4p\sigma$ configuration, lying just above the $3d\delta\ 4p\pi$ configuration, whereas the $^1\Sigma^+$ state from the configuration $4s\sigma\ 3d\sigma$ would be expected to be more stable than $4s\sigma\ 4p\sigma$, and is reasonably assigned to the state 5000 $cm^{-1}$ above the $B^1\Pi$ state. These reassignments presumably also apply to the states of the isoelectronic molecules such as TiO, although in these cases there are fewer states known than in ScF, and assignment of the configurations becomes rather more difficult. It is important to note that this work shows that arguments such as those proposed by Green (1971) in which the relative energies of orbitals are calculated from atomic data, are not valid as they do not take account of the differences in configurations between the atoms and molecules.

The configuration interaction calculations show that the $\Phi$ states are well described by single configuration wave functions; however, there is no wholly satisfactory explanation of the relatively poor value of the $^3\Phi$ - $a^3\Delta$ excitation energy. Atomic data show that it is not possible to interpret the discrepancy in terms of the differing correlation energies of a 4s and 3d electron, and a 4p and 3d electron. The explanation may lie in the greater importance of configurations in which an electron is excited from the F atom in the $\Phi$ states than in the $\Delta$ states, although there is little evidence to support this suggestion. The configuration interaction calculations do adequately account for the intensities of the $^1\Pi$-$X^1\Sigma^+$ transitions ; the clear differences in magnitudes of matrix elements corresponding to one-electron and two-electron excitations allow rationalisation of which cases are not well described by single configuration wave functions, and may allow predictions of other cases in which configuration interaction may be important. These arguments may be extended to TiO and other molecules, although it is worth noting that the problems of the transition intensities do not arise in TiO, where only one $^1\Pi$ state is known.

## 3.9 Conclusions

In this chapter calculations were performed on several low-lying and excited states of ScF. For the low-lying states, whose electronic structure is well-known, the calculated spectroscopic constants were in close agreement with experimental results. Calculations were performed on the excited $\Phi$ and $\Pi$ states; it was shown to be necessary to reassign the configurations of the observed $^3\Phi$ states, such that the lower state is described as $3d\delta 4p\pi$, and not $3d\delta 3d\pi$ as previously thought. However, the lowest $^3\Pi$ state was shown to be derived from the configuration $4s\sigma 3d\pi$; differences in electron repulsion therefore play an important role in determining the ordering of the states in transition metal diatomic molecules, and this removes a discrepancy between the relative energies of the 3d and 4p electrons in ScO and ScF. It was shown that there is no appreciable configuration mixing between the $\Phi$ states. It was also concluded that the observed $^3\Delta$ state is derived from the configuration $3d\delta 4p\sigma$, and not $3d\delta 3d\sigma$ as previously thought.

In the $\Pi$ states it was found that there is appreciable mixing between the configurations $4s\sigma 4p\pi$, $3d\delta 3d\pi$ and $3d\delta 4p\pi$, and this helps to explain the distribution of intensities between the four observed $^1\Pi - X^1\Sigma^+$ transitions. The lowest $\Pi$ state, from the configuration $4s\sigma\ 3d\pi$, is shown to be well represented by a single configuration. This difference from the $\Phi$ states was explained by the difference in magnitude of the off-diagonal matrix elements representing one-electron and two-electron excitations. Figure 3.4 summarises the electron configurations of the states of ScF proposed in this thesis.

These conclusions on the electronic structure of ScF may be carried over to molecules with isoelectronic valence shells, such as TiO and YF. However, in these cases, there are rather less experimental data available than for ScF, and the unambiguous assignment of configurations to observed states is more difficult.

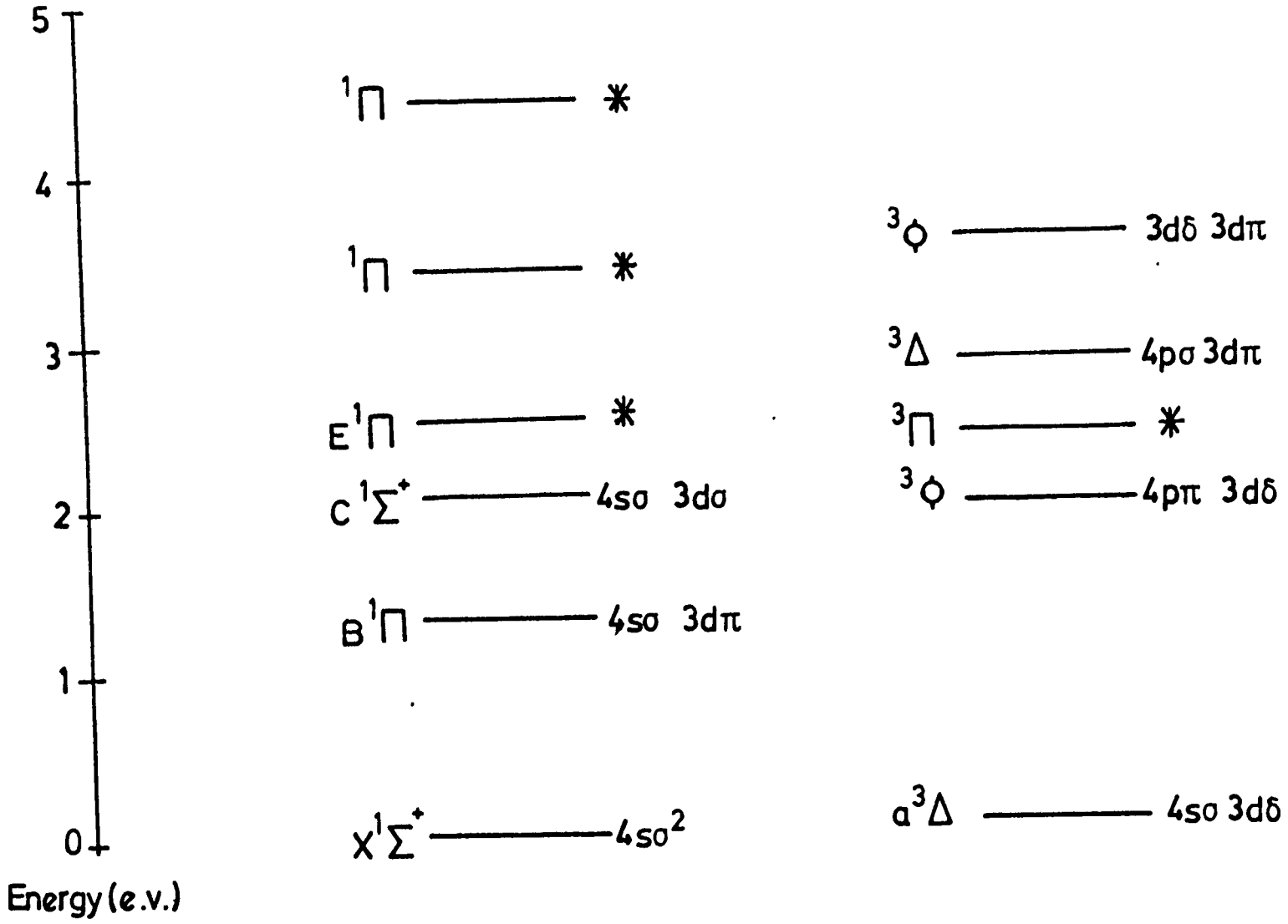



Figure 3.4.

Proposed Configurations for the Electronic States of ScF.

* These states may not be described by a single configuration.

## Chapter 4

## THE ELECTRONIC STRUCTURE OF THE TRANSITION METAL HYDRIDES


| | Page No. |
|---|---|
| 4.1 The Transition Metal Monohydrides | 96 |
| 4.1.1 Introduction | 96 |
| 4.1.2 Previous Work | 96 |
| 4.1.3 Electronic Structure | 99 |
| 4.1.4 Correlation Energy | 102 |
| 4.2 Scandium Monohydride | 108 |
| 4.2.1 Introduction | 108 |
| 4.2.2 Approximate Hartree-Fock Calculations | 108 |
| 4.2.3 Correlation Energy | 109 |
| 4.2.4 Discussion | 112 |
| 4.3 Titanium and Vanadium Monohydrides | 124 |
| 4.3.1 Introduction | 124 |
| 4.3.2 Approximate Hartree-Fock Calculations on TiH and VH | 124 |
| 4.3.3 Correlation Energy of TiH | 125 |
| 4.3.4 Near Degeneracy Effects in TiH and VH | 128 |
| 4.3.5 Discussion | 134 |
| 4.4 Iron Monohydride | 138 |
| 4.4.1 Introduction | 138 |
| 4.4.2 Approximate Hartree-Fock Calculations | 139 |
| 4.4.3 Discussion | 139 |
| 4.5 Nickel and Palladium Monohydrides | 144 |
| 4.5.1 Introduction | 144 |
| 4.5.2 Approximate Hartree-Fock Calculations | 144 |
| 4.5.3 Discussion | 145 |
| 4.6 Conclusions | 152 |

Tables


| | | Page No. |
|---|---|---|
| Table 4.1 | Molecular States Given by the Ground States of Both M+H and $M^{+}+H^{-}$ | 101 |
| Table 4.2 | Comparison of Different H Basis Sets in Calculations on MnH | 110 |
| Table 4.3 | S.T.O. Basis Functions for Calculations on ScH | 111 |
| Table 4.4 | Hartree-Fock Calculations on ScH | 113 |
| Table 4.5 | Calculated and Experimental Energies in Sc | 114 |
| Table 4.6 | Correlation Energy of the $^{1}\Sigma^{+}$ State of ScH | 115 |
| Table 4.7 | Correlation Energy of the $^{3}\Delta$ State of ScH | 116 |
| Table 4.8 | Correlation Energy of the $^{3}\Pi$ State of ScH | 117 |
| Table 4.9 | Correlation Energy of the $^{3}\Sigma^{+}$ State of ScH | 118 |
| Table 4.10 | Correlation Energy of the $^{3}\Phi$ State of ScH | 119 |
| Table 4.11 | Correlation Energy of the $^{3}\Sigma^{-}$ State of ScH | 120 |
| Table 4.12 | Correlation Energies in ScH | 121 |
| Table 4.13 | S.T.O. Basis Functions for TiH and VH | 126 |
| Table 4.14 | Hartree-Fock Calculations on TiH and VH | 127 |
| Table 4.15 | Calculated and Experimental Energies in Ti | 129 |
| Table 4.16 | Correlation Energy of the $^{4}\Phi$ State of TiH | 130 |
| Table 4.17 | Correlation Energy of the $^{4}\Delta$ State of TiH | 131 |
| Table 4.18 | Correlation Energy of the $^{2}\Delta$ State of TiH | 132 |
| Table 4.19 | Correlation Energies in TiH | 133 |
| Table 4.20 | Configuration Interaction Calculations on TiH and VH | 135 |
| Table 4.21 | S.T.O. Basis Functions for FeH | 140 |
| Table 4.22 | Calculated Spectroscopic Constants of FeH | 141 |
| Table 4.23 | Population Analysis of the Valence Orbitals of FeH | 142 |
| Table 4.24 | S.T.O. Basis Functions for PdH | 146 |
| Table 4.25 | S.T.O. Basis Functions for NiH | 147 |
| Table 4.26 | Calculated Spectroscopic Constants for PdH and NiH | 148 |


Figure


| | | |
|---|---|---|
| Figure 4.1 | Bonding in PdH and NiH | 150 |

## 4.1 The Transition Metal Monohydrides

### 4.1.1 Introduction

The monofluorides and monoxides of the transition metals have been extensively studied, and in several cases, such as VO and ScF, are well understood. However, the simplest transition metal diatomic molecules, the monohydrides, still largely remain a mystery, with even their electronic ground states rarely being unambiguously identified. Until recently many of the first row, and almost all of the second and third row transition metal monohydrides had never been observed experimentally, in spite of their potential astrophysical importance. Hydrogen and the transition metals are important stellar elements, and recently two transition metal hydrides, NiH and FeH, have been identified in solar spectra (Lambert and Mallia 1971, Carroll and McCormack 1972). Electronic spectra have now been observed for all the first row transition metal monohydrides, yet in five cases it has not proved possible to analyse the spectra at all, and in many of the remaining cases only two states are known, and it is rarely definitely known whether the lower state is the ground state. The work described in this chapter is an attempt to clarify some of the problems presented by the electronic structure of the transition metal monohydrides by ab initio calculations, to predict the nature of the ground states of these molecules, and to attempt to suggest rationalisations of the calculated orderings of the electronic states.

### 4.1.2 Previous Work on Transition Metal Hydrides.

Experimental work on the transition metal monohydrides dates back to 1934 (Gaydon and Pearse 1934), but after a productive decade in which five hydrides were discovered, relatively few advances have been made. The last decade has seen a revival of interest, and many bands have been more thoroughly studied, and new systems discovered.

CrH was first discovered by Gaydon and Pearse in 1937 using an electric arc; they observed bands in the ultra-violet regions of the spectrum.

Klemen and Liljeqvist (1955) showed that these bands are from two separate systems, and also described a $^6\Sigma^+$-$^6\Sigma^+$ transition in the infra-red. They observed the systems in emission in a King furnace operating at 1700-1900°K. O'Connor (1969) studied CrH and CrD in absorption and emission in a heavy current discharge tube, and from the marked change in intensity of emission between CrH and CrD, concluded that the upper state of the system at 3680 Å in CrH is predissociated. The state is probably $^6\Pi$. Klemen and Uhler (1959) observed perturbations in the infra-red system, and suggested that the upper $^6\Sigma^+$ state could be perturbed by a stable $^8\Sigma^+$ state.

MnH was first observed by Gaydon and Pearse (1938) in emission in a discharge tube, and in an arc. It has since been observed in emission and absorption in a King furnace, and a full description of the bands has been given by Nevin and Stephens (1953). The system between 5100 Å and 6200 Å has been analysed as a $^7\Pi$-$^7\Sigma^+$ transition, and further bands at higher and lower energies have been observed, but not fully analysed. Red degraded bands at 4500 Å and 4800 Å may involve quintet states.

The spectra of FeH and FeD have been observed by Carroll and McCormack (1972) in a King furnace in both emission and absorption. They were unable to complete an analysis, but did show that the lines observed were identical to those observed in the solar spectrum.

Cobalt hydride was first observed by Heimer (1936, 1937a) in a King furnace in emission. The bands were analysed as $^3\Phi_4$-$^3\Phi_4$, although the experimental observation is only that $\Omega=4$ in both states, and it has been suggested that the transition is more correctly described as $\Omega=4$-$\Omega=4$ in Hund's case (c) coupling. Correlation rules suggest that the state is derived mainly from $^3\Phi$, though $^5\Delta$ or $^1\Gamma$ cannot be ruled out. Recently weaker lines have been analysed by Klynning and Kronekvist (1973) as the $\Omega=3$-$\Omega=3$ component of the transition, and they estimated the spin-orbit coupling constant in the ground state to be approximately 800 $cm^{-1}$. They further reported that there were still some lines unaccounted for in their analysis, and that those could be

part of the $\Omega$=2-$\Omega$=2 component.

NiH was the first transition metal monohydride to be reported, by Gaydon and Pearse (1934, 1935). They used a flame containing nickel carbonyl vapour, and a high tension discharge between nickel electrodes through a flame of hydrogen burning in air, as source, and found two systems in the orange-red and red regions of the spectrum. The orange-red bands were analysed as $^2\Delta_{5/2}$-$^2\Delta_{5/2}$ sub-bands, and the red bands as $^2\Delta_{5/2}$-$^2\Delta_{5/2}$ sub-bands of another transition. Both systems have the same lower state. Heimer (1937b) used a King furnace and discovered another $^2\Delta_{5/2}$-$^2\Delta_{5/2}$ sub-band, and in 1965 Aslund et al. reported the $^2\Delta_{3/2}$-$^2\Delta_{3/2}$ sub-bands of the same transition, and also a very weak $^2\Delta_{3/2}$-$^2\Delta_{5/2}$ sub-band.

PdH and PdD were observed in absorption in a King furnace at 3100°K by Malmberg et al. (1968). They observed twelve bands of the type $^2\Sigma$-$^2\Sigma$ in the region 3100-6400 Å, all originating from one state, and probably corresponding to two separate upper states. Bands belonging to PtH were observed by Scullman (1965) in absorption in a King furnace, again above 3000°K, the high temperature being necessitated by the low volatility of the metal. The bands were analysed as two separate $^2\Delta_{5/2}$-$^2\Delta_{5/2}$ sub-bands, but no $^2\Delta_{3/2}$-$^2\Delta_{3/2}$ bands were observed, which was interpreted as indicating that the state is inverted.

Recently d'Incan and coworkers have obtained the spectrum of LaH in emission from a hollow cathode, and a preliminary analysis suggests that the lower state in the transition is $^3\Delta$. Further work is in progress, and this may prove to be an important and versatile source of transition metal hydrides. As the apparatus may be operated at liquid nitrogen temperatures, the rotational temperature is low, which appreciably simplifies the band spectra (Chojnicki, private communication).

Smith (1973) has reported spectra obtained in absorption behind reflected shock waves for all the first row transition metal hydrides. He was able to observe the bands reported by other workers, except for those in the infra-red,

which were not detected for technical reasons, and has also reported a large number of new bands. Unfortunately he was not able to analyse any of the new bands obtained, and it is not yet clear whether the shock tube will become recognised as a versatile and useful source of the spectra of transition metal hydrides. It does have the merit of being able to produce temperatures of 3000°K-4000°K relatively easily, and can produce spectra which are hard to obtain in emission in arcs and discharges where the excited states are probably predissociated.

There have been two ab initio calculations published on transition metal hydrides. In 1972 Walker et al. published a study of FeH using many body perturbation theory with a single centre basis set. They obtained approximate potential curves for eighteen states, and calculated the dissociation energy. This calculation is considered in greater detail in section 4.4. Bagus and Schaefer (1973) performed ab initio self-consistent field calculations on the high spin $^7\Sigma^+$ and $^7\Pi$ states of MnH. They varied the basis set extensively, and predicted spectroscopic constants in very satisfactory agreement with experiment. They calculated the dipole moments and an extensive range of other one-electron expectation values, and discussed the electronic structure of the two states, concluding that the metal 3d orbitals remained essentially unchanged on molecule formation.

4.1.3 Electronic Structure of the Transition Metal Hydrides

The electronic structure of the monohydrides of the transition metals has been discussed by Cheetham and Barrow (1967). They pointed out that the ground states of the atoms of the first transition series resemble those of the atoms of the third transition series, whereas those of the second transition series often correspond to a different configuration. Thus the first transition series ground states are all of the type $3d^n4s^2$, except for Cr and Cu ($d^{n+1}s$), whereas in the second transition series the ground states of Nb, Mo, Ru and Rh are all $4d^n5s$, and Pd has the ground state $4d^{10}$. It might therefore be expected that the ground states of the hydrides of the first transition series

resemble those of the third transition series, whereas the hydrides of the second transition series may often be individual.

If it is assumed that there is some degree of interaction between the covalent and ionic representations of the hydrides M-H and $M^+ H^-$, then the nature of the ground state may be determined by the ground state of the positive ion $M^+$ as well as of the neutral atom. Cheetham and Barrow pointed out that the symmetries of the molecular ground states could be predicted to be one of those states given by both of the combinations M+H and $M^+ + H^-$, and that in all known cases the prediction is correct, though not necessarily unique. Their predictions are shown in Table 4.1. In contrast the molecular ground states sometimes correlate with excited states of the united atom (MnH, NiH, PtH) and this seems to be a much less useful model for describing transition metal hydrides.

The excited states of the transition metal hydrides have been discussed in terms of a simple covalent picture, in which there are three low-lying orbitals:

| | | | |
|---|---|---|---|
| $\sigma_1$ | (n-1)d + ns | + H (1s) | bonding |
| $\sigma_2$ | (n-1)d - ns | | non-bonding |
| $\sigma_3^x$ | (n-1)d + ns | - H (1s) | anti-bonding |

The extent of d-s mixing varies considerably across the transition series, and the non-bonding $\sigma_2$ orbital becomes almost completely dσ after the transition series. In the ionic description, $\sigma_1$ is nearly 1s(H), $\sigma_2$ is M(ns), and $\sigma_3^x$ is M(n-1)d, and much less strongly anti-bonding. All the analysed transitions of the hydrides may be described as $\sigma_3^x \leftarrow \sigma_2$, with a corresponding increase in bond length of 0.1-0.2 Å, except for the transition in MnH, which is $\pi(4p) \leftarrow \sigma_3^x$, and is violet degraded.

This description of the transition metal hydrides is satisfactory in that it explains the qualitative features of the observed spectra, but nevertheless leaves unanswered many problems concerning the nature of the

Table 4.1

Molecular States Given by the Ground States of Both M+H and $M^+ + H^-$

| Element | States | Element | States | Element | States |
|---|---|---|---|---|---|
| Sc | $^3\Delta$, $^3\Pi$, $^3\Sigma$ | Y | $^1\Sigma$ | La | $\underline{^3\Delta}$, $^3\Pi$, $^3\Sigma$ |
| Ti | $^4\Phi$, $^4\Delta$, $^4\Pi$, $^4\Sigma$ | Zr | $^4\Phi$, $^4\Delta$, $^4\Pi$, $^4\Sigma$ | Hf | $^2\Delta$, $^2\Pi$, $^2\Sigma$ |
| V | $^5\Delta$, $^5\Pi$, $^5\Sigma$ | Nb | $^5\Delta$, $^5\Pi$, $^5\Sigma$ | Ta | $^5\Phi$, $^5\Delta$, $^5\Pi$, $^5\Sigma$ |
| Cr | $\underline{^6\Sigma}$ | Mo | $^6\Sigma$ | W | $^6\Delta$, $^6\Pi$, $^6\Sigma$ |
| Mn | $\underline{^7\Sigma}$ | Tc | $^7\Sigma$ | Re | $^7\Sigma$ |
| Fe | $^6\Delta$, $^6\Pi$, $^6\Sigma$ | Ru | $^4\Phi$, $^4\Delta$, $^4\Pi$, $^4\Sigma$ | Os | $^6\Delta$, $^6\Pi$, $^6\Sigma$ |
| Co | $\underline{^3\Phi}$, $^3\Delta$, $^3\Pi$, $^3\Sigma$ | Rh | $^3\Phi$, $^3\Delta$, $^3\Pi$, $^3\Sigma$ | Ir | $^3\Phi$, $^3\Delta$, $^3\Pi$, $^3\Sigma$ |
| Ni | $\underline{^2\Delta}$, $^2\Pi$, $^2\Sigma$ | Pd | $\underline{^2\Sigma}$ | Pt | $\underline{^2\Delta}$, $^2\Pi$, $^2\Sigma$ |

Observed states are underlined.

orbitals involved in the states. There are still virtually no data for many of the hydrides, and it would be unsafe to assume that such generalisations as have been made above will prove a completely satisfactory account of the electronic structure of all the transition metal monohydrides.

4.1.4 Correlation Energy

It is a relatively straightforward process to obtain approximate Hartree-Fock wave functions for the transition metal monohydrides to such an accuracy as to effectively reproduce the exact Hartree-Fock results, provided that convergence problems may be overcome. This does not mean that it is possible to predict unequivocally the ground states of these molecules, or to calculate reliably excitation energies, due to the neglect of the correlation energy of the molecule. Because Hartree-Fock wave functions in many cases represent dissociation to the wrong atomic limits, the potential curves are generally too steep on the right hand side, which typically produces a value of $\omega_e$ which is too high, and a value of $r_e$ which is slightly too low.

It is not computationally feasible to perform the very extensive configuration interaction which would be necessary to identify electronic ground states, or to predict reliable spectroscopic constants for the transition metal monohydrides, and a different approach is used in the work described in this chapter. Although molecular correlation energies are generally rather poorly understood, atomic correlation energies have been much more widely studied. This is partly because of the vast amount of very reliable data on atomic energy levels (Moore 1949), and partly because of the greater ease in performing ab initio calculations on atoms by virtue of the simplification of the problem caused by spherical symmetry. The use of atomic data in estimation of molecular correlation energies has been quite common, and tables of pair correlation energies have been given (e.g. Allen et al. 1963). These have proved useful where molecular orbitals correspond closely to atomic-type orbitals, but are of more limited value when the molecular orbitals are a linear combination of several atomic-type orbitals, as is often the case with

valence orbitals. Liu and Verhaegen (1970, 1971) have described a method for obtaining molecular correlation energies which takes account of the fact that molecular orbitals may not correspond to a single atomic-type orbital, and have used the method to estimate correlation energies in the first-row hydrides. They estimate the absolute accuracy of their calculations to be 0.1 e.v. This method is applicable to the estimation of correlation energies in transition metal hydrides, and is employed in this work.

Consider a single-determinantal wave function of a state Y of the molecule AB,

$$\Psi(AB(Y)) = |(\phi_1)^{N_1}(\phi_2)^{N_2} \ldots\ldots (\phi_n)^{N_n}|$$

where the molecular orbital $\phi_i$ has occupancy $N_i$. If the atomic populations of the different $\phi_i$ are calculated, then let the coefficients $Q_{ip}$ express the population of atomic orbital $\chi_p$ in the molecular orbital $\phi_i$. Using Mulliken's definition (Mulliken 1955)

$$Q_{ip} = \sum_q C_{ip}\, C_{iq}\, S_{pq}.$$

where the $C_{iq}$ are L.C.A.O. coefficients, and $S_{pq}$ is the overlap integral between $\chi_p$ and $\chi_q$. The molecular orbital $\phi_i$ may now be decomposed into atomic contributions

$$(\phi_i)^{N_i} = \sum_p (\chi_p^{Q_{ip}})^{N_i} + \sum_q (\chi_q^{Q_{iq}})^{N_i}$$

where $\chi_p$ is centred on atom A, and $\chi_q$ on atom B. As the molecular orbitals are orthonormal,

$$\sum_p (Q_{ip})^{N_i} + \sum_q (Q_{iq})^{N_i} = 1.$$

To extend this analysis to the entire wave function, the contributions of $\chi_p$ in all the molecular orbitals of the same occupancy are summed:

$$(P_p)^{N_i} = \sum_j (Q_{jp})^{N_j}\, \delta(N_i, N_j)$$

If interatomic correlation effects are neglected, then the total molecular 'wave function' may be split into distinct 'wave functions' centred on one atom only. From these it is possible to build Slater determinants by extracting the coefficients P and multiplying them to obtain a weight for each determinant. All the terms for one atom are then included in the product of sums:

$$\prod_{p} \sum_{N_i} P_p^{N_i} \chi_p^{N_i} = \sum_{N_1} \cdots \sum_{N_i} \cdots \sum_{N_n} x^{N_1 \cdots N_i \cdots N_n} |X|^{N_1 \cdots N_i \cdots N_n} ,$$

where $x^{N_1 \cdots N_i \cdots N_n}$ represents the product of the $P_p^{N_i}$'s and contains implicitly once, and only once, all the subscripts p, q, r and $|X|^{N_i \cdots N_j \cdots N_n}$ is the analogous product of $\chi_p^{N_i}$'s. A typical term would be

$P_p^{N_i} P_q^{N_i} P_r^{N_j} P_s^{N_k} |\chi_p^{N_i} \chi_q^{N_i} \chi_r^{N_j} \chi_s^{N_k}|$. From this the correlation energy of the molecule may be reduced to a sum of correlation energies of atomic determinants.

$$E_{CORR} = \sum_{M} \left( \sum_{N_1} \cdots \sum_{N_i} x^{N_1 \cdots N_i} E_{CORR} |X|^{N_1 \cdots N_i} \right)_M \qquad (1)$$

where the M summation extends over atoms. This equation may be used numerically to calculate the correlation energy of the molecule. If $|X|^{N_1 \cdots N_i}$ corresponds to an irreducible representation of the atom, then its correlation energy is that of the corresponding atomic state; if not, its correlation energy is given by a linear combination of the states to which it corresponds.

The method therefore consists of describing the molecular orbitals by a Mulliken population analysis, neglecting interatomic effects, and decomposing the resulting atomic wavefunction into a sum of atomic determinants, whose correlation energies are determined. An example makes the use of the method clearer. Consider the $A^3\Pi$ state of NH, with population analyses given below.

$$\Psi = |1\sigma^2\ 2\sigma^2\ 3\sigma\ 1\pi^3|$$

$$1\sigma^2 = (2s_N^{1\cdot00})^2$$

$$2\sigma^2 = (2s_N^{0\cdot89})^2 + (2p_N^{0\cdot03})^2 + (1s_H^{0\cdot08})^2$$

$$3\sigma = (2s_N^{0\cdot09})^1 + (2p_N^{0\cdot66})^1 + (1s_H^{0\cdot25})^1$$

$$1\pi^3 = (2p_N^{1\cdot00})^3$$

We thus have the atomic structures:

$$[(1s^{1\cdot00})^2(2s^{0\cdot89})^2(2s^{0\cdot09})^1(2p_0^{0\cdot03})^2(2p_0^{0\cdot66})^1(2p_1^{1\cdot00})^2(2p_{-1}^{1\cdot00})^1]_N$$

$$+ [1s^{0\cdot08})^2(1s^{0\cdot25})^1]_H .$$

Hence

$$E_{CORR} = 1.00\times0.89\times1.00\times0.03\times1.00\ |1s^2\ 2s^2\ 2p_1^2\ 2p_0^2\ 2p_{-1}|$$

$$+ 1.00\times0.89\times1.00\times0.66\times1.00\ |1s^2\ 2s^2\ 2p_1^2\ 2p_0\ 2p_{-1}|$$

$$+ 1.00\times0.89\times1.00\times0.31\times1.00\ |1s^2\ 2s^2\ 2p_1^2\ 2p_0|$$

$$+ 1.00\times0.09\times1.00\times0.03\times1.00\ |1s^2\ 2s\ 2p_1^2\ 2p_0^2\ 2p_{-1}|$$

$$+ 1.00\times0.09\times1.00\times0.66\times1.00\ |1s^2\ 2s\ 2p_1^2\ 2p_0\ 2p_{-1}|$$

$$+ 1.00\times0.09\times1.00\times0.31\times1.00\ |1s^2\ 2s\ 2p_1^2\ 2p_{-1}|$$

$$+ 1.00\times0.02\times1.00\times0.03\times1.00\ |1s^2\ 2p_1^2\ 2p_0^2\ 2p_{-1}|$$

$$+ 1.00\times0.02\times1.00\times0.66\times1.00\ |1s^2\ 2p_1^2\ 2p_0\ 2p_{-1}|$$

$$+ 1.00\times0.02\times1.00\times0.31\times1.00\ |1s^2\ 2p_1^2\ 2p_{-1}|$$

$$+ 0.08\ |1s^2|$$

$$= 0.03\ E_{CORR}\ (N^{2-},\ ^2P^0) + 0.59\ E_{CORR}\ (N^-,\ ^3P) + 0.28\ E_{CORR}$$
$$(N,\ \tfrac{1}{2}\ ^2D^0 + \tfrac{1}{2}\ ^2P^0) + 0.06\ E_{CORR}\ (N,\ ^4P) + 0.03\ E_{CORR}\ (N^+,\ \tfrac{1}{2}\ ^3D^0$$
$$+ \tfrac{1}{2}\ ^3P^0) + 0.01\ E_{CORR}\ (N^+,\ ^3P) + 0.08\ E_{CORR}\ (H^-,\ ^1S).$$

The problem of obtaining molecular correlation energies is now reduced to that of obtaining atomic correlation energies. The correlation energy of the $H^-$ ion is well-known, but those for the transition metals are not adequately documented, and so numerical Hartree-Fock calculations have been carried out on the relevant states of the transition metal atoms and ions, and the resulting energies compared with experimental data to obtain correlation energies. This method is satisfactory provided that sufficient data are available; it gives only relative values of correlation energies, not absolute values, but this is not important in the problems considered in this work. It was found that the only cases where sufficient data were not available were those which had rather small coefficients in the expansion (1), and any reasonable estimate of the correlation energy would then suffice. Problems also arise in estimating the correlation energies of negative ions. Ideally these are obtained by extrapolating the corresponding values for the isoelectronic atom and positive ions, but in practice this is not possible in the transition metals, as sufficient data to obtain a meaningful extrapolation are never available. Correlation energies are relatively insensitive to change in nuclear charge, and instead of an extrapolation procedure, the correlation energies of negative ions were obtained from those of the isoelectronic atom by scaling the atomic value by the ratio of the nuclear charges. Almost any other reasonable method of estimating these correlation energies would give results which are essentially identical; the coefficients of the negative ions are typically rather small.

The accuracy of this method in the transition metal monohydrides is almost impossible to estimate. Liu and Verhaegen claimed an absolute accuracy of 0.1 e.v. in the first row hydrides; it would be unreasonable to expect such accuracy for heavier molecules, as the accuracy with which the atomic data may be obtained decreases from the first to the third row, although only relative correlation energies are calculated in this work, so systematic errors are less important. However, the transition metal hydrides have

appreciably larger charge on the H atom than the first row hydrides, so presumably the error from the neglect of interatomic correlation energy is larger. Excitation energies would be expected to be calculated rather more accurately than dissociation energies; contributions which are difficult to assess often cancel between different electronic states, but do not do so between the ground state and the separated atoms. An assessment of the accuracy of the method must probably await further experimental results; at present there is insufficient data to allow a test of the method. However, if the method is accurate to 0.25 e.v., more than twice Liu and Verhaegen's estimate, it is still certainly of great value in calculations on the transition metal monohydrides.

## 4.2 Scandium Monohydride

### 4.2.1 Introduction

Scandium monohydride is the first of the transition metal hydrides, and has been observed by Smith in absorption in a shock tube. He described the bands as consisting of one or two maxima, with diffuse complicated structure on either side, and not clearly degraded either way. The absorption was in the region 5450 Å to 5650 Å, with a maximum at 5560 Å, which corresponds to an excitation energy of 18,000 $cm^{-1}$. The isotope shift from ScH to ScD was small, and it was concluded that this was a (0,0) band, but no (1,0) or (0,1) bands could be found. No rotational analysis was reported, but Smith commented that the complexity of the transition was somewhat surprising if the transition involved triplet states. Simple correlation arguments suggest that the ground state is $^3\Delta$, $^3\Pi$ or $^3\Sigma^+$, although the ground state of ScF, which has an isoelectronic valence shell, is $^1\Sigma^+$. As *ab initio* molecular orbital calculations have proved a reliable source of information on the ground states of transition metal diatomic molecules, calculations were performed on ScH to investigate the electronic structure of the low-lying states (Scott and Richards 1974b).

### 4.2.2 Approximate Hartree-Fock Calculations

The calculations were carried out in the matrix Hartree-Fock approximation using the open-shell method of Roothaan and Bagus (1963) as implemented in the ALCHEMY programme. There are two main problems in choosing a basis set for these calculations; firstly one or two Slater-type orbitals are not sufficient to obtain a good representation of the hydrogen atom, and secondly it is necessary to use a reasonably large basis set for the metal atom to prevent the calculation from building up too much charge on the hydrogen atom, as the calculation is performed variationally. The double zeta set of Clementi *et al*. (1967) was used to represent the metal atom; this provides a very satisfactory representation of both the Sc atom and the $Sc^+$ ion without requiring an unwieldy number of basis functions. The basis set is augmented

by the addition of two 4p functions, which are not included in Clementi's set, but which make important contributions on molecule formation, and one 4f function, to represent angular polarisation. The exponents for the 4p functions are those optimised in work on ScF (see Chapter 3); the contribution of the 4f functions is small, and their exponent was not optimised. In this basis set the energy of the Sc atom ($^2$D) is calculated to be -759.722155 a.u., within 0.0134 a.u. of the Hartree-Fock limit. Bagus and Schaefer (1973), in their calculation on MnH, showed that the exact choice of the basis set for the H atom is not particularly important, provided that a sufficiently flexible set is used. Table 4.2 summarises their results on the effects of varying the hydrogen basis on the energy and population analysis of MnH. The basis set used for H in this work is of comparable size to those considered by Bagus and Schaefer. Full details of the basis set are given in Table 4.3.

Calculations were performed on eight states which could be expected, on the basis of orbital energies, to be low-lying. For each state the energy was calculated at five internuclear separations around the equilibrium value, and the resulting potential curves analysed by the programme MCFIT (see Chapter 1), to give values of $r_e$ and $\omega_e$. The energies and calculated spectroscopic constants are given in Table 4.4. The population analyses and orbital energies of some of the low-lying states are given in Tables 4.6-4.11. The state of lowest energy is calculated to be the $^3\Delta$ state from the configuration

$$1\sigma^2\ 2\sigma^2\ 3\sigma^2\ 4\sigma^2\ 5\sigma^2\ 6\sigma^2\ 7\sigma\ 1\pi^4\ 2\pi^4\ 1\delta.$$

### 4.2.3 Correlation Energy

Correlation energies were estimated by the method of Liu and Verhaegen (section 4.1.4) for six states of the molecule ScH, and for the separated atoms Sc($^2$D) + H($^2$S). The wave function for each state was decomposed by a Mulliken population analysis, and the appropriate atomic determinants identified. Where the determinants do not correspond to a single atomic state, the appropriate linear combination of states was evaluated, and these are given in

Table 4.2

Comparison of Different H Basis Sets in Calculations on MnH

| | A | B | C | D | E |
|---|---|---|---|---|---|
| 1s exponent | 1.566 | 1.225 | 1.9 | 2.2 | 1.0 |
| 1s exponent | 0.888 | 0.8 | 0.888 | 1.0 | 0.45 |
| 2s exponent | 2.2 | 2.5 | 2.3 | 2.2 | 1.0 |
| 2s exponent | | | 0.6 | 1.0 | 0.45 |
| 3s exponent | | | 2.2 | | |
| 2p exponent | 1.376 | 1.8 | 2.0 | 2.9 | 1.21 |
| 2p exponent | | 1.2 | 1.2 | 1.7 | 0.85 |
| 3p exponent | | | | 2.9 | 1.2 |
| | | | | | |
| $E(H^-)$ | -0.4573 | -0.4772 | -0.4877 | -0.4786 | -0.4878 |
| $H^-$ virial | -1.749 | -1.883 | -1.995 | -1.901 | -2.002 |
| E(MnH)+1150 | -0.42126 | -0.4213 | -0.42156 | -0.42123 | -0.42127 |
| MnH virial | -1.99996 | -1.99996 | -1.99996 | -1.99996 | -1.99996 |
| H population | 1.47 | 1.57 | 1.52 | 1.47 | 1.46 |

Table 4.3

STO Basis Functions for Calculations on ScH

| Function | Type | Atom | Exponent |
|---|---|---|---|
| 1 | 1sσ | Sc | 17.29 |
| 2 | 1sσ | Sc | 22.7566 |
| 3 | 2sσ | Sc | 8.2528 |
| 4 | 2sσ | Sc | 10.8582 |
| 5 | 3sσ | Sc | 3.4054 |
| 6 | 3sσ | Sc | 5.3205 |
| 7 | 4sσ | Sc | 1.9277 |
| 8 | 4sσ | Sc | 1.0507 |
| 9 | 2pσ | Sc | 7.6297 |
| 10 | 2pσ | Sc | 13.4947 |
| 11 | 3pσ | Sc | 4.2055 |
| 12 | 3pσ | Sc | 2.6867 |
| 13 | 4pσ | Sc | 3.5863 |
| 14 | 4pσ | Sc | 1.0837 |
| 15 | 3dσ | Sc | 1.8554 |
| 16 | 3dσ | Sc | 4.5843 |
| 17 | 4fσ | Sc | 2.75 |
| 18 | 1sσ | H | 0.83 |
| 19 | 1sσ | H | 1.45 |
| 20 | 2sσ | H | 1.85 |
| 21 | 2pσ | H | 1.14555 |
| 22 | 3dσ | H | 1.85 |
| 23 | 2pπ | Sc | 7.6297 |
| 24 | 2pπ | Sc | 13.4947 |
| 25 | 3pπ | Sc | 4.2055 |
| 26 | 3pπ | Sc | 2.6867 |
| 27 | 4pπ | Sc | 3.5863 |
| 28 | 4pπ | Sc | 1.0837 |
| 29 | 3dπ | Sc | 1.8554 |
| 30 | 3dπ | Sc | 4.5843 |
| 31 | 4fπ | Sc | 2.75 |
| 32 | 2pπ | H | 1.14555 |
| 33 | 3dπ | H | 1.85 |
| 34 | 3dδ | Sc | 1.8554 |
| 35 | 3dδ | Sc | 4.5843 |

Appendix B. Numerical Hartree-Fock calculations were then performed on thirty-five states of the atoms and ions of Sc and Ti. The results of these calculations, together with the corresponding experimental data, are given in Table 4.5. The contributions to the correlation energies of each of the states are given in Tables 4.6-4.11. Where it is not possible to calculate the correlation energy of a particular state because it has not been experimentally observed, an estimate of the correlation energy is obtained by comparison with ions of the same charge. In these cases the value is given to one decimal place; it can be seen that generally the exact value of the estimate is not very important. The correlation energy of the $H^-$ ion ($1s^2$) is taken as 1.088 e.v. (Clementi 1963). Table 4.12 gives the predicted excitation energies of the states of ScH after the semi-empirical estimates of correlation energy have been taken into account. It is not possible to make a critical assessment of the value of the method on the basis of the figures, but two points are worth making. It is encouraging to note that the estimates of the correlation energies of the various states are in line with chemical intuition, and seem to be of reasonable magnitude. In particular, the calculations are not dominated by contributions from highly charged ions, which presumably are rather poor models for describing the electron distribution in ScH. Secondly, the value of this approach over more simple approaches where molecular orbitals are described only by their major component is illustrated in Table 4.7, where the major contribution (4s 3d) has a coefficient of only 0.44. The remaining 56% of the Sc correlation energy is derived from other configurations which would have been neglected in other treatments.

4.2.4 Discussion

Two electronic states are shown to be low-lying in ScH, the $^3\Delta$ and $^1\Sigma^+$ states. These two states are analogous to the experimental ground states in ScF, which has an isoelectronic valence shell. The calculated energy difference is certainly less than the accuracy of the calculation, but the calculations do suggest that both states are sufficiently low-lying to be

Table 4.4

Hartree-Fock Calculations on ScH

| | | R | E | | | R | E |
|---|---|---|---|---|---|---|---|
| $^3\Delta$ | ($\sigma\delta$) | 3.2 | -760.2795263 | $^3\Pi$ | ($\sigma\pi$) | 3.2 | -760.2700623 |
| | | 3.4 | .2875124 | | | 3.4 | .2775409 |
| | | 3.6 | .2906404 | | | 3.6 | .2804432 |
| | | 3.8 | .2902497 | | | 3.8 | .2800452 |
| | | 4.0 | .2873414 | | | 4.0 | .2772938 |
| $^1\Delta$ | ($\sigma\delta$) | 3.4 | .2762101 | $^1\Pi$ | ($\sigma\pi$) | 3.2 | .2567268 |
| | | 3.6 | .2794371 | | | 3.4 | .2640058 |
| | | 3.8 | .2790779 | | | 3.6 | .2667397 |
| | | 4.0 | .2761539 | | | 3.8 | .2662037 |
| | | 4.2 | .2714293 | | | 4.0 | .2633421 |
| $^3\Sigma^+$ | ($\sigma\sigma$) | 3.2 | .2647145 | $^1\Sigma^+$ | ($\sigma^2$) | 3.0 | .2612399 |
| | | 3.4 | .2723852 | | | 3.2 | .2678227 |
| | | 3.6 | .2756238 | | | 3.4 | .2689043 |
| | | 3.8 | .2756357 | | | 3.6 | .2660704 |
| | | 4.0 | .2733301 | | | 3.8 | .2605066 |
| $^3\Phi$ | ($\delta\pi$) | 3.2 | .1926050 | $^3\Sigma^-$ | ($\delta^2$) | 3.4 | .1374895 |
| | | 3.4 | .1993171 | | | 3.6 | .1442639 |
| | | 3.6 | .2013045 | | | 3.8 | .1473748 |
| | | 3.8 | .1999040 | | | 4.0 | .1478125 |
| | | 4.0 | .1961145 | | | 4.2 | .1463178 |

| Configuration | State | $T_e$ ($cm^{-1}$) | $r_e$ (Å) | $\omega_e$ ($cm^{-1}$) |
|---|---|---|---|---|
| $7\sigma 1\delta$ | $^3\Delta$ | 0 | 1.94 | 1440 |
| $7\sigma 3\pi$ | $^3\Pi$ | 2240 | 1.94 | 1400 |
| $7\sigma 8\sigma$ | $^3\Sigma^+$ | 3270 | 1.96 | 1350 |
| $7\sigma 1\delta$ | $^1\Delta$ | 2460 | 1.94 | 1450 |
| $7\sigma 3\pi$ | $^1\Pi$ | 5260 | 1.94 | 1400 |
| $7\sigma^2$ | $^1\Sigma^+$ | 4780 | 1.77 | 1690 |
| $1\delta 3\pi$ | $^3\Phi$ | 19650 | 1.91 | 1490 |
| $1\delta^2$ | $^3\Sigma^-$ | 31370 | 2.08 | 1190 |

Table 4.5

Calculated and Experimental Energies in Sc

| Species | Configuration | State | Exptl. Energy (e.v.) | Calc. Energy (e.v.) | $\Delta E_{CORR}$ |
|---|---|---|---|---|---|
| $Sc^{3+}$ | | $^1S$ | 44.193 | 41.382 | -2.810 |
| $Sc^{2+}$ | d | $^2D$ | 19.440 | 17.506 | -1.933 |
| | s | $^2S$ | 22.593 | 20.541 | -2.052 |
| | p | $^2P$ | 27.155 | 24.850 | -2.305 |
| $Sc^{+}$ | sd | $^3D$ | 6.559 | 5.348 | -1.211 |
| | sp | $^3P$ | 11.400 | 9.590 | -1.810 |
| | pd | $^3F$ | 9.973 | 8.497 | -1.476 |
| | | $^3D$ | 10.023 | 8.504 | -1.519 |
| | | $^3P$ | 10.237 | 8.885 | -1.352 |
| | $d^2$ | $^3F$ | 7.154 | 6.146 | -1.008 |
| | | $^3P$ | 8.049 | 7.341 | -0.708 |
| | | $^1D$ | 7.904 | 7.126 | -0.778 |
| | | $^1G$ | 8.315 | 7.664 | -0.651 |
| | $s^2$ | $^1S$ | 8.004 | 7.444 | -0.560 |
| Sc | $s^2d$ | $^2D$ | 0 | 0 | 0 |
| | spd | $^4F$ | 1.952 | 0.950 | -1.002 |
| | | $^4D$ | 1.984 | 0.997 | -0.987 |
| | | $^4P$ | 2.286 | 1.300 | -0.986 |
| | $sd^2$ | $^4F$ | 1.426 | 1.006 | -0.420 |
| | | $^4P$ | 2.215 | 2.068 | -0.147 |
| | $d^3$ | $^2D$ | 4.490 | 5.599 | 1.109 |
| | $pd^2$ | $^4G$ | 3.603 | 2.914 | -0.689 |
| $Ti^{+}$ | $s^2d$ | $^2D$ | 0 | 0 | 0 |
| Ti | $sd^3$ | $^3H$ | -7.696 | -6.978 | 0.718 |
| | | $^3G$ | -8.064 | -7.410 | 0.654 |
| | | $^3D$ | -7.781 | -6.836 | 0.945 |
| | $s^2d^2$ | $^3F$ | -9.920 | -9.515 | 0.405 |
| | | $^1D$ | -9.044 | -8.223 | 0.821 |
| | | $^1G$ | -8.441 | -7.492 | 0.949 |
| | $spd^2$ | $^5G$ | -7.943 | -8.597 | -0.654 |
| | | $^5D_1$ | -7.643 | -8.245 | -0.602 |
| | | $^5S^1$ | -6.831 | -7.039 | -0.208 |
| | | $^5D_2$ | -6.753 | -6.974 | -0.221 |

Table 4.6

Correlation Energy of the $^1\Sigma^+$ State of ScH

Population Analysis, R=3.4 a.u.

| | 4s | 4p | 3d | 1s | $\epsilon^{SCF}$ |
|---|---|---|---|---|---|
| 6σ (2) | .042 | .018 | .134 | .799 | -0.4058 |
| 7σ (2) | .831 | .047 | .168 | -.042 | -0.2323 |

$$0.873\ |4s^2| + 0.127\ |.....|$$
$$0.065\ |4p_0^2| + 0.935\ |.....|$$
$$0.302\ |3d_0^2| + 0.698\ |.....|$$
$$0.757\ |1s^2| + 0.243\ |.....|$$

| | | | | |
|---|---|---|---|---|
| | .570 | $\|4s^2\|$ | - .570 × .560 = | - .319 |
| + | .246 | $\|4s^2 3d_0^2\|$ | .246 × .859 = | .211 |
| + | .083 | $\|....\|$ | - .083 × 2.810 = | - .233 |
| + | .040 | $\|4s^2 4p_0^2\|$ | .040 × .7 = | .028 |
| + | .036 | $\|3d_0^2\|$ | - .036 × .696 = | - .025 |
| + | .017 | $\|4s_0^2 4p^2 3d_0^2\|$ | .017 × 2.5 = | .042 |
| + | .006 | $\|4p_0^2\|$ | - .006 × .7 = | - .004 |
| + | .003 | $\|4p_0^2 3d_0^2\|$ | .003 × .7 = | .002 |
| + | .757 | $\|1s^2\|$ | .757 × 1.088 = | .824 |
| | | | | .526 |

Table 4.7

Correlation Energy of the $^3\Delta$ State of ScH

Population Analysis, R=3.6 a.u.

| | 4s | 4p | 3d | 1s | $\varepsilon^{SCF}$ |
|---|---|---|---|---|---|
| 6σ (2) | .067 | .026 | .055 | .846 | -0.3566 |
| 7σ (1) | .690 | .285 | .014 | .011 | -0.2199 |
| 1δ (1) | | | 1.000 | | -0.3312 |

$$
\begin{aligned}
&0.067\ |4s^2| + 0.690\ |4s| + 0.243\ |....| \\
&0.026\ |4p_0^2| + 0.285\ |4p_0| + 0.689\ |....| \\
&0.055\ |3d_0^2| + 0.014\ |3d_0| + 0.931\ |....| \\
&\qquad\qquad 1.000\ |3d_2|
\end{aligned}
$$

| | | | | |
|---|---|---|---|---|
| .443 | $\|4s3d_2\|$ | | $-$ .443 × 1.211 = | $-$ .536 |
| .183 | $\|4s4p_0 3d_2\|$ | | $-$ .183 × .922 = | $-$ .182 |
| .156 | $\|3d_2\|$ | | $-$ .156 × 1.933 = | $-$ .302 |
| .043 | $\|4s^2 3d_2\|$ | | .043 × .000 = | .000 |
| .026 | $\|4s3d_0^2 3d_2\|$ | | .026 × .685 = | .018 |
| .064 | $\|4p_0 3d_2\|$ | | $-$ .064 × 1.505 = | $-$ .096 |
| .018 | $\|4s^2 4p_0 3d_2\|$ | | .018 × .7 = | .012 |
| .017 | $\|4s4p_0^2 3d_2\|$ | | .017 × .7 = | .012 |
| .011 | $\|4s4p_0 3d_0^2 3d_2\|$ | | .011 × 1.5 = | .016 |
| .009 | $\|3d_0^2 3d_2\|$ | | .009 × 1.109 = | .010 |
| .007 | $\|4s3d_0 3d_2\|$ | | $-$ .007 × .420 = | $-$ .003 |
| .003 | $\|4s4p_0 3d_0 3d_2\|$ | | $-$ .003 × .628 = | $-$ .002 |
| .003 | $\|4s^2 3d_0^2 3d_2\|$ | | $-$ .003 × 1.5 = | .005 |
| .002 | $\|3d_0 3d_2\|$ | | $-$ .002 × 1.008 = | $-$ .002 |
| .001 | $\|4s^2 3d_0 3d_2\|$ | | .001 × .387 = | .000 |
| .846 | $\|1s^2\|$ | | .846 × 1.088 = | .920 |
| | | | | $-$ .126 |

Table 4.8

Correlation Energy of the $^3\Pi$ State of ScH

Population Analysis, R=3.6 a.u.

| | 4s | 4p | 3d | 1s | $\epsilon^{SCF}$ |
|---|---|---|---|---|---|
| $6\sigma$ (2) | .088 | .034 | .048 | .824 | - 0.3481 |
| $7\sigma$ (1) | .696 | .277 | .012 | .015 | - 0.2199 |
| $3\pi$ (1) | | | 1.000 | | - 0.3232 |

$$
\begin{aligned}
&0.088\ |4s^2| + 0.696\ |4s| + 0.216\ |....| \\
&0.034\ |4p_0^2| + 0.277\ |4p_0| + 0.689\ |....| \\
&0.048\ |3d_0^2| + 0.012\ |3d_0| + 0.940\ |....| \\
&\qquad\qquad 1.000\ |3d_1|
\end{aligned}
$$

| | | |
|---|---|---|
| .451 $\|4s3d_1\|$ | - .451 × 1.211 | = - .546 |
| .181 $\|4s4p_0 3d_1\|$ | - .181 × .995 | = - .180 |
| .140 $\|3d_1\|$ | - .140 × 1.933 | = - .271 |
| .057 $\|4s_0 3d_1\|$ | .057 × .000 | = .000 |
| .056 $\|4p_0 3d_1\|$ | - .056 × 1.446 | = - .081 |
| .023 $\|4s3d_0^2 3d_1\|$ | .023 × .685 | = .016 |
| .023 $\|4s^2 4p_0 3d_1\|$ | .023 × .7 | = .015 |
| .022 $\|4s4p_0^2 3d_1\|$ | .022 × .7 | = .015 |
| .009 $\|4s4p_0 3d_0^2 3d_1\|$ | .009 × 1.5 | = .013 |
| .007 $\|3d_0^2 3d_1\|$ | .007 × 1.109 | = .008 |
| .006 $\|4s3d_0 3d_1\|$ | - .006 × .256 | = - .002 |
| .003 $\|4s^2 3d_0^2 3d_1\|$ | .003 × 1.5 | = .004 |
| .002 $\|4s4p_0 3d_0 3d_1\|$ | - .002 × .628 | = - .001 |
| .002 $\|3d_0 3d_1\|$ | - .002 × .828 | = - .002 |
| .001 $\|4s^2 3d_0 3d_1\|$ | .001 × .729 | = .001 |
| .824 $\|1s^2\|$ | .824 × 1.088 | = .897 |
| | | - .140 |

Table 4.9

Correlation Energy of the $^3\Sigma^+$ State of ScH

Population Analysis, R=3.6 a.u.

| | 4s | 4p | 3d | 1s | $\varepsilon^{SCF}$ |
|---|---|---|---|---|---|
| 6σ (2) | .106 | .050 | .047 | .785 | - 0.3669 |
| 7σ (1) | .178 | .039 | .810 | | - 0.3202 |
| 8σ (1) | .507 | .440 | .033 | | - 0.2235 |

$$
\begin{aligned}
.106\ |4s^2| &+ .685\ |4s| + .209\ |....| \\
.050\ |4p_0^2| &+ .479\ |4p_0| + .471\ |....| \\
.047\ |3d_0^2| &+ .843\ |3d_0| + .110\ |....|
\end{aligned}
$$

| | | | | |
|---|---|---|---|---|
| .277 | $\|4s4p_03d_0\|$ | - .277 × .996 | = | - .276 |
| .272 | $\|4s3d_0\|$ | - .272 × 1.211 | = | - .329 |
| .084 | $\|4p_03d_0\|$ | - .084 × 1.426 | = | - .120 |
| .083 | $\|3d_0\|$ | - .083 × 1.933 | = | - .160 |
| .043 | $\|4s^24p_03d_0\|$ | .043 × .7 | = | .030 |
| .042 | $\|4s^23d_0\|$ | .042 × .000 | = | - .000 |
| .036 | $\|4s4p_0\|$ | - .036 × 1.810 | = | - .065 |
| .035 | $\|4s\|$ | - .035 × 2.052 | = | - .072 |
| .015 | $\|4s4p_03d_0^2\|$ | .015 × 0.406 | = | .006 |
| .015 | $\|4s3d_0^2\|$ | - .015 × 0.351 | = | - .005 |
| .029 | $\|4s4p_0^23d_0\|$ | .029 × .7 | = | .020 |
| .011 | $\|4p_0\|$ | - .011 × 2.305 | = | - .025 |
| .011 | $\|....\|$ | - .011 × 2.810 | = | - .031 |
| .009 | $\|4s4p_0^2\|$ | - .009 × .2 | = | .002 |
| .006 | $\|4s^24p_0\|$ | - .006 × .2 | = | .001 |
| .005 | $\|3d_0^2\|$ | - .005 × .696 | = | - .003 |
| .785 | $\|1s^2\|$ | .785 × 1.088 | = | .854 |
| | | | | - .213 |

Table 4.10

Correlation Energy of the $^3\Phi$ State of ScH

Population Analysis, R=3.4 a.u.

| | 4s | 4p | 3d | 1s | $\epsilon^{SCF}$ |
|---|---|---|---|---|---|
| $6\sigma$ (2) | .097 | .000 | .071 | .827 | - 0.3564 |
| $3\pi$ (1) | | .974 | .026 | | - 0.1237 |
| $1\delta$ (1) | | | 1.000 | | - 0.3278 |

| | | |
|---|---|---|
| .097 $\|4s^2\|$ | | + .903 $\|....\|$ |
| | .974 $\|4p_1\|$ | + .026 $\|....\|$ |
| .071 $\|3d_0^2\|$ | | + .929 $\|....\|$ |
| | .026 $\|3d_1\|$ | + .974 $\|....\|$ |
| | 1.000 $\|3d_2\|$ | |

| | | | |
|---|---|---|---|
| .796 $\|4p_1 3d_2\|$ | - .796 × 1.476 | = | - 1.175 |
| .085 $\|4s^2 4p_1 3d_2\|$ | .085 × .7 | = | .060 |
| .063 $\|3d_0^2 4p_1 3d_2\|$ | .063 × .7 | = | .044 |
| .021 $\|3d_2\|$ | - .021 × 1.933 | = | - .041 |
| .021 $\|4p_1 3d_1 3d_2\|$ | - .021 × .689 | = | - .014 |
| .010 $\|4s^2 3d_2\|$ | .010 × .000 | = | .000 |
| .007 $\|4s^2 3d_0^2 4p_1 3d_2\|$ | .007 × 2.5 | = | .017 |
| .002 $\|4s^2 4p_1 3d_1 3d_2\|$ | .002 × 1.5 | = | .003 |
| .827 $\|1s^2\|$ | .827 × 1.088 | = | .900 |
| | | | - .209 |

Table 4.11

Correlation Energy of the $^3\Sigma^-$ State of ScH

Population Analysis, R=4.0 a.u.

| | 4s | 4p | 3d | 1s | $\epsilon^{SCF}$ |
|---|---|---|---|---|---|
| 6σ (2) | .102 | .021 | .019 | .849 | - 0.2715 |
| 1δ (2) | | | 1.000 | | - 0.1225 |

$$
\begin{aligned}
.012\ &|4s^2| &+&\ .898\ |....| \\
.021\ &|4p_0^2| &+&\ .979\ |....| \\
.019\ &|3d_0^2| &+&\ .981\ |....| \\
1.000\ &|3d_2^2|
\end{aligned}
$$

| | | | | |
|---|---|---|---|---|
| .862 | $\|3d_2^2\|$ | - .862 × | .768 | = - .662 |
| .098 | $\|4s^2 3d_2^2\|$ | .098 × | .796 | = .078 |
| .018 | $\|4p_0^2 3d_2^2\|$ | .018 × | .5 | = .009 |
| .016 | $\|3d_0^2 3d_2^2\|$ | .016 × | .5 | = .008 |
| .002 | $\|4s^2 4p_0^2 3d_2^2\|$ | .002 × | 2.5 | = .005 |
| .002 | $\|3d_0^2 4p_0^2 3d_2^2\|$ | .002 × | 2.5 | = .005 |
| .849 | $\|1s^2\|$ | .849 × | 1.088 | = .924 |
| | | | | .367 |

Table 4.12

Correlation Energies in ScH

| Configuration | State | Relative Correlation Energy ($cm^{-1}$) | Correlated $T_e$ ($cm^{-1}$) |
|---|---|---|---|
| $7\sigma 1\delta$ | $^3\Delta$ | 0 | 480 |
| $7\sigma 3\pi$ | $^3\Pi$ | -100 | 2820 |
| $7\sigma 8\sigma$ | $^3\Sigma^+$ | -700 | 4450 |
| $7\sigma^2$ | $^1\Sigma^+$ | 5260 | 0 |
| $1\delta 3\pi$ | $^3\Phi$ | -670 | 20800 |
| $1\delta^2$ | $^3\Sigma^-$ | 3980 | 27870 |
| $Sc(^2D)+H(^2S)$ | | 1020 | 14530 |

observed in an absorption experiment, as kT has a value of about 2000 $cm^{-1}$ at 3000°K, which is a typical shock tube temperature. It is more doubtful whether any of the other states are sufficiently low-lying to give rise to the strongest feature of the absorption spectrum, and so the bands observed by Smith may be tentatively assigned to a transition from the $^3\Delta$ or $^1\Sigma^+$ state. The calculations cannot unequivocally identify the upper state of the transition, although it is interesting to note that a $^3\Phi$ state is predicted to lie at 20,000 $cm^{-1}$. The corresponding transition in ScF is a strong feature of the absorption spectrum, the transition being loosely $4p \leftarrow 4s$, but this is not the only possible assignment of the transition.

The ground state of ScH is not necessarily correctly predicted by the correlation rules of Cheetham and Barrow, which predict the ground state to be $^3\Delta$, $^3\Pi$ or $^3\Sigma^+$. The relative energies of the configurations which may loosely be described as $4s^2$, $4s3d$ and $3d^2$ are of some importance, as these three types of configuration are the contenders for the ground state across the transition series. In ScH the $4s^2$ configuration is predicted to be the ground state; in later transition metal hydrides states with two 4s electrons become excited states, as the 3d orbital becomes more stable across the series. The configuration 4s3d is typical of the high spin configurations which provide the ground states of the molecules from TiH to FeH, whereas the $3d^2$ configuration, which is highly excited in ScH, becomes more stable across the series, finally becoming the ground state at CoH. The d orbital population of the $7\sigma$ orbital in the $^3\Delta$ state ScH is only 0.01; this reflects the fact that in ScH the 4s orbital is appreciably more stable than the 3d, and there is very little mixing between the two orbitals. The splitting of the d orbitals is predicted to be in the order $\delta < \pi < \sigma$, which is the same as that found in the fluorides, but the magnitude of the splitting is now appreciably smaller. In ScF the $^3\Delta$-$^3\Pi$ splitting is calculated to be over 5000 $cm^{-1}$, whereas in ScH it is less than 2300 $cm^{-1}$. It would not be expected that transitions to the $\Pi$ or $\Sigma^+$ states, which are strong features of the ScF

spectrum, would be observed in ScH, where they will lie deep in the infrared.

The nature of the $3\pi$ orbital in ScH is of some significance; as in ScF, the lowest $^3\Phi$ state is derived from the configuration $3d\delta 4p\pi$, and not $3d\delta 3d\pi$ as might have been expected as the lowest $^3\Pi$ is from the configuration $4s\sigma 3d\pi$. This effect has been discussed in Chapter 3, and may be attributed to the relatively high repulsion between 4s and 4p electrons.

The dissociation energy of ScH is calculated to be 1.8 e.v. It is hard to assess the accuracy of this figure; dissociation energies are probably less accurate than excitation energies, as there is no cancellation of errors from atomic states whose correlation energies are hard to estimate. The calculated value probably acts as a lower bound to the dissociation energy, as the interatomic correlation effects, which stabilise the molecule relative to the separated atoms, have been neglected. The value of 1.8 e.v. is certainly reasonable; it compares with an experimental value of 1.7 e.v. for the neighbouring molecule CaH (Kopp et al. 1966).

## 4.3 Titanium and Vanadium Monohydrides

### 4.3.1 Introduction

Titanium and vanadium monohydrides are both potentially of astrophysical importance as constituents of cool stars, although to date it has not proved possible to identify any lines in stellar spectra with either of these molecules. The only terrestrial observations of the molecules have been by Smith (Smith and Gaydon 1972, Smith 1973), who was unable to analyse the bands he discovered. TiH showed three systems, one between 4700 Å and 4800 Å, one between 5210 Å and 5500 Å, and a rather weak system at 5030 Å to 5110 Å. VH showed absorption in the region 4400 Å to 4800 Å. The isotope shifts in each case suggested that these are (0,0) bands, or part of the (0,0) sequence. Smith claimed that correlation arguments suggest that the ground state of TiH is doublet, quartet or sextet, $\Sigma$, $\Pi$, $\Delta$ or $\Phi$, which is not a great help, and commented that the spectra seemed to be compatible with multiplicities of 5 for VH, and at least 4 for TiH. In order to obtain more detailed information on the nature of the low-lying states in TiH and VH, ab initio molecular orbital calculations were performed for both of these molecules (Scott and Richards 1974a, c), and the results are presented below.

### 4.3.2 Approximate Hartree-Fock Calculations on TiH and VH

The calculations described in this section are similar to those on ScH (section 4.2.2). They were performed using the ALCHEMY programme, and a basis set derived from the double zeta set of Clementi et al. (1967). The basis set is augmented by two 4p functions and one 4f function, although because none of the states considered have a 4p orbital occupied, optimisation of the 4p exponents is not particularly important. The 4p exponents are chosen to be 4.0536 and 1.5450 for Ti, and 4.05 and 1.7 for V, and it is expected that these can give a reasonable representation of the 4p orbital contributions. The 4f exponent is again chosen to be 2.75, and the H basis is similar to that used for ScH. Full details of the basis sets are given

in Table 4.13; in this representation the energy of the Ti atom ($^3F$) is -848.38434 a.u., within 0.0209 a.u. of the Hartree-Fock limit.

Calculations were performed on nine low-lying states of TiH, and seven low-lying states of VH, selected on the basis of orbital energies, at five values of the internuclear separation around the equilibrium value, and the potential curves analysed by the programme MCFIT. The calculated spectroscopic constants are summarised in Table 4.14. It is expected that, as is usual in Hartree-Fock calculations, the $r_e$ values will be a few per cent too small, and the $\omega_e$ values too large, although the trends in vibration frequency should be correctly predicted. The calculations give the state of lowest energy of TiH to be the $^4\Phi$ state from the configuration

$$1\sigma^2\ 2\sigma^2\ 3\sigma^2\ 4\sigma^2\ 5\sigma^2\ 6\sigma^2\ 7\sigma\ 1\pi^2\ 2\pi^4\ 3\pi\ 1\delta,$$

and that of VH to be the $^5\Delta$ state from the configuration

$$1\sigma^2\ 2\sigma^2\ 3\sigma^2\ 4\sigma^2\ 5\sigma^2\ 6\sigma^2\ 7\sigma\ 1\pi^4\ 2\pi^4\ 3\pi^2\ 1\delta.$$

The 7σ orbitals are mainly 4s(M), and the 8σ, 3π and 1δ orbitals, of which the 8σ is not occupied in the ground states, are mainly 3d(M). Population analyses and orbital energies of the valence orbitals of the low-lying states are given in Tables 4.16-4.18.

### 4.3.3 Correlation Energy of TiH

As in the case of ScH, the correlation energy of the states of TiH is estimated by the method of Liu and Verhaegen from atomic data. Correlation energies were estimated for two of the quartet states, one doublet state, and for the separated atoms. The correlation energies of the remaining quartet states are discussed in section 4.3.4. It is not necessary to compute correlation energies for VH, as the low spin states are now too highly excited to be considered for the ground state. Numerical Hartree-Fock calculations were carried out for twenty-seven states of the Ti and V atoms and ions, and the

Table 4.13

STO Basis Functions for TiH and VH

| Function | Type | Atom | Exponent | | Function | Type | Atom | Exponent | |
|---|---|---|---|---|---|---|---|---|---|
| | | | Ti | V | | | | Ti | V |
| 1. | 1sσ | M | 19.1672 | 20.6421 | 19. | 1sσ | H | 1.45 | 1.45 |
| 2. | 1sσ | M | 24.3682 | 26.1496 | 20. | 2sσ | H | 1.85 | 1.85 |
| 3. | 2sσ | M | 8.6061 | 9.1890 | 21. | 2pσ | H | 1.1455 | 1.145 |
| 4. | 2sσ | M | 13.0122 | 12.7217 | 22. | 3dσ | H | 1.85 | 1.85 |
| 5. | 3sσ | M | 3.1804 | 3.3876 | 23. | 2pπ | M | 8.2114 | 8.7784 |
| 6. | 3sσ | M | 4.2714 | 4.6018 | 24. | 2pπ | M | 14.6952 | 16.0868 |
| 7. | 4sσ | M | 0.9906 | 0.9417 | 25. | 3pπ | M | 5.0016 | 4.4957 |
| 8. | 4sσ | M | 1.7265 | 1.6209 | 26. | 3pπ | M | 2.9769 | 2.8683 |
| 9. | 2pσ | M | 14.6952 | 8.7784 | 27. | 4pπ | M | 4.0536 | 4.05 |
| 10. | 2pσ | M | 8.2114 | 16.0868 | 28. | 4pπ | M | 1.5450 | 1.7 |
| 11. | 3pσ | M | 5.0016 | 4.4957 | 29. | 3dπ | M | 1.983 | 2.2166 |
| 12. | 3pσ | M | 2.9769 | 2.8683 | 30. | 3dπ | M | 4.6227 | 5.1853 |
| 13. | 4pσ | M | 4.0536 | 4.05 | 31. | 4fπ | M | 2.75 | 2.75 |
| 14. | 4pσ | M | 1.5450 | 1.7 | 32. | 2pπ | H | 1.1455 | 1.145 |
| 15. | 3dσ | M | 1.983 | 2.2166 | 33. | 3dπ | H | 1.85 | 1.85 |
| 16. | 3dσ | M | 4.6227 | 5.1853 | 34. | 3dδ | M | 1.983 | 2.2166 |
| 17. | 4fσ | M | 2.75 | 2.75 | 35. | 3dδ | M | 4.6227 | 5.1853 |
| 18. | 1sσ | H | 0.915 | 0.915 | 36. | 3dδ | H | | 1.85 |

Table 4.14

Hartree-Fock Calculations on TiH and VH

| | Configuration | State | $T_e$ ($cm^{-1}$) | $r_e$ (Å) | $\omega_e$ ($cm^{-1}$) |
|---|---|---|---|---|---|
| TiH | $7\sigma 3\pi 1\delta$ | $^4\Phi$ | 0 | 1.86 | 1510 |
| | $7\sigma 8\sigma 1\delta$ | $^4\Delta$ | 3510 | 1.95 | 1410 |
| | $7\sigma 3\pi^2$ | $^4\Sigma^-$ | 4360 | 1.86 | 1460 |
| | $7\sigma 3\pi 1\delta$ | $^4\Pi$ | 5190 | 1.86 | 1510 |
| | $7\sigma 1\delta^2$ | $^4\Sigma^-$ | 7510 | 1.85 | 1550 |
| | $7\sigma^2 1\delta$ | $^2\Delta$ | 11680 | 1.70 | 1790 |
| | $7\sigma 1\delta^2$ | $^2\Sigma^-$ | 11810 | 1.86 | 1550 |
| | $7\sigma 8\sigma 3\pi$ | $^4\Pi$ | 12610 | 1.93 | 1380 |
| | $7\sigma^2 3\pi$ | $^2\Pi$ | 16530 | 1.68 | 1780 |
| VH | $7\sigma 3\pi^2 1\delta$ | $^5\Delta$ | 0 | 1.79 | 1550 |
| | $7\sigma 8\sigma 3\pi 1\delta$ | $^5\Phi$ | 4080 | 1.89 | 1430 |
| | $7\sigma 8\sigma 1\delta^2$ | $^5\Sigma^-$ | 5020 | 1.90 | 1470 |
| | $7\sigma 3\pi 1\delta^2$ | $^5\Pi$ | 6200 | 1.79 | 1600 |
| | $7\sigma 8\sigma 3\pi 1\delta$ | $^5\Pi$ | 9860 | 1.89 | 1440 |
| | $7\sigma 8\sigma 3\pi^2$ | $^5\Sigma^-$ | 16200 | 1.88 | 1410 |
| | $7\sigma^2 3\pi 1\delta$ | $^3\Phi$ | 16320 | 1.62 | 1870 |

results, together with the corresponding atomic data, are given in Table 4.15. Where it is necessary to construct linear combinations of atomic states to correspond to determinants, these are given in Appendix B. The contributions to the correlation energies of each of the states are given in Tables 4.16-4.18. Table 4.19 gives the energies of the states after the correlation energy corrections have been applied; the accuracy of the method has been discussed in section 4.2.3.

4.3.4 Near Degeneracy Effects in TiH and VH

Table 4.14 gives the results of Hartree-Fock calculations on TiH and VH; these differ from the results on ScH in one important respect, namely that there are two pairs of states of the same symmetry which are near-degenerate with each other. The method of Liu and Verhaegen for estimating correlation energies takes no account of near-degeneracy effects, which must be treated separately. It is therefore necessary to perform a 2×2 configuration interaction calculation for both the $\Sigma^-$ and $\Pi$ states. A problem arises as to how to perform this C.I. calculation; the ALCHEMY programme performs a variational calculation on the lower state, obtains a wave function for the higher state by use of virtual orbitals, and then performs configuration interaction between these two states. Unfortunately the upper state is not well represented by virtual orbitals, with the result that the energy difference between the states is too large, and the resultant mixing coefficients too small. The procedure used in these calculations is different. The off-diagonal matrix element between the states is calculated in the virtual orbital approximation by the ALCHEMY programme, but the diagonal elements are both taken from variational calculations. This procedure may be judged by performing analogous calculations on the Ti atom, where the corresponding states, which are all components of the $^4F$ state, are degenerate. It is then found that the difference in energies between the states calculated in this way is less than 10 $cm^{-1}$, and any errors introduced in this way are almost certainly smaller than the energy differences between the states in TiH and

Table 4.15

Calculated and Experimental Energies in Ti

| Species | Configuration | State | Exptl. Energy (e.v.) | Calc. Energy (e.v.) | $\Delta E_{CORR}$ (e.v.) |
|---|---|---|---|---|---|
| $Ti^{3+}$ | $d$ | $^2D$ | 47.803 | 44.536 | - 3.267 |
| $Ti^{2+}$ | $d^2$ | $^3F$ | 19.666 | 17.832 | - 1.834 |
| | | $^3P$ | 20.958 | 19.497 | - 1.461 |
| $Ti^{+}$ | $sd^2$ | $^4F$ | 6.029 | 4.966 | - 1.063 |
| | | $^4P$ | 7.237 | 6.568 | - 0.669 |
| | $s^2d$ | $^2D$ | 9.113 | 8.975 | - 0.138 |
| | $pd^2$ | $^4G$ | 9.712 | 8.369 | - 1.343 |
| | | $^4D$ | 10.054 | 9.954 | - 1.009 |
| | | $^4D$ | 11.036 | 10.079 | - 0.957 |
| | | $^4S$ | 10.963 | 8.745 | - 1.309 |
| | $d^3$ | $^2H$ | 7.580 | 7.275 | - 0.305 |
| | | $^2G$ | 7.125 | 6.801 | - 0.324 |
| | | $^2D$ | 7.577 | 7.445 | - 0.132 |
| Ti | $s^2d^2$ | $^3F$ | - 0.802 | - 0.540 | 0.262 |
| | | $^3P$ | 0.226 | 1.208 | 0.802 |
| | $sd^3$ | $^5F$ | 0 | 0 | 0 |
| | | $^5P$ | 0.909 | 1.305 | 0.396 |
| | $spd^2$ | $^5G$ | 1.175 | 0.378 | - 0.797 |
| | | $^5D$ | 1.472 | 1.936 | - 0.343 |
| | | $^5S$ | 2.279 | 0.730 | - 0.742 |
| | | $^5D$ | 2.365 | 2.002 | - 0.363 |
| $V^{+}$ | $sd^3$ | $^5F$ | 0 | 0 | 0 |
| V | $s^2d^3$ | $^2G$ | - 5.736 | - 3.337 | 1.880 |
| | | $^2H$ | - 5.217 | - 3.902 | 1.834 |
| | | $^2D$ | - 5.299 | - 3.117 | 2.182 |
| | $sd^4$ | $^4H$ | - 5.242 | - 3.444 | 1.798 |
| | | $^4F$ | - 5.151 | - 3.189 | 1.962 |
| | | $^4P$ | - 5.193 | - 3.257 | 1.957 |

Table 4.16

Correlation of the $^4\Phi$ State of TiH

Population Analysis, R=3.5 a.u.

| | 4s | 4p | 3d | 1s | $\varepsilon^{SCF}$ |
|---|---|---|---|---|---|
| $6\sigma$ (2) | .099 | .024 | .051 | .819 | - 0.3516 |
| $7\sigma$ (1) | .818 | .131 | .038 | .015 | - 0.2244 |
| $1\delta$ (1) | | | 1.000 | | - 0.4127 |
| $3\pi$ (1) | | | 1.000 | | - 0.3986 |

$$
\begin{aligned}
0.099\ &|4s^2| + 0.818\ |4s| + 0.083\ |....| \\
0.024\ &|4p_0^2| + 0.131\ |4p_0| + 0.845\ |....| \\
0.051\ &|3d_0^2| + 0.038\ |3d_0| + 0.911\ |....| \\
&\qquad 1.000\ |3d_1 3d_2|
\end{aligned}
$$

| | | | | | | | |
|---|---|---|---|---|---|---|---|
| .630 | $\|4s3d_1 3d_2\|$ | - | .630 | × | 1.063 | = | - .670 |
| .098 | $\|4s4p_0 3d_1 3d_2\|$ | - | .098 | × | .780 | = | - .076 |
| .064 | $\|3d_1 3d_2\|$ | - | .064 | × | 1.834 | = | - .117 |
| .076 | $\|4s^2 3d_1 3d_2\|$ | | .076 | × | .262 | = | .020 |
| .035 | $\|4s3d_0^2 3d_1 3d_2\|$ | | .035 | × | 1.810 | = | .063 |
| .026 | $\|4s3d_0 3d_1 3d_2\|$ | | .026 | × | .000 | = | .000 |
| .018 | $\|4s4p_0^2 3d_1 3d_2\|$ | | .018 | × | 1.8 | = | .032 |
| .012 | $\|4s^2 4p_0 3d_1 3d_2\|$ | | .012 | × | 1.8 | = | .021 |
| .010 | $\|4p_0 3d_1 3d_2\|$ | - | .010 | × | 1.330 | = | - .013 |
| .005 | $\|4s4p_0 3d_0^2 3d_1 3d_2\|$ | | .005 | × | 2.7 | = | .013 |
| .004 | $\|4s4p_0 3d_0 3d_1 3d_2\|$ | | .004 | × | 1.8 | = | .007 |
| .004 | $\|3d_0^2 3d_1 3d_2\|$ | | .004 | × | .0 | = | .000 |
| .004 | $\|4s^2 3d_0^2 3d_1 3d_2\|$ | | .004 | × | 2.7 | = | .011 |
| .819 | $\|1s^2\|$ | | .819 | × | 1.088 | = | .891 |
| | | | | | | | .188 |

Table 4.17

Correlation Energy of the $^4\Delta$ State of TiH

Population Analysis, R=3.7 a.u.

| | 4s | 4p | 3d | 1s | $\epsilon^{SCF}$ |
|---|---|---|---|---|---|
| 6σ (2) | .122 | .044 | .033 | .744 | - 0.3534 |
| 7σ (1) | .083 | .162 | .713 | .037 | - 0.3459 |
| 8σ (1) | .689 | .088 | .214 | .008 | - 0.2846 |
| 1δ (1) | | | 1.000 | | - 0.4375 |

$$
\begin{aligned}
&.122\ |4s^2| + .772\ |4s| + .106\ |....| \\
&.044\ |4p_0^2| + .250\ |4p_0| + .706\ |....| \\
&.033\ |3d_0^2| + .927\ |3d_0| + .040\ |....| \\
&\qquad\qquad 1.000\ |3d_2|
\end{aligned}
$$

| | | | | | | |
|---|---|---|---|---|---|---|
| .505 | $\|4s3d_03d_2\|$ | - | .505 | × 1.063 | = | - .537 |
| .179 | $\|4s4p_03d_03d_2\|$ | - | .179 | × .770 | = | - .138 |
| .080 | $\|4s^23d_03d_2\|$ | | .080 | × .262 | = | .021 |
| .069 | $\|3d_03d_2\|$ | - | .069 | × 1.834 | = | - .127 |
| .031 | $\|4s4p_0^23d_03d_2\|$ | | .031 | × 1.8 | = | .055 |
| .028 | $\|4s^24p_03d_03d_2\|$ | | .028 | × 1.8 | = | .050 |
| .025 | $\|4p_03d_03d_2\|$ | - | .025 | × 1.325 | = | - .033 |
| .022 | $\|4s3d_2\|$ | - | .022 | × 1.6 | = | - .037 |
| .018 | $\|4s3d_0^23d_2\|$ | | .018 | × .5 | = | .009 |
| .005 | $\|4s^24p_0^23d_03d_2\|$ | | .005 | × 3.0 | = | .015 |
| .004 | $\|4p_0^23d_03d_2\|$ | | .004 | × .5 | = | .002 |
| .003 | $\|3d_2\|$ | - | .003 | × 3.267 | = | - .010 |
| .003 | $\|4s^23d_0^23d_2\|$ | | .003 | × 1.873 | = | .006 |
| .003 | $\|4s^23d_2\|$ | - | .003 | × .138 | = | .000 |
| .006 | $\|4s4p_03d_0^23d_2\|$ | | .006 | × 1.8 | = | .011 |
| .794 | $\|1s^2\|$ | | .794 | × 1.088 | = | .864 |
| | | | | | | .165 |

Table 4.18

Correlation Energy of the $^2\Delta$ State of TiH

Population Analysis, R=3.2 a.u.

| | 4s | 4p | 3d | 1s | $\epsilon^{SCF}$ |
|---|---|---|---|---|---|
| $6\sigma$ (2) | .021 | .018 | .181 | .774 | - 0.4177 |
| $7\sigma$ (2) | .822 | .011 | .235 | - .064 | - 0.2397 |
| $1\delta$ (1) | | | 1.000 | | - 0.4571 |

$$
\begin{aligned}
.843\ &|4s^2| &+&\ .157\ |....| \\
.029\ &|4p_0^2| &+&\ .971\ |....| \\
.416\ &|3d_0^2| &+&\ .584\ |....| \\
1.000\ &|3d_2|
\end{aligned}
$$

| | | | | | |
|---|---|---|---|---|---|
| .478 | $\|4s^2 3d_2\|$ | - .478 | × .138 | = - | .065 |
| .340 | $\|4s^2 3d_0^2 3d_2\|$ | .340 | × 1.873 | = | .637 |
| .089 | $\|3d_2\|$ | - .089 | × 3.267 | = - | .290 |
| .063 | $\|3d_0^2 3d_2\|$ | - .063 | × .250 | = - | .015 |
| .012 | $\|4s^2 4p_0^2 3d_2\|$ | .012 | × 1.8 | = | .022 |
| .010 | $\|4s^2 4p_0^2 3d_0^2 3d_2\|$ | .010 | × 4.0 | = | .040 |
| .002 | $\|4p_0^2 3d_0^2 3d_2\|$ | .002 | × 1.8 | = | .004 |
| .002 | $\|4p_0^2 3d_2\|$ | - .002 | × .6 | = - | .001 |
| .710 | $\|1s^2\|$ | .710 | × 1.088 | = | .773 |
| | | | | | 1.104 |

Table 4.19

Correlation Energies in TiH

| Configuration | State | Relative Correlation Energy ($cm^{-1}$) | Correlated $T_e$ ($cm^{-1}$) |
|---|---|---|---|
| $7\sigma 3\pi 1\delta$ | | 0 | 0 |
| $7\sigma 8\sigma 1\delta$ | | -180 | 3700 |
| $7\sigma^2 1\delta$ | | 7390 | 4300 |
| Ti ($^3$F) + H ($^2$S) | | 600 | 12700 |

VH. The results of the configuration interaction calculations are given in Table 4.20. The mixing coefficients of the $\Sigma^-$ and $\Pi$ states are those for the equilibrium internuclear separation.

4.3.5 Discussion

The ground states of TiH and VH are predicted to be $^4\Phi$ and $^5\Delta$ respectively, from the high-spin configurations $7\sigma 3\pi 1\delta$ and $7\sigma 3\pi^2 1\delta$. These may be described loosely as $4s3d^2$ and $4s3d^3$. The low-spin configurations, in which the $7\sigma$ orbital, which is mainly 4s, is doubly occupied, are calculated to lie 0.5 e.v. higher in TiH after a oorrelation energy correction, and if the correlation energy correction is rather similar in VH, then the low-spin states lie a further 0.5 e.v. higher than in TiH. The variationally calculated low-spin states still correspond mainly to configurations of the type $4s^2 3d^n$, rather than $3d^{n+2}$, although the $3d^{n+2}$ configurations become the ground states of the later transition metal hydrides. TiH thus resembles the parent positive ion $Ti^+$ in having one 4s electron in the ground state, but not a second, preferring to have the maximum possible number of unpaired spins. VH also has one 4s electron in the ground state, though here it differs from the ion $V^+$, which has a $^5D$ ground state ($d^4$). That the correlation rules of Cheetham and Barrow correctly predict the ground state of VH must therefore be regarded as fortuitous; the symmetries of the low-lying states of TiH and VH are identical, and only the sign of the ligand-field splitting, which is not considered by Cheetham and Barrow, prevents the low-lying $^5\Phi$ state from being the ground state; Cheetham and Barrow predict the ground state of TiH to be $^4\Phi$, $^4\Delta$, $^4\Pi$ or $^4\Sigma$, but allow only $^5\Delta$, $^5\Pi$ or $^5\Sigma$ for VH.

The results of the Hartree-Fock calculations on TiH are significant, as they illustrate the importance of a factor not previously considered in transition metal diatomic molecules. If the states of these molecules are described by single configuration wave functions, then differences in the repulsion energies between d electrons become important. Thus although the ligand stabilises the $d\delta$ orbital relative to the $d\pi$ orbital, the configuration

Table 4.20

Configuration Interaction Calculations on TiH and VH

| Configuration | State | $T_e$ ($cm^{-1}$) | $r_e$ (Å) | $\omega_e$ ($cm^{-1}$) |
|---|---|---|---|---|
| $0.90\|\sigma\sigma\pi\|-0.43\|\sigma\pi\delta\|$ | $^4\Pi$ | 15140 | 1.90 | 1440 |
| $0.81\|\sigma\delta^2\|-0.59\|\sigma\pi^2\|$ | $^4\Sigma^-$ | 11220 | 1.85 | 1520 |
| $\|\sigma\sigma\delta\|$ | $^4\Delta$ | 3510 | 1.95 | 1410 |
| $0.90\|\sigma\pi\delta\|+0.43\|\sigma\sigma\pi\|$ | $^4\Pi$ | 2750 | 1.89 | 1430 |
| $0.81\|\sigma\pi^2\|+0.59\|\sigma\delta^2\|$ | $^4\Sigma^-$ | 650 | 1.86 | 1490 |
| $\|\sigma\pi\delta\|$ | $^4\Phi$ | 0 | 1.86 | 1510 |
| | | | | |
| $0.93\|\sigma\sigma\pi^2\|-0.37\|\sigma\sigma\delta^2\|$ | $^5\Sigma^-$ | 18330 | 1.87 | 1430 |
| $0.82\|\sigma\sigma\pi\delta\|-0.57\|\sigma\pi\delta^2\|$ | $^5\Pi$ | 13970 | 1.82 | 1580 |
| $\|\sigma\sigma\pi\delta\|$ | $^5\Phi$ | 4080 | 1.89 | 1430 |
| $0.93\|\sigma\sigma\delta^2\|+0.37\|\sigma\sigma\pi^2\|$ | $^5\Sigma^-$ | 2880 | 1.90 | 1450 |
| $0.82\|\sigma\pi\delta^2\|+0.57\|\sigma\sigma\pi\delta\|$ | $^5\Pi$ | 2260 | 1.85 | 1460 |
| $\|\sigma\pi^2\delta\|$ | $^5\Delta$ | 0 | 1.79 | 1550 |

$7\sigma 1\delta^2$ lies above the configuration $7\sigma 3\pi 1\delta$, as the repulsion between two $d\delta$ electrons is higher than that between a $d\delta$ and $d\pi$ electron. Similarly the lowest $^4\Sigma^-$ state is derived from the configuration $7\sigma 3\pi^2$ and not $7\sigma 1\delta^2$, as would have been supposed, as the $\pi$-$\pi$ repulsion energy is less than the $\delta$-$\delta$ repulsion energy. Furthermore, the $\sigma$-$\pi$ repulsion energy is greater than the $\sigma$-$\delta$ repulsion energy; it is suggested in section 4.5 that this may be the explanation for the nature of the ground state of NiH. In TiH, it is shown below that configuration interaction greatly reduces the significance of these deductions, as the low-lying states may be considered as the states of the parent atom, slightly perturbed by the presence of a hydrogen atom. But in cases where the molecule is not well described as a perturbed atom, as may be the case in NiH and possibly in TiF and VO, they may be of critical importance in determining the ordering of states.

In both VH and TiH the calculations show six high-spin states; four of the states are very low-lying, and the other two lie together about 1.5 e.v. higher. These six states are recognisable as the four components of the $^4F$ state of the $Ti^+$ ion ($4s3d^2$) and the $^5F$ state of the $V^+$ ion ($4s3d^3$), and the two components of the $^4P$ and $^5P$ states from the same configurations. It is therefore not necessary to calculate correlation energies for the $\Sigma^-$ and $\Pi$ states, as these will be very close to those of the $\Delta$ and $\Phi$ states, whose correlation energies are essentially identical. The conclusion is therefore that in TiH and VH the H atom is acting only as a small perturbation on the electronic states of the metal atoms or ions. (The hydrides are intermediate between M-H and $M^+$-$H^-$, and their structure may be regarded as a H atom perturbing an M atom, or an $H^-$ ion perturbing an $M^+$ ion.) This differs appreciably from the situation in VO, which formally has an isoelectronic valence shell with TiH, in which the ground state is $^4\Sigma^-$, and is assigned the configuration $\sigma\delta^2$ (Carlson and Moser 1966). The ordering of the low-lying states in TiH, $^4\Phi < ^4\Sigma^- < ^4\Pi < ^4\Delta$, is exactly the opposite of that found in VH, $^5\Delta < ^5\Pi < ^5\Sigma^- < ^5\Phi$, and similarly the components of the P states are ordered $^4\Sigma^- < ^4\Pi$ in TiH, and

$^5\Pi < ^5\Sigma^-$ in VH. As the high-spin $sd^5$ configuration is spherically symmetrical, the states of VH ($sd^3$) may be regarded as the 'hole' states corresponding to the states of TiH ($sd^2$); this explains why the perturbation in VH has the opposite sense to that in TiH. In ScH it was shown that the ligand stabilises the d orbitals in the sense $\delta < \pi < \sigma$, and this ordering is compatible with the calculated ordering in TiH and VH. The calculated spectroscopic constants show a steady variation with the perturbation, the most stable states having the highest vibration frequencies and lowest internuclear separations.

This description of the low-lying states of TiH and VH may be extended to the neighbouring CrH. If the lowest lying states in CrH correspond loosely to the configuration $sd^4$, which is reasonable considering the nature of the ground states of ScH, TiH and VH, then the ordering of the $^6\Delta$, $^6\Pi$ and $^6\Sigma^+$ in CrH may be deduced from the ordering of the $^3\Delta$, $^3\Pi$ and $^3\Sigma^+$ states of ScH, the corresponding 'hole' states. This predicts that the ground state of CrH should be $^6\Sigma^+$; the only state which has been observed in absorption experiments on CrH is $^6\Sigma^+$.

## 4.4 Iron Monohydride

### 4.4.1 Introduction

The molecule FeH occupies an important place in the transition metal monohydrides, lying between the high-spin molecule MnH and the low-spin CoH. MnH has a $^7\Sigma^+$ ground state, from the configuration $\sigma^2\pi^2\delta^2\sigma\sigma^*$, where the anti-bonding $\sigma^*$ orbital is occupied, whereas the $^3\Phi$ ground state of CoH is presumably derived from the configuration $\sigma^2\pi^3\delta^3\sigma^2$, where the $\sigma$ orbital is now doubly occupied. In spite of its potential astrophysical importance, there has been only one experimental investigation of FeH; Carroll and McCormack (1972) obtained the spectrum in absorption and emission in a King furnace. They did not report an analysis, remarking only that the transition appeared to be between states of high multiplicity.

There has been one theoretical study of FeH, by Walker et al. (1973) who used many body perturbation theory with a single-centre basis set. This technique had previously given good results for CH. They predicted that their spectroscopic constants should be reliable, except for the vibration frequencies which they expected to be too large. Their main conclusion was that the ground state of FeH is $^6\Sigma^+$, from the configuration $\sigma^2\pi^2\delta^2\sigma^2\sigma$, and that two other states are low-lying, a $^6\Pi$ state at 5900 $cm^{-1}$ ($\sigma^2\pi^3\delta^2\sigma\sigma$) and a $^6\Delta$ state at 9200 $cm^{-1}$ ($\sigma^2\pi^2\delta^3\sigma\sigma$). The quartets from the low-spin configurations $\sigma^2\pi^2\delta^3\sigma^2$ and $\sigma^2\pi^3\delta^2\sigma^2$ were calculated to lie at 27,900 $cm^{-1}$ and 37,000 $cm^{-1}$ respectively. Thus the ligand-field splitting of the d orbitals was predicted to be $d\sigma<d\pi<d\delta$ in the high-spin states, and $d\delta<d\pi$ in the low-spin states. These results seem rather surprising in view of the calculations described in the previous sections, and of the calculation of Bagus and Schaefer on MnH, in which the splitting has been $d\delta<d\pi<d\sigma$, and where the magnitude of the splitting has been appreciably smaller. It also seemed worthwhile to investigate the energy difference between the high-spin and low-spin states, as in the neighbouring molecule CoH the ground state is thought to be low-spin.

Hartree-Fock calculations have previously been shown to be a reliable source of data on transition metal diatomic molecules, and such calculations have therefore been performed on the low-lying states of FeH (Scott and Richards 1974d).

4.4.2 Approximate Hartree-Fock Calculations

The calculations were performed in the matrix Hartree-Fock approximation as implemented in the ALCHEMY programme. The basis set is derived from the double zeta set of Clementi et al. (1967), augmented by two 4p functions and one 4f function. In this basis the energy of the Fe atom ($^4$D) is -1262.3558 a.u., within 0.0867 a.u. of the Hartree-Fock limit. The hydrogen basis set is similar to that used in calculations on other monohydrides described in this chapter. Full details of the basis set are given in Table 4.21. Calculations were performed on five states, three high-spin and two low-spin, at five internuclear separations around the equilibrium value. Spectroscopic constants were obtained by the programme MCFIT. Table 4.22 gives the spectroscopic constants, along with those calculated by Walker et al. Table 4.23 gives population analyses and orbital energies of the valence orbitals at the equilibrium internuclear distance. The ground state is calculated to be the $^6\Delta$ state from the configuration $1\to6\sigma^2 7\sigma 8\sigma 1\pi^4 2\pi^4 3\pi^2 1\delta^3$. The doubly occupied $6\sigma$ orbital has a higher orbital energy than the singly occupied $7\sigma$ orbital. The $7\sigma$, $3\pi$ and $1\delta$ orbitals are mainly 3d(Fe), in agreement with the suggestion that the 3d orbitals remain largely unchanged on molecule formation in the early transition metal hydrides. The bonding is mainly between the 4s, 4p and 1s (H) orbitals; the antibonding $8\sigma$ orbital is a linear combination of 4s and 4p orbitals.

4.4.3 Discussion

The low-spin states of FeH ($^4\Delta$ and $^4\Pi$) are calculated to lie about 3 e.v. above the ground state. This is the same general result as that obtained by Walker et al., who obtained a similar excitation energy, and the splitting is rather smaller in this work. Correlation energy corrections have not been

Table 4.21

S.T.O. Basis Functions of FeH

| Type | Symmetry | Centre | Exponent |
|---|---|---|---|
| 1s | σ | Fe | 23.0020 |
| 1s | σ | Fe | 28.9800 |
| 2s | σ | Fe | 10.6180 |
| 2s | σ | Fe | 14.7057 |
| 3s | σ | Fe | 3.9551 |
| 3s | σ | Fe | 5.5099 |
| 4s | σ | Fe | 1.1331 |
| 4s | σ | Fe | 2.0826 |
| 2p | σ,π | Fe | 10.5045 |
| 2p | σ,π | Fe | 19.6544 |
| 3p | σ,π | Fe | 5.9885 |
| 3p | σ,π | Fe | 3.6793 |
| 4p | σ,π | Fe | 1.9 |
| 4p | σ,π | Fe | 1.1 |
| 3d | σ,π,δ | Fe | 2.6139 |
| 3d | σ,π,δ | Fe | 6.0576 |
| 4f | σ,π,δ | Fe | 2.75 |
| 1s | σ | H | 0.915 |
| 1s | σ | H | 1.45 |
| 2s | σ | H | 1.85 |
| 2p | σ,π | H | 1.145 |
| 3d | σ,π,δ | H | 1.85 |

Table 4.22

Calculated Spectroscopic Constants of FeH

| | | This work | | | Walker et al. | | |
|---|---|---|---|---|---|---|---|
| Configuration | State | $T_e(cm^{-1})$ | $r_e(\AA)$ | $\omega_e(cm^{-1})$ | $T_e(cm^{-1})$ | $r_e(\AA)$ | $\omega_e(cm^{-1})$ |
| $\sigma^2\pi^2\delta^3\sigma\sigma$ | $^6\Delta$ | 0 | 1.73 | 1650 | 0 | 1.60 | 2535 |
| $\sigma^2\pi^2\delta^2\sigma^2\sigma$ | $^6\Sigma^+$ | 1520 | 1.72 | 1600 | -9200 | 1.49 | 2820 |
| $\sigma^2\pi^3\delta^2\sigma\sigma$ | $^6\Pi$ | 1620 | 1.72 | 1620 | -3300 | 1.56 | 2465 |
| $\sigma^2\pi^2\delta^3\sigma^2$ | $^4\Delta$ | 23430 | 1.53 | 1910 | 18700 | 1.42 | 2900 |
| $\sigma^2\pi^3\delta^2\sigma^2$ | $^4\Pi$ | 26560 | 1.48 | 2060 | 27800 | 1.41 | 2950 |

Table 4.23

Population Analysis of the Valence

Orbitals of FeH, $^6\Delta$

| Orbital | Occupancy | Orbital energy | 4s(Fe) | 4p(Fe) | 3d(Fe) | 1s(H) | 2p(H) |
|---|---|---|---|---|---|---|---|
| 6σ | 2 | -0.39969 | 0.28 | 0.11 | 0.04 | 1.54 | 0.03 |
| 7σ | 1 | -0.63919 | 0.00 | 0.10 | 0.89 | 0.01 | 0.00 |
| 8σ | 1 | -0.30895 | 0.59 | 0.31 | 0.07 | 0.02 | 0.00 |
| 3π | 2 | -0.69088 | - | 0.00 | 1.99 | - | 0.01 |
| 1δ | 3 | -0.59393 | - | - | 3.00 | - | - |

applied in this work, and they would be expected to stabilise the low-spin states relative to the high-spin states, although if this effect is about 1 e.v., as suggested in ScH and TiH, the excitation energy is still about 2 e.v., which is quite large if the low-spin states are to be the ground state in CoH. The possibility must be considered that the $^3\Phi$ state in CoH could be derived from the high-spin configuration $\sigma^2\pi^3\delta^3\sigma\sigma^*$, with configuration interaction causing a reversal of the normal ordering $^5\Phi < ^3\Phi$.

The calculated ordering of the high-spin states is predicted to be $^6\Delta < ^6\Sigma^+ \sim ^6\Pi$; the calculated splitting between the $^6\Sigma^+$ and $^6\Pi$ states is probably of comparable magnitude to the accuracy of the calculation. As the states are all essentially components of the $sd^6$ configuration of the $Fe^+$ ion, it would be expected that correlation energy differences between them would be rather small, and it may therefore be concluded that the ground state of FeH is $^6\Delta$, with two low-lying states, $^6\Pi$ and $^6\Sigma^+$. This removes the problem of understanding the previous predictions of the ligand field splittings of the d-orbitals; the splitting is such as to make the dδ orbital the most stable, and the magnitudes of the splittings are comparable to those found in calculations on other transition metal hydrides.

The lack of agreement between the spectroscopic constants calculated by Walker et al. and those in this work is disappointing. Not only are the absolute values of the constants appreciably different, but there are also few similarities in the trends in the constants between different states. This may be due to the difficulty in representing adequately the rather high electron density on the hydrogen atom in the single centre basis set, and may reflect the fact that the perturbations due to the extra nucleus and due to the extra electron converge at rather different rates. In view of the proved reliability of the matrix Hartree-Fock calculations, it must be concluded that the single centre method is not currently sufficiently accurate to be a useful tool for the investigation of the electronic states of the transition metal hydrides.

## 4.5 Nickel and Palladium Monohydrides

### 4.5.1 Introduction

The monohydrides of the congeners nickel, palladium and platinum have all been observed experimentally, and in each case absorption is observed from only one low-lying state, which is probably the ground state in each case. In NiH and PtH this state has $^2\Delta$ symmetry, but PdH has a $^2\Sigma^+$ ground state. This presents two problems; to explain why the ground state changes from NiH to PdH, and to explain why the ground states of NiH and PtH are not $^2\Pi$. A simple crystal field model would predict the $^2\Pi$ state from the configuration $\sigma^2\pi^3\delta^4\sigma^2$ to lie below the $^2\Delta$ state, which corresponds to the configuration $\sigma^2\pi^4\delta^3\sigma^2$, as the $d\delta$ orbital ought to be stabilised relative to the $d\pi$ orbital by the negatively charged hydrogen atom.

Cheetham and Barrow (1967) have pointed out that the ground states of the Ni and Pt atoms are $^3D(d^9s)$, whereas the ground state of the Pd atom is $^1S$ $(d^{10})$. They also suggested that a small splitting causing the $\pi$ orbital to be more stable than the $\delta$ orbital could be caused by a stronger interaction of the $d\pi$ orbital with a $2p\pi$ orbital on the H atom than of the $3d\delta$ with a $3d\delta$ orbital on H, or by a stronger interaction of the non-bonding d orbitals with the hydrogen nucleus than with the electron charge density.

Ab initio molecular orbital calculations are particularly suited to the investigation of this problem. Calculation of wave functions for the low-lying states of NiH and PdH should confirm the identity of the ground states, which are not definitely known from the experimental work, and provide information on the splittings between the low-lying states. Further calculations should be capable of testing the two hypotheses advanced for explaining why the $^2\Delta$ state lies below the $^2\Pi$ state in NiH.

### 4.5.2 Approximate Hartree-Fock Calculations

The basis set employed for calculations of NiH is similar to those described in the earlier sections of this chapter. It is derived from the double zeta of Clementi et al. (1967). It is however not computationally

possible to use a basis set of similar quality for the calculations on PdH, and instead only the valence orbitals are represented by double zeta functions. The core orbitals are represented by the minimal basis set of Richardson et al. (1973). This procedure is expected to be satisfactory for the qualitative conclusions which are drawn from these calculations. Details of the basis sets are given in Tables 4.24 and 4.25.

Calculations were performed on the $^2\Delta$ and $^2\Pi$ states of NiH, and on the $^2\Sigma^+$, $^2\Delta$ and $^2\Pi$ states of PdH. Extensive efforts were made to obtain convergence on the $^2\Sigma^+$ state of NiH, but in vain. However, calculations in the virtual orbital approximation suggest strongly that the $^2\Sigma^+$ state is not very low-lying. The spectroscopic constants derived from the potential curves are shown in Table 4.26, along with population analyses of the valence orbitals.

4.5.3 Discussion.

The calculations satisfactorily predict that the ground states of NiH and PdH are $^2\Delta$ and $^2\Sigma^+$ respectively, which confirms the experimental information. However, they also provide further important information on the low-lying states of NiH and PdH. In PdH, the $^2\Pi$ and $^2\Delta$ states are predicted to lie about 1 e.v. above the ground state, and are virtually degenerate. In NiH, the splitting between the $^2\Delta$ and $^2\Pi$ states is about 0.6 e.v., which is rather larger than any of the splittings between a $d\pi$ and $d\delta$ orbital calculated in other transition metal hydrides, and also in the opposite sense.

The electronic structure of PdH may be understood in terms of simple covalent bonding between the $4d\sigma$ and $1s\sigma$ orbitals. If we assume that there are no $\pi$ or $\delta$ orbitals on the ligand atom, then the $d\pi$ and $d\delta$ orbitals are split only by the crystal field effect of the negative hydrogen atom, and if the polarity of the molecule is not large, this effect may be very small. Thus the ground state of the PdH molecule is expected to be $^2\Sigma^+$, with two essentially degenerate excited states, in exact agreement with the calculations and population analysis. This is shown in Figure 4.1.

Table 4.24

S.T.O. Basis Functions for PdH

| Type | Centre | Exponent | Type | Centre | Exponent |
|---|---|---|---|---|---|
| 1sσ | Pd | 45.065 | 2pπ | Pd | 20.953 |
| 2sσ | Pd | 16.926 | 3pπ | Pd | 9.676 |
| 3sσ | Pd | 9.749 | 4pπ | Pd | 4.560 |
| 4sσ | Pd | 4.889 | 5pπ | Pd | 2.013 |
| 5sσ | Pd | 1.408 | 3dπ | Pd | 15.576 |
| 5sσ | Pd | 2.112 | 3dπ | Pd | 8.797 |
| 2pσ | Pd | 20.953 | 4dπ | Pd | 4.517 |
| 3pσ | Pd | 9.676 | 4dπ | Pd | 2.086 |
| 4pσ | Pd | 4.560 | 4fπ | Pd | 2.75 |
| 5pσ | Pd | 2.013 | 2pπ | H | 1.145 |
| 3dσ | Pd | 15.576 | 3dπ | H | 1.85 |
| 3dσ | Pd | 8.797 | 3dδ | Pd | 15.576 |
| 4dσ | Pd | 4.517 | 3dδ | Pd | 8.797 |
| 4dσ | Pd | 2.086 | 4dδ | Pd | 4.517 |
| 4fσ | Pd | 2.75 | 4dδ | Pd | 2.086 |
| 1sσ | H | 0.915 | 4fδ | Pd | 2.75 |
| 1sσ | H | 1.45 | 3dδ | H | 1.85 |
| 2sσ | H | 1.85 | | | |
| 2pσ | H | 1.145 | | | |
| 3dσ | H | 1.85 | | | |

Table 4.25

S.T.O. Basis Functions for NiH

| Type | Centre | Exponent | Type | Centre | Exponent |
|---|---|---|---|---|---|
| 1sσ | Ni | 24.3414 | 1sσ | H | 0.915 |
| 1sσ | Ni | 30.4042 | 1sσ | H | 1.45 |
| 2sσ | Ni | 11.54231 | 2sσ | H | 1.85 |
| 2sσ | Ni | 15.96082 | 2pσ | H | 1.1455 |
| 3sσ | Ni | 4.4269 | 3dσ | H | 1.85 |
| 3sσ | Ni | 6.2680 | 2pπ | Ni | 11.34775 |
| 4sσ | Ni | 1.2148 | 2pπ | Ni | 20.26566 |
| 4sσ | Ni | 2.2966 | 3pπ | Ni | 6.62284 |
| 2pσ | Ni | 11.34775 | 3pπ | Ni | 4.02084 |
| 2pσ | Ni | 20.26566 | 4pπ | Ni | 2.0135 |
| 3pσ | Ni | 6.62284 | 3dπ | Ni | 2.83057 |
| 3pσ | Ni | 4.02084 | 3dπ | Ni | 6.63049 |
| 4pσ | Ni | 2.0135 | 4fπ | Ni | 2.75 |
| 3dσ | Ni | 2.83057 | 2pπ | H | 1.1455 |
| 3dσ | Ni | 6.63049 | 3dπ | H | 1.85 |
| 4fσ | Ni | 2.75 | 3dδ | Ni | 2.83057 |
| | | | 3dδ | Ni | 6.63049 |

Table 4.26

Calculated Spectroscopic Constants for PdH and NiH

| | State | Configuration | $T_e$ ($cm^{-1}$) | $R_e$ (Å) | $\omega_e$ ($cm^{-1}$) |
|---|---|---|---|---|---|
| PdH | $^2\Pi$ | $\sigma^2\pi^3\delta^4\sigma^2$ | 7790 | 1.79 | 1400 |
| | $^2\Delta$ | $\sigma^2\pi^4\delta^3\sigma^2$ | 7550 | 1.71 | 1400 |
| | $^2\Sigma^+$ | $\sigma^2\pi^4\delta^4\sigma$ | 0 | 1.55 | 1740 |
| NiH | $^2\Pi$ | $\sigma^2\pi^3\delta^4\sigma^2$ | 5530 | 1.49 | 1940 |
| | $^2\Delta$ | $\sigma^2\pi^4\delta^3\sigma^2$ | 0 | 1.43 | 2100 |

Population Analysis

PdH $^2\Sigma^+$, R=3.0 a.u.

| | 5s | 5p | 4d | 1s |
|---|---|---|---|---|
| 9σ | 0.11 | 0.03 | 0.76 | 1.09 |
| 10σ | 0.11 | 0.01 | 0.59 | 0.29 |

NiH $^2\Delta$, R=2.7 a.u.

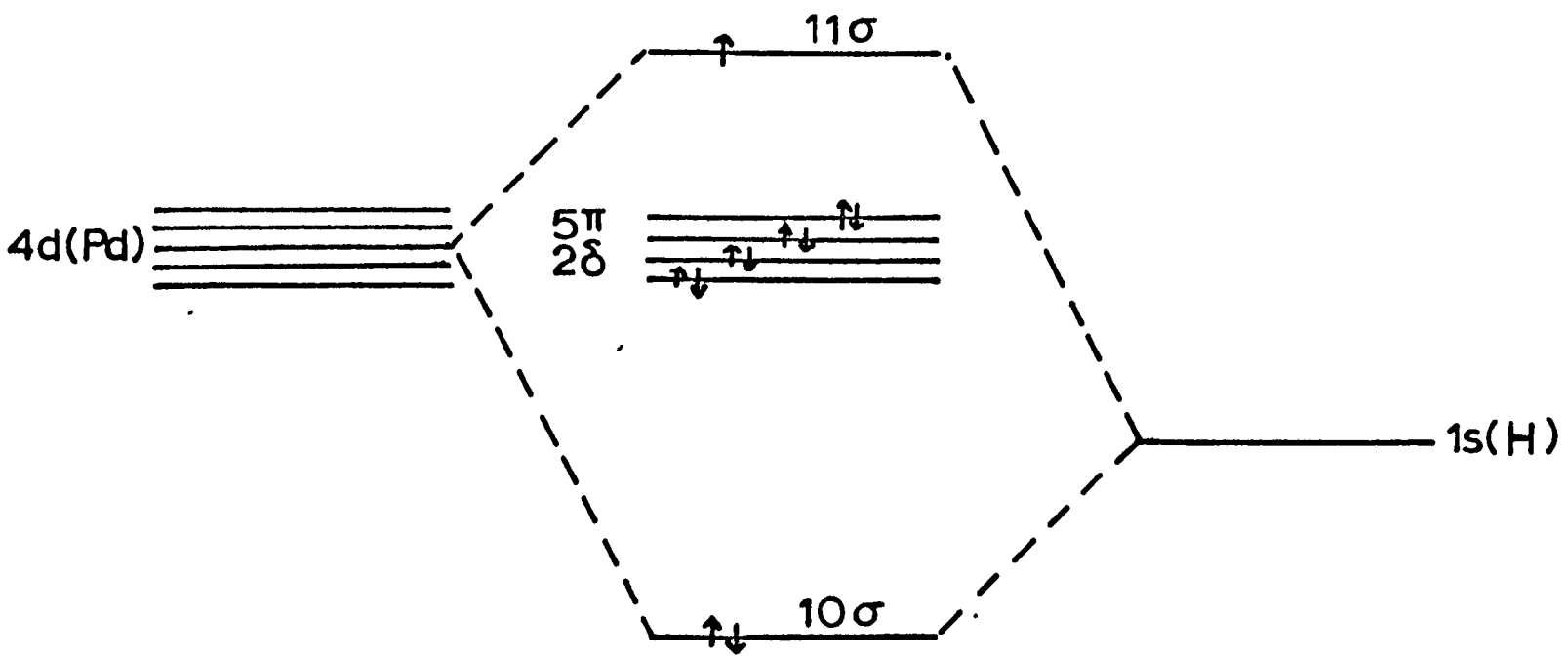
| | 4s | 4p | 3d | 1s |
|---|---|---|---|---|
| 6σ | -0.11 | -0.02 | 0.91 | 1.22 |
| 7σ | 1.21 | 0.03 | 0.64 | 0.14 |

In NiH the population analysis reveals that the situation is rather different. Covalent bonding must be considered between not only the 3dσ and 1sσ orbitals, but also the 4sσ orbital, which is relatively lower-lying in Ni than Pd. The effect of this is to stabilise the anti-bonding combination of 3dσ and 1sσ, so that it falls below the 3dπ and 3dδ orbitals, which are non-bonding in this approximation. By the aufbau principle, the two lower sigma orbitals are now doubly occupied, leaving seven electrons to occupy the dπ and dδ orbitals. This would predict two very low-lying states, $^2\Delta$ and $^2\Pi$, with an excited $^2\Sigma^+$ state. This is also shown in Figure 4.1.

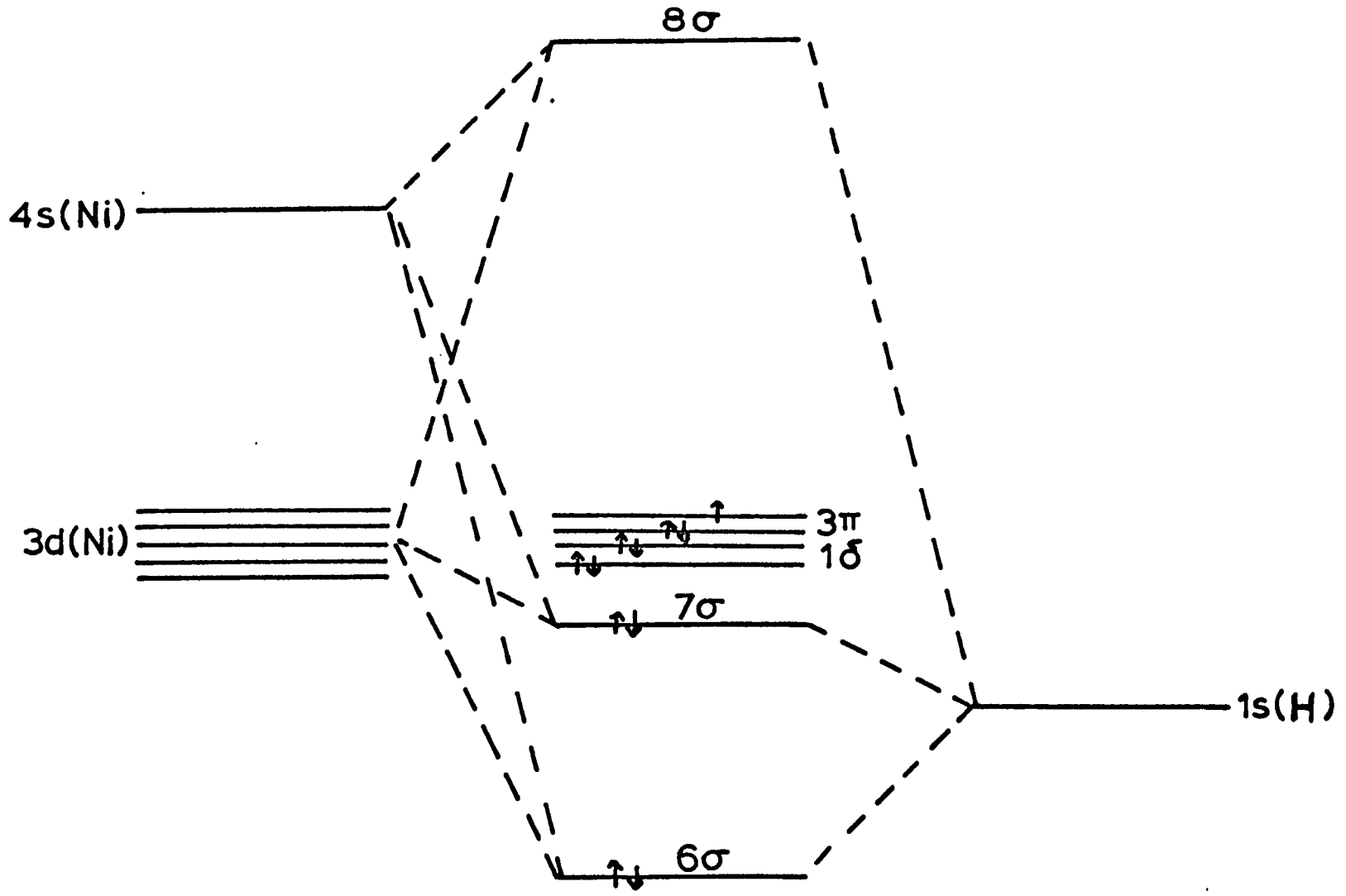
It is still necessary to account for the large stabilisation of the dπ orbital relative to the dδ orbital. A calculation on NiH using no 2pπ or 3dδ basis functions on the H atom produces an essentially unchanged value of the $^2\Pi$-$^2\Delta$ splitting, so it is not possible to maintain that the effect is caused by covalent stabilisation of the dπ orbital by 2pπ on H. This possibility is rendered improbable by the near degeneracy of the $^2\Pi$ and $^2\Delta$ states in PdH in any case. Furthermore, a calculation of the electrostatic effect of a single S.T.O. of the same size as the 1s orbital on a single S.T.O. representing the 3d orbitals shows that, even if the molecule were assumed to have no polarity at all, the electrostatic effect of the hydrogen nucleus is an order of magnitude too small to account for a splitting of 0.6 e.v. between the $^2\Pi$ and $^2\Delta$ states.

It is suggested here that the splitting may be caused by the difference in magnitudes of the repulsion between a dδ and dσ electron, and the repulsion between a dπ and dσ electron. In PdH, the population analysis shows that the $^2\Pi$ and $^2\Delta$ states may be regarded as different spatial components of a $d^9$ configuration, which in the absence of the ligand would be degenerate. Any splitting between them may therefore be attributed to the effect of the ligand. But in NiH, the population analysis reveals that this is not the case. The unoccupied anti-bonding orbital has mainly 4sσ character, but also an appreciable 3dσ character, and thus the H atom is effectively depopulating the 3dσ

Figure 4.1.




The Bonding in PdH.




The Bonding In NiH.

orbital. The population analysis suggests that the population of the 3d orbital is about 1.5, although it is not meaningful to place a great quantitative significance on this number. Because the repulsion between a dπ and dσ electron is necessarily greater than that between a dδ and dσ electron, assuming the same spatial part for each orbital, this effect stabilises the dπ orbital relative to the dδ. A simple calculation of the J and K integrals between d orbitals of the same size as those in NiH reveals that, if the d orbital occupancy is considered proportional to the repulsion energies, the magnitude of the effect would be expected to be about 0.75 e.v. The significance of this calculation is not that it justifies a quantitative use of a population analysis which is clearly incorrect as integrals of the type $\langle sd|\hat{g}|dd\rangle$ are neglected, nor that it suggests that the wave function may be exactly represented by a population analysis, but that it suggests that the proposed cause of the splitting may give rise to a splitting at least of the correct order of magnitude; this is more than can be said for the other proposed explanations of the splitting.

It is therefore suggested that the explanation of the change in ground state from PdH to NiH, and the increase in the $^2\Delta$-$^2\Pi$ splitting, may both be attributed to the relative increase in stability of the s orbital in going from the second to the first transition series. This increase, which is manifested in the change of ground state from Ni to Pd, is caused by the increase in penetration of the d orbital in going from the first to the second transition series.

## 4.6 Conclusions

This chapter has shown some of the ways in which molecular orbital calculations may be used in the investigation of the electronic structure of transition metal monohydrides. Three types of configurations have been shown to be important, and they may be loosely described as $s^2d^{n-2}$, $sd^{n-1}$ and $d^n$. In ScH and TiH, the $s^2d^{n-2}$ configuration is very low-lying, but becomes much less important across the series. From TiH to FeH the $sd^{n-1}$ configuration always gives rise to the ground state; however, the d electrons are largely non-bonding in these molecules, and it was shown that the conventional ways of describing diatomic molecules by single configuration wave functions may be inadequate. Limited configuration interaction showed that the molecules could be regarded as perturbed atoms, and that the perturbation stabilised the d orbitals in the order $\delta>\pi>\sigma$. It was further shown that a single centre perturbation technique was not capable of producing reliable results for transition metal hydrides. Towards the end of the series, the configuration $d^n$ becomes the most stable configuration, and the d orbitals become involved in bonding. However in NiH the s orbital contribution is still not negligible, and this gives rise to the d orbitals being stabilised in the order $\delta<\pi<\sigma$. In the second transition series, the d orbitals are relatively more stable, and PdH may be understood in terms of simple covalent bonding between the 4d and 1s orbitals alone.

Further theoretical work is required to investigate the nature of the low-lying states of CoH, where the high- and low-spin configurations are of comparable energies, but the most urgent need is for experimental work to test the accuracy of the theoretical calculations and provide further data. Theoretical and experimental work are complementary, and both will be required before it can be said that the electronic structures of the transition metal hydrides are fully understood.

## REFERENCES


60 L.C. Allen, E. Clementi and H.M. Gladney, 1963, Rev.Mod.Phys. 35 465.

P.S. Bagus, 1971, 'ALCHEMY Studies of Small Molecules', Proc. Seminar Selected Topic in Mol.Phys., Ludwigsburg (IBM Germany).

P.S. Bagus, A.D. McLean, M. Yoshimine and B. Liu, 1471, Users' Manual for ALCHEMY (unpublished).

32 P.S. Bagus and H.J.T. Preston, 1973, J.Chem.Phys. 59, 2986.

31 P.S. Bagus and H.F. Schaefer, 1973, J.Chem.Phys. 58, 1844.

W.J. Balfour and J.B. Tatum, 1973, J.Mol.Spect. 48, 313.

4 R.F. Barrow, 1971, in Essays in Structural Chemistry, ed. A.J. Downs, D.A. Long and L.A.K. Staveley (Macmillan, London).

R.F. Barrow (ed.), 'Diatomic Molecules, A Critical Bibliography of Spectroscopic Data' (Pergamon, Oxford).

R.F. Barrow, M.W. Bastin, D.L.G. Moore and C.J. Pott, 1967, Nature 215, 1072.

3 R.F. Barrow and C. Cousins, 1971, Adv.High Temp.Chem. 4, 161.

17 A.M. Bass, N.A. Kuebler and L.S. Nelson, 1964, J.Chem.Phys. 40, 3121.

R.A. Berg and O. Sinanoglu, 1960, J.Chem.Phys. 32, 1082.

G. Berthier, 1954, Comptes Rendues Acad.Sci. 238, 91.

M. Born and J.R. Oppenheimer, 1926, Ann.Physik 79, 361.

42 L. Brewer and D.W. Green, 1969, High Temp.Sci. 1, 26.

L. Brillouin, 1933, 'Les Champs Self-Consistent de Hartree et de Fock' (Hermann et Cie, Paris).

P.E. Cade and W.M. Huo, 1967, J.Chem.Phys. 47, 614.

P.E. Cade and W.M. Huo, 1967, J.Chem.Phys. 47, 649.

16 A.B. Callear and R.G.W. Norrish, 1960, Proc.R.Soc. A 259, 304.

K.D. Carlson and C.R. Claydon, 1967, Adv.High Temp.Chem. 1, 43.

K.D. Carlson, C.R. Claydon and C.M. Moser, 1967, J.Chem.Phys. 46, 4963.

K.D. Carlson, E. Ludeña and C.M. Moser, 1965, J.Chem.Phys. 43, 2408.

K.D. Carlson and C.M. Moser, 1966, J.Chem.Phys. 44, 3259.

41 K.D. Carlson and C.M. Moser, 1967, J.Chem.Phys. 46, 35.

26 K.D. Carlson and R.K. Nesbet, 1964, J.Chem.Phys. 41, 1051.

50 P.K. Carroll and P. McCormack, 1972, Astrophys.J. 177, L33.

C.J. Cheetham and R.F. Barrow, 1967, Adv.High Temp.Chem. 1, 7.

E. Clementi, 1963, J.Chem.Phys. 38, 2248.

E. Clementi, 1964, J.Chem.Phys. 40, 1944.

E. Clementi, R. Matcha and A. Veillard, 1967, J.Chem.Phys. 47, 1865.

E.A. Colbourn, 1973, J.Phys. B 6, 2618.

J.P. Colpa and M.F.J.Islip, 1973, Mol.Phys. 25, 701.

G. Das, 1973, J.Chem.Phys. 58, 5104.

G. Das and A.C. Wahl, 1972, J.Chem.Phys. 56, 1769.

R.L. Diebner and J.G. Kay, 1969, J.Chem.Phys. 51, 3547.

R.N. Dixon and S.E. Hull, 1969, Chem.Phys.Lett. 3, 317.

O. Edqvist, E. Lindholm, L.E. Selin and L. Åsbrink, 1970, Phys.Scripta, 1, 25.

V.A. Fock, 1930, Z.Phys. 61, 126.

A.Fröman, 1958, Phys.Rev. 112, 870.

A.G. Gaydon and R.W.B. Pearse, 1934, Nature 134, 287.

A.G. Gaydon and R.W.B. Pearse, 1935, Proc.R.Soc. A 148, 312.

A.G. Gaydon and R.W.B. Pearse, 1938, Proc.Phys.Soc. 50, 201.

D.W. Green, 1971, J.Phys.Chem. 75, 3103.

L.V. Gurvich and E.A. Shenyavskaya, 1963, Opt.Spekt. (USSR) (Eng. translation), 14, 161.

H. Hartman and E. Clementi, 1964, Phys.Rev. 133, 1295.

D.R. Hartree, 1928, Proc.Camb.phil.Soc.math.phys.Sci. 24, 328.

W. Hayes and T.E. Nevin, 1955, Proc.R.Irish Acad. A 57, 15.

A. Heimer, 1936, Naturwiss. 26, 413.

A. Heimer, 1937a, Z.Phys. 104, 448.

A. Heimer, 1937b, Z.Phys. 105, 56.

G.A. Henderson, W.T. Zemka and A.C. Wahl, 1973, J.Chem.Phys. 58, 2654.

G. Herzberg, 1950, 'Spectra of Diatonic Molecules' (Van Nostrand, Princeton, N.J.).

F. Hund, 1925, Z.Phys. 33, 345.

E. Hylleraas, 1929, Z.Phys. 54, 347.

N. Jonathan, A. Morris, K.J. Ross and D.J. Smith, 1971, J.Chem.Phys. 54, 4954.

53 B. Klemen and B. Liljeqvist, 1955, Ark.Fys. 9, 345.

55 B. Klemen and U. Uhler, 1959, Cam.J.Phys. 37, 537.

60 L. Klynning and M. Kronekvist, 1973, Phys.Scripta 7, 31.

69 I. Kopp, M. Kronekvist and A. Guntsch, 1966, Ark.Fys. 32, 371.

49 D.L. Lambert and E.A. Mallia, 1971, Mon.Not.R.Astr.Soc. 151, 437.

C. Linton and S.R. Singhal, 1974, J.Mol.Spec. 51, 194.

67 H.P.D. Liu and G. Verhaegen, 1970, J.Chem.Phys. 53, 735.

68 H.P.D. Liu and G. Verhaegen, 1971, Int.J.Quantum Chem. 5, 103.

63 C. Malmberg, R. Scullman and P. Nylen, 1969, Ark.Fys. 39, 495.

D. McLeod and W. Weltner, 1966, J.Phys.Chem. 70, 3298.

R. McWeeny and B.T. Sutcliffe, 1969, 'Methods in Molecular Quantum Mechanics' (Academic Press, London).

62 C.E. Moore, 1949, Nata.Bur.Stand.Circ. No. 467.

R.S. Mulliken, 1955, J.Chem.Phys. 23, 1833.

57 T.E. Nevin and D.V. Stephens, 1953, Proc.R. Irish Acad. A55, 109.

29 R.K. Nesbet, 1964, Phys.Rev. 135, 460.

54 S. O'Connor, 1969, J.Phys. B 2, 541.

P.A.G. O'Hare, 1974, J.Chem.Phys. 60, 4084.

P.A.G. O'Hare and A.C. Wahl, 1972, J.Chem.Phys. 56, 4516.

C.L. Pekeris, 1959, Phys.Rev. 115, 1216.

38 J.G. Phillips, 1950, Astrophys.J. 111, 314.

J.G. Phillips, 1952, Astrophys.J. 115, 567.

40 J.G. Phillips and S.P. Davis, 1971, Astrophys.J. 167, 209.

J.A. Pople and R.K. Nesbet, 1954, J.Chem.Phys. 22, 571.

J.D. Power and R.M. Pitzer, 1974, Chem.Phys.Lett. 24, 478.

J. Raftery and W.G. Richards, 1971, Int.J.Mass.Spec.Ion.Phys. 6, 269.

23 J. Raftery, P.R. Scott and W.G. Richards, 1972, J.Phys. B 5, 1293.

10 P.R. Rao, R.K. Asundi and J.K. Brody, 1962a, Can.J.Phys. 40, 412.

11 P.R. Rao, R.K. Asundi and J.K. Brody, 1962b, Can.J.Phys. 40, 423

P.R. Rao, J.K. Brody and R.K. Asundi, 1962c, Can.J.Phys. 40, 1443.

W.G. Richards and J.A. Horsley, 1971, 'Ab Initio Molecular Orbital Calculations for Chemists' (O.U.P. London).

W.G. Richards, J. Raftery and R.K. Hinkley, 1974, Spec.Publs.Chem.Soc. in the press.

W.G. Richards, T.E.H. Walker, L. Farnell and P.R. Scott, 1974, 'Supplement to Bibliography of Ab Initio Molecular Wave Functions 1970-1973' (Clarendon Press, Oxford).

W.G. Richards, T.E.H. Walker and R.K. Hinkley, 1971, 'Bibliography of Ab Initio Molecular Wave Functions' (Clarendon Press, Oxford).

J.W. Richardson, M.J. Blackman and J.E. Ranochak, 1973, J.Chem.Phys. 58, 3010.

C. Roetti and E. Clementi, 1974, J.Chem.Phys. 60, 3342.

C.C.J. Roothaan, 1951, Rev.Mod.Phys. 23, 69.

C.C.J. Roothaan, 1960, Rev.Mod.Phys. 32, 179.

C.C.J. Roothaan and P.S. Bagus, 1963, in 'Methods in Comp.Physics' Vol. 2 (Academic Press, N.Y.).

B. Rosen (ed.), 1970, 'Donées Spectroscopiques Rélatives aux Molécules Diatomiques' (Pergamon Press, Oxford).

G.M. Schwenzer, D.H. Liskow, H.F. Schaefer III, P.S. Bagus, B. Liu, A.D. McLean and M. Yoshimine, 1973, J.Chem.Phys. 58, 3181.

P.R. Scott, 1972, B.A. Thesis, Oxford.

P.R. Scott, J. Raftery and W.G. Richards, 1973a, J.Phys. B 6, 881.

P.R. Scott, J. Raftery and W.G. Richards, 1973b, Colloquium on High Resolution Molecular Spectroscopy, Tours, France.

P.R. Scott and W.G. Richards, 1974a, J.Phys. B 7, 500.

P.R. Scott and W.G. Richards, 1974b, J.Phys. B in the press.

P.R. Scott and W.G. Richards, 1974c, J.Phys. B in the press.

P.R. Scott and W.G. Richards, 1974d, J.Chem.Phys. submitted for publication.

P.R. Scott and W.G. Richards, 1974e, Chem.Phys.Lett. in the press.

R. Scullman, 1965, Ark.Fys. 28, 255.

J.C. Slater, 1929, Phys.Rev. 34, 1293.

J.C. Slater, 1930, Phys.Rev. 35, 210.

J.C. Slater, 1931, Phys.Rev. 38, 1109.

R.E. Smith, 1973, Proc.R.Soc. A 332, 113.

R.E. Smith and A.G. Gaydon, 1971, J.Phys. B 4, 797.

S.P. So and W.G. Richards, 1974, J.Phys. B in the press.

J.A.C. Todd, 1967, B.A. Thesis, Oxford.

J.A.C. Todd, 1973, D.Phil. Thesis, Oxford.

J.H. Walker, T.E.H. Walker and H.P. Kelly, 1972, J.Chem.Phys. 57, 2094.

T.E.H. Walker, 1971, J.Phys.B 4, 399.

W. Weltner, 1967, Science 155, 155.

W. Weltner and D. McLeod, 1965, J.Phys.Chem. 69, 3488.

W. Weltner, D. McLeod and P.H. Kasai, 1967, J.Chem.Phys. 46, 3172.

## Appendix A

## THE ROOTHAAN DOUBLE HAMILTONIAN METHOD

Roothaan (1960) proposed this method for open-shell wave functions in which the energy expectation value could be expressed as:

$$E = 2\sum_i \varepsilon_i^N + \sum_{ij} (2J_{ij}-K_{ij}) + f\{2\sum_u \varepsilon_u^N + f\sum_{uv} (2uJ_{uv}-bK_{uv}) + \sum_{uj} (2J_{uj}-K_{uj})\}$$

which is a special case of the more general expression

$$E = \sum_I \sum_i 2f_I \varepsilon_i^N + \sum_{IJ} \sum_{ij} f_I f_J (2a_{IJ}J_{ij}-b_{IJ}K_{ij})$$

where I and J are 'shells' between which the interactions take a similar form. All wave functions consisting of a single spin eigenfunction have energy expressions which may be expressed in this way. The method is first outlined for a single open shell, and then in matrix notation for the general case.

For a single open shell, the conditions for a stationary expectation value, subject to the orthonormality constraint, are

$$(\hat{h} + 2\hat{J}_c - \hat{K}_c + 2\hat{J}_o - \hat{K}_o)|i\rangle = \sum_j \theta_{ij}|j\rangle + \sum_v \theta_{iv}|v\rangle \qquad (1)$$

$$f(\hat{h} + 2\hat{J}_c - \hat{K}_c + 2a\hat{J}_o - b\hat{K}_o)|u\rangle = \sum_j \theta_{uj}|j\rangle + \sum_v \theta_{uv}|v\rangle \qquad (2)$$

where i,j are closed-shell orbitals, and u,v open-shell orbitals. Unitary transformations of the $\phi_i$ and $\phi_u$ may be chosen to make $\theta_{ij}$ and $\theta_{uv}$ diagonal, so that

$$(\hat{h} + 2\hat{J}_c - \hat{K}_c + 2\hat{J}_o - \hat{K}_o)|i\rangle = \varepsilon_i|i\rangle + \sum_v \theta_{iv}|v\rangle \qquad (3)$$

$$f(\hat{h} + 2\hat{J}_c - \hat{K}_c + 2a\hat{J}_o - b\hat{K}_o)|u\rangle = \varepsilon_u|u\rangle + \sum_j \theta_{uj}|j\rangle \qquad (4)$$

Applying $\langle u|$ to (3) and $\langle i|$ to (4),

$$\langle u|\hat{h} + 2\hat{J}_c - \hat{K}_c + 2\hat{J}_o - \hat{K}_o|i\rangle = \varepsilon_i \langle u|i\rangle + \sum_v \theta_{iv} \langle u|v\rangle$$

$$= \theta_{iu} \qquad (5)$$

$$f \langle i|\hat{h} + 2\hat{J}_c - \hat{K}_c + 2a\hat{J}_o - b\hat{K}_o|u\rangle = \theta_{iu} \qquad (6)$$

Subtracting (5) multiplied by f from (6), and using hermiticity, gives

$$\theta_{iu}(1-f) = -f \langle i|2(1-a)\hat{J}_o - (1-b)\hat{K}_o|u\rangle$$

If $\alpha = \frac{1-a}{1-f}$ and $\beta = \frac{1-b}{1-f}$,

$$\theta_{iu} = -f \langle i|2\alpha\hat{J}_o - \beta\hat{K}_o|u\rangle = \theta_{ui}$$

Substituting in equation (3) and (4)

$$(\hat{h} + 2\hat{J}_c - \hat{K}_c + 2\hat{J}_o - \hat{K}_o)|i\rangle = \varepsilon_i|i\rangle - f \sum_v \langle i|2\alpha\hat{J}_o - \beta\hat{K}_o|v\rangle |v\rangle$$

$$f(\hat{h} + 2\hat{J}_c - \hat{K}_c + 2a\hat{J}_o - b\hat{K}_o)|u\rangle = \varepsilon_u|u\rangle - f \sum_j \langle u|2\alpha\hat{J}_o - \beta\hat{K}_o|j\rangle |j\rangle$$

Defining coupling operators $\hat{L}_o$ and $\hat{L}_c$

$$\hat{L}_o|i\rangle = f \sum_v \langle i|2\alpha J_o - \beta K_o|v\rangle |v\rangle$$

and $\hat{L}_c|u\rangle = \sum_j \langle u|2\alpha\hat{J}_o - \beta\hat{K}_o|j\rangle |j\rangle$,

we obtain $$(\hat{h} + 2\hat{J}_c - \hat{K}_c + 2\hat{J}_o - \hat{K}_o + \hat{L}_o)|i\rangle = \varepsilon_i|i\rangle \qquad (7)$$

$$f(\hat{h} + 2\hat{J}_c - \hat{K}_c + 2a\hat{J}_o - b\hat{K}_o + \hat{L}_c)|u\rangle = \varepsilon_u|u\rangle \qquad (8)$$

which have the required eigenvalue form.

For the case of many open-shells, if the orbitals are expanded in a basis set $\{\chi\}$, then

$$E = 2 \sum_I f_I \underline{R}_I : \underline{h} + \sum_{IJ} f_I f_J \underline{R}_I \{2a_{IJ}J - b_{IJ}K\} : R_J \qquad (9)$$

where $R_I$ are the density matrices for each shell

$$R_I = \underline{C}_I \underline{C}_I^+$$

Defining $\underline{J}_J = J:R_J$, $\underline{K}_J = K:\underline{R}_J$ and $\underline{G}_I = \sum_J f_J\{2a_{IJ}\underline{J}_J - b_{IJ}\underline{K}_J\}$,

$$E = \sum_I f_I \underline{R}_I : (2\underline{h} + \underline{G}_I). \tag{10}$$

If this expression is minimised with respect to variations in $\underline{C}_I$, then for each I

$$f_I\ (\underline{h}+\underline{G}_I)C_I = \vec{\varepsilon}_I\ \underline{S}\ \underline{C}_I + \sum_{J\neq I} \underline{S}\ \underline{C}_J\ \underline{\theta}_{IJ} \tag{11}$$

where $\underline{\theta}_{IJ}$ is a matrix of off-diagonal Lagrangian multipliers. Multiplying (11) by $\underline{C}_K^+$,

$$f_I\ \underline{C}_K^+\ (\underline{h}+\underline{G}_I)\ \underline{C}_I = \theta_{IK} \tag{12}$$

as $$\underline{C}_K^+\ \underline{S}\ \underline{C}_I = 0$$

Using hermiticity $\underline{\theta}_{IK} = \underline{\theta}_{KI}^+ = f_K\ \underline{C}_K^+\ (\underline{h}+\underline{G}_K)\ C_I$,

and $$-\underline{\theta}_{IK}\ (f_I - f_K) = f_I f_K\ \underline{C}_K^+\ (\underline{G}_I - \underline{G}_K)\ \underline{C}_I \tag{13}$$

Now $$\underline{G}_I - \underline{G}_K = \sum_L f_L\ \{(2a_{IL}\underline{J}_L - b_{IL}\underline{K}_L) - (2a_{KL}\underline{J}_L - b_{KL}\underline{K}_L)\}$$

$$= \sum f_L\ \{2(a_{IL}-a_{KL})\underline{J}_L - (b_{IL}-b_{KL})\underline{K}_L\} \tag{14}$$

Substituting (14) into (13), putting $\frac{a_{IL}-a_{KL}}{f_I-f_K} = \alpha_{IKL}$, $\frac{b_{IL}-b_{KL}}{f_I-f_K} = \beta_{IKL}$

$$\underline{\theta}_{IK} = -f_I f_K\ \{C_K^+ \sum_L f_L\ (2\alpha_{IKL}\underline{J}_L - \beta_{IKL}\underline{K}_L)\ C_I\}$$

which substituted in equation (11) gives

$$f_I(\underline{h}+\underline{G}_I)\underline{C}_J = \vec{\varepsilon}_I\ \underline{S}\ \underline{C}_I - f_I \sum_{J\neq I} f_J\ \underline{S}\ \underline{R}_J \sum_L f_L\ (2\alpha_{IJL}\underline{J}_L - \beta_{IJL}\underline{K}_L)\ \underline{C}_I$$

Defining the coupling matrix $\underline{L}_{IJ}$

$$\underline{L}_{IJ} = f_J \, \underline{S} \, \underline{R}_J \sum_L f_L \, (2\alpha_{IJL}\underline{J}_L - \beta_{IJL}\underline{K}_L) \, ,$$

$$f_I \, (\underline{h}+\underline{G}_I + \sum_{J=I} L_{IJ}) \, C_I = \vec{\epsilon}_I \, \underline{S} \, \underline{C}_I .$$

There is thus a set of equations, one for each shell, in which the Fock matrix is modified by the addition of matrices representing the coupling to each other shell. The solutions of the variational problem are the eigenvectors (the matrices $\underline{C}_I$) of these equations.

## Appendix B

### ATOMIC CORRELATION ENERGIES

Configuration $d^2$

$$E\ |2\ \ 1| = E\ (^3F)$$
$$E\ |2\ \ 0| = E\ (^3F)$$
$$E\ |1\ \ 0| = .40E\ (^3F) + .60E\ (^3P)$$
$$E\ |2\ -1| = .60E\ (^3F) + .40E\ (^3P)$$
$$E\ |2\ -2| = .20E\ (^3F) + .80E\ (^3P)$$
$$E\ |1\ -1| = .80E\ (^3F) + .20E\ (^3P)$$
$$E\ |0\ \ \bar{0}| = .20E\ (^1S) + .29E\ (^1D) + .47E\ (^1G)$$

Configuration dp

$$E\ |2\ \ 1| = E\ (^3F)$$
$$E\ |2\ \ 0| = .33E\ (^3F) + .67E\ (^3D)$$
$$E\ |1\ \ 1| = .67E\ (^3F) + .33E\ (^3D)$$
$$E\ |1\ \ 0| = .53E\ (^3F) + .17E\ (^3D) + .30E\ (^3P)$$
$$E\ |0\ \ 1| = .40E\ (^3F) + .50E\ (^3D) + .10E\ (^3P)$$
$$E\ |2\ -1| = .07E\ (^3F) + .33E\ (^3D) + .60E\ (^3P)$$
$$E\ |1\ -1| = .20E\ (^3F) + .50E\ (^3D) + .30E\ (^3P)$$
$$E\ |0\ \ 0| = .60E\ (^3F) + .40E\ (^3P)$$
$$E\ |-1\ \ 1| = .20E\ (^3F) + .50E\ (^3D) + .30E\ (^3P)$$

Configuration $d^3$

$$E\ |0\ \ 2\ -2| = .80E\ (^4F) + .20E\ (^4P)$$
$$E\ |0\ \ 2\ -1| = .60E\ (^4F) + .40E\ (^4P)$$
$$E\ |2\ \ 0\ \ \bar{0}| = .30E\ (^2H) + .34E\ (^2G) + .25E(^2D_1) + .11E(^2D_2)$$

Configuration $d^2p$

$$E\ |2\ \ 1\ \ 0| = .25E\ (^4G) + .75E\ (^4F)$$
$$E\ |2\ \ 0\ \ 0| = .43E\ (^4G) + .33E\ (^4F) + .24E\ (^4D_F)$$
$$E\ |2\ -1\ \ 0| = .32E\ (^4G) + .05E\ (^4F) + .23E\ (^4D_F) + .20E\ (^4D_P) + .20E\ (^4P)$$
$$E\ |1\ \ 1\ \ 0| = .21E\ (^4G) + .03E\ (^4F) + .15E\ (^4D_F) + .30E\ (^4D_P) + .30E\ (^4P)$$
$$E\ |2\ -2\ \ 0| = .11E\ (^4G) + .09E\ (^4D_F) + .53E\ (^4D_P) + .27E\ (^4S)$$

Configuration $d^4$

$$E\ |2\ \ 0\ \ \bar{0}\ -2| = .38E\ (^3H) + .07E\ (^3F_1) + .27E\ (^3F_2) + .27E\ (^3P_1) + .02E(^3P_2)$$

where for the configuration dp,

E |1 0| is the correlation energy of the determinant $|d_1 p_0|$,

and

E ($^3$F) is the correlation energy of the $^3$F state from the configuration pd.